TRANSCRIPTION FACTOR FKH-9 REGULATES OXIDATIVE STRESS RESPONSES IN *CAENORHABDITIS ELEGANS*

ALESSIA LIBERTUCCI

A THESIS SUBMITTED TO THE FACULTY OF GRADUATE STUDIES

IN PARTIAL FULFILLMENT OF THE REQUIREMENTS FOR THE

DEGREE OF MASTER OF SCIENCE

GRADUATE PROGRAM IN BIOLOGY

YORK UNIVERSITY

TORONTO, ONTARIO

AUGUST 2023

Abstract

The biological process of energy production is an essential mechanism needed for the strength and survival of many living organisms. Although highly beneficial, energy production can also exert a negative effect through the creation of reactive oxygen species (ROS). ROS are highly reactive chemicals that are generated when oxygen molecules get reduced in the cell such as from mitochondrial oxidative metabolism. This production of ROS is a normal cellular event; however, its accumulation can cause oxidative stress by modifying compounds, interfering with signalling cascades, and damaging macromolecules. Therefore, the cell is known to have many detoxification systems that involve specific cellular signalling pathways. One pathway seen in *C. elegans* is the skinhead-1 (SKN-1) glutathione s-transferase-4 (GST-4) pathway. GST-4 is an important detoxification enzyme that helps reduce the accumulation of ROS in the cell, while the SKN-1 transcription factor regulates *gst-4* at the promoter. However, under non-oxidative stress-inducing conditions SKN-1 is hypothesized to be indirectly held in the cytoplasm by the BRCA1 associated protein-2 (BRAP-2). Recently, our lab discovered elevated *gst-4* levels in *brap-2(ok1492)* deletion mutants, however RNAi of the transcription factor forkhead-9 *(fkh-9)* in these mutants caused a decrease in *gst-4* expression. I have confirmed that FKH-9 is needed for *gst-4* expression levels in *brap-2(ok1492)* mutated worms. I have also uncovered its potential role in the signalling pathway as FKH-9 significantly increased SKN-1-mediated activity at the *skn-1c* promoter indicating a potential synergistic effect with SKN-1 to help increase SKN-1 transcription levels. Biological analysis of FKH-9 was also carried out and mutants were seen to have compromised longevity and survival under various stress-inducing conditions compared to wild-type (WT). Thus, my investigation ultimately presents an initial indication upon the role and function of FKH-9 in the *C. elegans* oxidative stress response.

Acknowledgments

Anyone who knows me knows that getting into Graduate school to obtain my Master's Degree has been my number one goal since high school. Completing this thesis after two years of hard work is therefore my biggest and most valuable milestone in my academic career thus far. It has definitely been a wild journey, but it has also been the absolute best of my life. I am extremely proud of myself for achieving this accomplishment, but I could not have done it alone. I am incredibly grateful to everyone who helped and supported me along the way, so I would like to dedicate this thesis to all of you.

First and foremost, I would like to thank my amazing supervisor Dr. Terrance J. Kubiseski. I cannot thank you enough for taking me on as a student and allowing me to conduct research in your lab. I heavily appreciated not only your constant mentorship and support, but the creativity you allowed me to express. You let me take full ownership of my project and trusted in my abilities to carry out this research. Most importantly though, what I heavily valued and will take with me as I endure future endeavors as a scientist, is your never-failing optimism and open-mindedness. Thank you for always helping me when I was stressing over my lab work and for teaching me to think outside the box. Next, to my advisor Dr. Hudak, thank you so much for your constant valuable insight and feedback. Your suggestions allowed me to think more critically about my project and helped me examine certain areas in different perspectives. I am very thankful for your gracious encouragement throughout these past two years! And to Dr. Magdalena Jaklewicz, thank you for taking the time to teach me how to capture beautiful images of my *C. elegans*. You are the microscopy queen always!

I would next like to send a massive shoutout to all the lab homies! The biggest thank you goes out to my wonderful lab partner, Fozia. Foz, I genuinely would not have been able to get through this without you. Thank you so much for welcoming me into the lab and for being such a great mentor. You were always so kind and generous and I feel very lucky to have met such a delightful person like you. Our lab shenanigans will always be my favorite memories! Next, to my besties Tanvir and Arnold. You two have done more for me than you could ever know. I am so incredibly grateful that this program brought us together because I do not think I could have survived without either of you! Thank you for the fun adventures, the weekend trips, the non-stop violations and all the laughs! Alongside this, I would like to thank my best friends Emily and Anabela. Thank you both for always being incredibly supportive and understanding of my academic goals. You two have stuck by me through it all and I love you both with all my heart! To Mom, Dad, and Nick, thank you for always trusting in my abilities to become the best version of myself that I could be. You always believed in me when I did not believe in myself, and I would not have made it this far without your continuous love and support.

Lastly, I need to send out a very special thank you by travelling back to high school. I discovered my love for biology in my Grade.10 science class and it was all thanks to my outstanding teacher. To Mr. Gillingham, thank you for being a prime example of what it means to be passionate about science. Your love and adoration for this field was what made me realize mine, and ever since then I have never looked back. Even more, that class gave me two of the most important friendships in my life. To Melina and Tia, thank you both for being on this journey with me since day one. We have come so far since the high school days, and I cannot wait to see what the future holds for all of us! I will never be able to express how much you both mean to me, but all I can say is (p)MAT forever!

P.S. – To whoever may read this: always stay curious and never stop questioning ♥

Table of Contents

List of Figures

List of Tables

List of Abbreviations

AAK	AMP Activated Kinase
AGE	Ageing Alteration
AKT	Protein Kinase B (PKB)
AMPK	AMP-Activated Protein Kinase
ARE	Antioxidant Response Element
AS	Arsenite
BRAP	Brca1 Associated Binding Protein
BRCA	Breast Cancer susceptibility gene
bZIP	Basic Leucine Zipper
CDC	Cell Division Control Protein
cDNA	Complementary DNA
C. elegans	*Caenorhabditis elegans*
CUL	Cullin
DAF	Abnormal Dauer Formation
DDB	UV-Damaged DNA Binding Protein
DHS	Dehydrogenases Short Chain
DNA	Deoxyribonucleic Acid
DTT	Dithiothreitol
E. coli	*Escherichia coli*
ER	Endoplasmic Reticulum
ERK	Extracellular Signal-Regulated Protein Kinase
ETC	Electron Transport Chain
E3	Ubiquitin ligase
FKH	Fork-Head Domain-Containing Protein
FMO	Flavin Monooxygenase
FOXO	Forkhead box O
GCS	Glutamate-Cysteine Ligase
GFP	Green Fluorescent Protein
GSK	Glycogen Synthase Kinase
GSTO	Glutathione-S-Transferase Omega
GST	Glutathione-S-Transferase
HIM	High Incidence of Males
HSP	Heat Shock Protein
IGF	Insulin Growth Factor
IIS	Insulin/Insulin-like growth factor Signaling
IRE	Serina/Threonine-Protein Kinase
JKK	JNK Kinase
JNK	Jun N-terminal Kinase
KEAP	Kelch-like ECH-Associated Protein
KSR	Kinase Suppressor of RAS
MAF	Musculoaponeurotic Fibrosarcoma
MAPK	Mitogen-Activated Protein Kinase

MAPKK	Mitogen-Activated Protein Kinase Kinase
MAPKKK	Mitogen-Activated Protein Kinase Kinase
MDT	Mediator Subunit
MEK	Erk Kinase
MPK	MAP Kinase
mRNA	messenger RNA
NGM	Nematode Growth Medium
NLS	Nuclear Localization Signal
PCR	Polymerase Chain Reaction
PDK	Phosphoinositide-Dependent Kinase
PIP_2	Phosphatidylinositol 4,5-bisphosphate
PIP_3	Phosphatidylinositol 3,4,5-triphosphate
PMK	P38 Map Kinase Family
p38	Protein 38 MAPK
qPCR	Quantitative Polymerase Chain Reaction
RT-PCR	Reverse Transcriptase Polymerase Chain Reaction
RAF	Rapidly Accelerated Fibrosarcoma
RAS	Rat Sarcoma Oncogene
RNA	Ribonucleic Acid
RNAi	RNA Interference
ROS	Reactive Oxygen Species
SDZ	SKN-1 Dependent Zygotic Transcript
SKN	Skinhead
SOD	Superoxide Dismutase
SWPCR	Single Worm PCR
TBA	Tubulin Alpha Chain
tBHP	*tert*-Butyl Hydroperoxide
TFs	Transcription Factors
TOR	Target of Rapamycin
UGT	UDP-Glucuronosyl Transferase
VIT	Vitellogenin
WDR	WD Repeat Protein
WNT	Wingless-Related Integration Site
WT	Wild Type
XBP	X-Box-Binding Protein 1

CHAPTER 1: INTRODUCTION AND LITERATURE REVIEW

1.0 Introduction:

1.1 General Introduction:

Aging is a natural and normal occurrence for a multitude of living beings. It is not something that can be stopped or hindered, but instead is part of the natural life cycle. Unfortunately, aging is accompanied with many debilitating diseases that cause sickness to the organism and its eventual demise. For example, cardiovascular disease remains the most common cause of death in older adults, with cancer being the second (Jaul & Barron, 2017). Due to this, understanding the mechanisms of aging remains to be a critical area of importance in cellular/molecular biology. The better we can understand the core mechanisms of aging, the better advancements we can make in research on human health. This, however, is certainly not an easy task to accomplish.

Although we do not have all the answers to explain the structure of aging, we have made substantial progress into grasping the underlying cellular/molecular causes. It is important to note that there is not one single and clear biological cause of aging, but instead many different components that contribute to aging overall. Through different biological theories we have uncovered causes of aging such as the accumulation of random molecular damage. This includes for example, somatic mutations, telomere shortening, protein damage and mitochondrial dysfunction (Mc Auley et al., 2017). Although our cells contain and carry out control systems to recognize, repair and remove cellular damage, these systems are not 100% effective.

One of the main cellular causes of aging remains to be mitochondrial dysfunction, as this leads to the formation of reactive oxygen species (ROS). With progressive decline in mitochondrial function with age, this causes an accumulation of ROS in the cell (Singh, 2006). At low concentrations, ROS are important to the cell as they can serve as signalling molecules.

However, the accumulation of ROS becomes a large issue because these chemicals can go on to modify compounds, interfere with signalling cascades and damage macromolecules such as lipids, proteins, and DNA (Klotz & Steinbrenner, 2017). With this high level of ROS in the cell, comes the imbalance between ROS and the ability of detoxification enzymes to ultimately remove them, resulting in oxidative stress. The cell must have a way to defend itself against this stress and one way it can achieve this is through cellular signalling pathways (Nita & Grzybowski, 2016).

Cellular signalling pathways are known to be quite intricate and complex, however it is critical to understand the pathways involved in oxidative stress to help develop therapeutics. Many signalling pathways are known to be conserved with counterparts in multiple different organisms such as worms, mice, and flies. These simple animals are often used in research as model organisms to help us investigate certain biological mechanisms. In this project, I used a microscopic nematode, *Caenorhabditis elegans,* to determine the role of the FKH-9 transcription factor in the oxidative stress response.

1.1.1 *Caenorhabditis elegans* as a Useful and Powerful Model Organism:

The eukaryotic, multicellular organism *Caenorhabditis elegans* is a free-living (non-parasitic), transparent nematode that feeds on microorganisms such as *Escherichia coli*. *C. elegans* are about 1-1.5mm in length, have a rapid life cycle (1-3 days), and can self-fertilize. Due to these unique characteristics, in 1965 Sydney Brenner decided to use *C. elegans* as a model organism in the lab to study animal development and behaviour (Goldstein, 2016). He quickly learned and appreciated the great potential they present for genetic cultivation as well as ease of laboratory use. Since then, *C. elegans* have continued to be used in the laboratory setting due to the multiple advantages they present.

Due to their small size, *C. elegans* are easy to manipulate in the lab. They can grow rapidly on petri dishes with *E. coli* to feed off. Due to their small size, scientific experimentation can be carried out in the context of a living and intact organism instead of only isolated cells. Also, hundreds of progenies are easily attainable in a short time due to their rapid life cycle which allows fast and readily available experimentation (Figure 1.1). *C. elegans* can also exhibit one of two sexes: hermaphrodites and males. The way we can visually distinguish males from hermaphrodites is by examining the tail region; males contain a small knick in their tail making it appear as a hook shape. Hermaphrodites do not contain this as they instead appear smooth throughout. Hermaphrodites contain both eggs and sperm and are able to lay up to 300 fertilized eggs (S. Zhang et al., 2020). Males contain only sperm and when present in the population, are preferred for fertilization. Due to this, males are very beneficial to use for genetic crosses.

Another strong advantage that *C. elegans* present is that although they are a relatively simple organism, they contain multiple molecular mechanisms and signalling pathways that are shared with higher, more complex organisms. For example, they contain many homologs of human related genes which presents a great opportunity for manipulation to study human disease (Qin et al., 2018). Please refer to Table 5 in the appendix for a list of mammalian homologs of *C. elegans* genes and their functions.

In 1998, *C. elegans* became the first multicellular organism to have its entire genome sequenced which gave them great laboratory significance (Yoshimura et al., 2019). Since then, many more genetic techniques have been carried out on this model organism such as: generating transgenic lines, using fluorescently tagged proteins to track location, RNAi to study protein effect/function and qRT-PCR to measure mRNA levels of genes to examine gene expression.

Figure 1.1: *C. elegans* on Petri Dish

Picture portraying hundreds of progenies of *C. elegans* feeding off *E. coli* on a 6cm petri dish. This plate contains eggs as well as mainly L3-L4 adult worms. Due to their rapid life cycle, this number of worms is attainable in only a few days providing a substantial amount of *C. elegans* for experimentation. It is also clear to see their small size, helping to depict how simplistic manipulation is in the lab.

Overall, *C. elegans* have proven to be a valuable model organism in the lab as it has given us valuable insight and understanding of various human diseases such as cancer, diabetes, and Alzheimer's. In this project, I have used this magnificent model organism to study the role of the FKH-9 transcription factor in the oxidative stress response, as well as its biological role in survival and lifespan.

1.2 Oxidative Stress

The cell undergoes and withstands multiple different chemical reactions, signalling systems and tasks on a day-to-day basis. Although it is the smallest unit of life, the cell works hard to keep itself viable and healthy by protecting itself against different stressors that could be detrimental. Although the cell carries out various reactions to promote its survival and growth, sometimes these are accompanied with by-products that can harm the cell. One specific class of potentially detrimental by-products includes Reactive Oxygen Species (ROS) which can put the cell under oxidative stress.

ROS are known as free radicals or oxygen radicals as they are essentially unstable oxygen molecules. An oxygen atom contains two unpaired electrons in its outermost shell and therefore the creation of ROS occurs when an oxygen atom gets reduced, making it highly reactive with other molecules in the cell (Bergamini et al., 2004). Examples of these oxygen molecules include the superoxide anion ($\cdot O_2^-$), the hydroxyl ion (OH^-), the hydroxyl radical ($OH\cdot$) and hydrogen peroxide (H_2O_2). These cellular forms of ROS can arise endogenously during natural metabolic events such as oxidative metabolism, or they may form from interactions an organism has with exogenous sources such as xenobiotics (Klotz & Steinbrenner, 2017; Nita & Grzybowski, 2016). At low concentrations, ROS is deemed as great importance to the cell as it aids in multiple different signalling pathways, however the issue arises when ROS

levels in the cell become elevated. The cell must have a way to combat this elevation, and it does so by using detoxification enzymes. However, when ROS levels reach a point of where they heavily out-weigh the amount of detoxification enzymes available in the cell, ROS can go on to modify compounds, interfere with signalling cascades and cause damage to lipids, proteins and DNA (Klotz & Steinbrenner, 2017). When this state occurs, the cell is officially known to be under "oxidative stress." Long-term oxidative stress is known to play a role in aging, but also in the development of chronic inflammation, cancer, and diabetes for example. Therefore, understanding the way in which this stress is caused and subsequently counter-acted by the cell holds great importance to our understanding of many human health diseases.

1.2.1 ROS Generation and Detoxification

As previously mentioned, ROS can be found in the cell as a by-product of normal cellular events. Although ROS can be produced by different cellular compartments such as the cell membrane, endoplasmic reticulum and peroxisomes for example, the mitochondria is known to be the major source of ROS as it generates about 90% of cellular ROS overall (Balaban et al., 2005). Specifically, the superoxide anion ($\cdot O_2^-$) is the most abundant ROS produced by the mitochondria, which goes on to be converted into other forms of ROS such as H_2O_2 and hydroxyl ions (OH^-) (Balaban et al., 2005; Duchen, 2004). ROS are specifically produced at the electron transport chain (ETC) during oxidative phosphorylation when molecular oxygen (O_2) gets reduced to $\cdot O_2^-$. During the process of their transport along the chain, electrons can leak out and interact with molecular oxygen molecules (O_2) to form the superoxide anion ($\cdot O_2^-$) (Tahara et al., 2009). This event mainly occurs at complexes I and III of the ETC making them major sources of superoxide and hydrogen peroxide (Tahara et al., 2009). It is also important to note that due to

the mitochondria being a major source of ROS, if this organelle becomes damaged in the cell, leakage of electrons will increase and result in a much higher production of ROS.

Besides oxidative phosphorylation, ROS can also be created from exogenous sources such as radiation, pollution, and diet for example. However, one of the main exogenous sources of ROS are xenobiotics. Xenobiotics are chemical substances within an organism that are not naturally present within that organism (Klotz & Steinbrenner, 2017). Often times, organisms can acquire xenobiotics through their environment (known as environmental toxins) (Klotz & Steinbrenner, 2017). In order to remove xenobiotics, xenobiotic metabolism must be carried out which involves biotransformation of these substances for transport and excretion out of the cell (Klotz & Steinbrenner, 2017). However, this biotransformation is usually accompanied with the large generation of ROS.

When a large amount of ROS is present in the cell, this can be detrimental as ROS molecules can oxidize and irreversibly damage proteins, lipids and DNA and also cause deterioration of cells and tissues (Figure 1.2). The way in which ROS damages proteins is by causing the oxidation of amino acid residues, the cleavage of peptide bonds and aggregation between proteins (Milkovic et al., 2019). ROS can damage lipids by causing lipid peroxidation; free radicals can oxidize an unsaturated lipid chain which leads to the formation of a hydro-peroxidised lipid and an alkyl radical (Yadav et al., 2019). This can result in alterations in cell membrane structure for example, ultimately affecting fluidity and damaging its integrity (Yadav et al., 2019). ROS can also cause major damage to DNA as its oxidation can result in alterations to DNA bases or double helix breaks (Poetsch, 2020). The hydroxyl radical (OH·) specifically can cause direct DNA damage by strand excision and also cause oxidative damage to pyrimidine and purine bases (Poetsch, 2020). It is clear to see the extensive and serious damage elevated

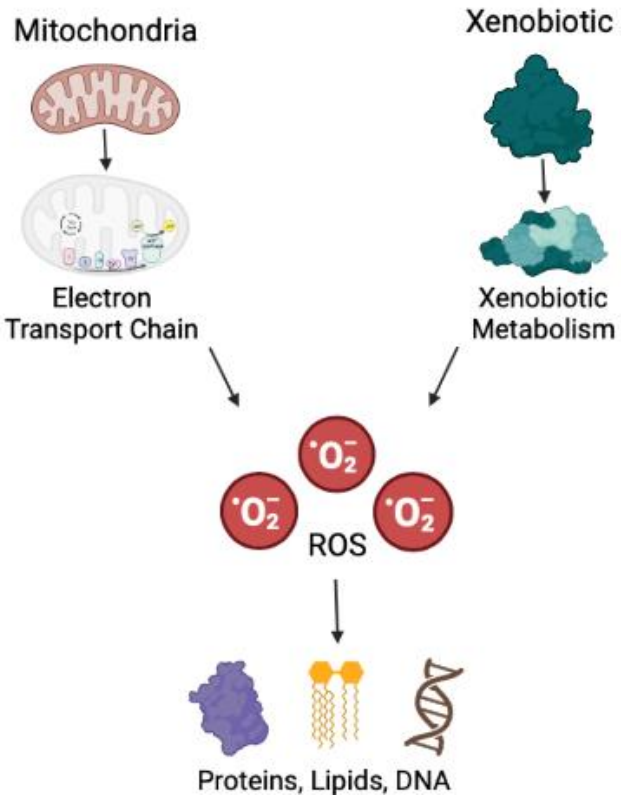

Figure 1.2: Exogenous and Endogenous Sources of ROS

ROS can be generated in the cell by both exogenous and endogenous sources. The main endogenous source includes the mitochondria. Electrons can leak out of the ETC and interact with oxygen molecules which causes them to become reduced and transformed into the superoxide anion. A main exogenous source of ROS includes xenobiotics. Once in the cell, xenobiotic metabolism must occur for the export of the foreign chemical. This biotransformation results in the generation of ROS. Subsequent high levels of ROS in the cell can be detrimental as they can go on to damage proteins, lipids, and DNA.

ROS levels can cause to the cell. Therefore, it is crucial for the cell to contain detoxification enzymes that can help combat these high ROS levels and prevent cellular destruction.

There are three different phases of detoxification enzymes that play a role in balancing ROS (Figure 1.3). Phase I enzymes solubilize targets by oxygen molecule transfer (Xu et al., 2005). Phase II enzymes catalyze the conjugation of the targets to neutralize their reactivities, and phase III consists of transporters that are responsible for pumping out the targets resulting in official detoxication (Xu et al., 2005). In *C. elegans*, an important class of phase II detoxification enzymes includes the Glutathione S-Transferases (GSTs). When the cell is under oxidative stress due to a toxic environment for example, the *gst* detoxification genes become activated to fight the stress and balance the ROS. In a study conducted by Hasegawa et al. 2010, *C. elegans* were seen to prominently upregulate *gst-4* levels when exposed to acrylamide and paraquat (oxidative stress-inducing reagents). The *gst-4* expression levels correlated with the oxidative stress tolerance in a dose-dependent manner (Hasegawa et al., 2010). The specific way in which GST-4 reduces ROS is by conjugating a reduced form of glutathione to ROS and subsequently removing ROS reactivities. The abundance of glutathione in the cell is ultimately what enables the detoxification system. This is because by adding glutathione to ROS this makes the compound more polar and the cell can more easily dispose of it. Therefore, GST-4 is needed for the cell to protect itself against toxic environments that may upregulate ROS.

Another class of genes involved in the oxidative stress response includes the Superoxide Dismutase (SODs) which are known as phase I detoxification genes. SODs function to attenuate oxidative stress by converting superoxide into oxygen and hydrogen peroxide which ultimately reduces ROS levels in the cell (Azadmanesh & Borgstahl, 2018). These different phases of

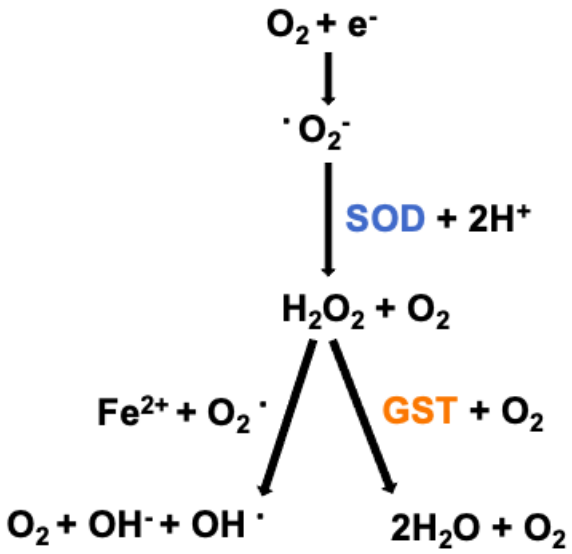

Figure 1.3: The Formation and Detoxification of ROS

ROS molecules can form in the cell when an oxygen molecule becomes reduced (with the addition of an electron). When this occurs, the superoxide anion ($\cdot O_2^-$) forms which is a type of reactive oxygen species. Phase I detoxification enzymes will act on the ROS first, such as superoxide dismutase (SODs), by solubilizing the target with oxygen molecule transfer. SODs can transform $\cdot O_2^-$ into oxygen (O_2) and hydrogen peroxide (H_2O_2) through the addition of hydrogen molecules. Following this, phase II detoxification enzymes, such as glutathione-S-transferase (GSTs), will act on the H_2O_2. GSTs will catalyze the conjugation of glutathione to the target to neutralize it and to therefore form water (H_2O) and oxygen molecules. If phase II enzymes do not act on the H_2O_2 created from phase I, then iron (Fe^{2+}) will be able to react with it instead and this will produce more forms of ROS (OH^-, $OH^{\cdot}$) along with O_2.

detoxification enzymes are integral to the cell's health and stability, as without them present, the cell would not be able to save itself and repair the disturbances caused by ROS.

1.2.2 Aging and Longevity in *C. elegans*

The biological process of aging is quite complex as many different factors contribute to the timely progression. Simply put, aging results from the accumulation of damage within cells, compromising cell function and ultimately leading to cell death. Unfortunately, ROS and oxidative stress can be large contributors to aging and shortened lifespan due to the damage it can cause to the cell. The free radical theory of aging states that organisms age because cells accumulate free radical damage over time; essentially, the accumulation of ROS over an organism's lifetime and how it deals with this damage determines its lifespan (Wickens, 2001). Examining this theory of aging with *C. elegans* has provided bountiful valuable information on finding disease genes that play a role in the aging process, as well as on establishing that aging was indeed something that could be studied genetically.

There are many advantages that come with using *C. elegans* as a model organism to study aging such as their genetic tractability, short lifespan, and age-dependant physiological changes (Son et al., 2019). For example, aged *C. elegans* display a decline in their anatomical and functional features such as tissue integrity, motility, learning, memory and immunity (Son et al., 2019). They also exhibit many age-associated changes in the expression of microRNAs and stress-responsive genes. Due to this, there are abundant molecular tools available to use on *C. elegans* such as transgenic lines, gene knockouts and RNAi knockdowns. Due to their simplicity, *C. elegans* remain to be a recommended model for studies on signal mapping mechanisms involved in the aging process.

Mutations in the *age-1* gene specifically were found in the first forward-genetic screen and this mutation resulted in a significant increase in lifespan in *C. elegans* (Klass, 1983). With further mutation mapping, studies have shown that single gene mutations can have dramatic effects on an organism's lifespan; this heavily sparked an enormous trend in studying aging with *C. elegans* specifically. One of the most significant finds involved the realization of the importance of the insulin/IGF-1 signalling (IIS) pathway in regulating lifespan. Studying this pathway in *C. elegans* has played a large role in determining which genes affect lifespan and longevity (Longo et al., 2015). Overall, the dissection of this pathway, as well as others that play a role in longevity, are bringing us closer and closer to understanding the molecular mechanisms responsible for the complex phenomenon of aging.

1.3 Cellular Signalling Pathways Involved in the *C. elegans* Oxidative Stress Response

The cell must take on many intricate and complicated tasks, usually at the same time, to carry out all the functions necessary for growth and survival. A large player that aids in multiple cellular functions are known as transcription factors (TFs). TFs are proteins that contain domains that bind to promoter or enhancer regions of DNA and modulate the rate of transcription of a specific gene by either promoting or suppressing transcription (Lickwar et al., 2012). This consequently regulates the amount of mRNA produced by the gene and therefore the amount of protein created in the cell. Many TFs are common to several different types of cells, while others can be cell specific. TFs ultimately work to allow proper functioning of the organism in areas such as development, inflammatory responses, energy metabolism, cellular differentiation and much more. Due to the important roles that TFs play, any mutations could be detrimental to cell and overall organismal health. For example, TF mutations have been known to contribute to

many different diseases such as cancer, autoimmunity, neurological disorders and diabetes (Lee & Young, 2013).

Due to how impactful mutations in TFs can be, it is no surprise that they are tightly regulated and controlled in the cell through cellular signalling pathways. Signalling pathways can be rather complex and can be activated through either extrinsic or intrinsic factors. These signalling pathways are ultimately what activate or inhibit TFs to subsequently control gene expression. Many of the MAP kinase (MAPK) and IIS pathways are involved in signalling cascades that regulate TFs. These specific pathways have been shown to play roles in oxidative stress, aging, and lifespan (Gami & Wolkow, 2006). Here, I discuss the major pathways in *C. elegans* that are important to this thesis which affect two key regulators known as SKN-1 and DAF-16.

1.3.1 The Insulin/Insulin-like Signalling (IIS) Pathway

One of the most well-known cellular signalling pathways involved in aging/longevity includes the insulin/insulin-like signalling (IIS) pathway. In *C. elegans* specifically, this pathway plays a role in multiple different areas such as metabolism, growth, development, and behaviour. The way in which this pathway works starts with insulin-like peptides (ILPs) that bind to and activate an insulin receptor at the cell membrane known as DAF-2 (IGF-1 ortholog) through auto-phosphorylation. With DAF-2 activation, this recruits and activates the p110 catalytic subunit of the phosphoinositide 3 kinase (AGE-1/PI3K). AGE-1 then goes on to catalyze the conversion of PIP_2 into PIP_3 (Weinkove et al., 2006). The subsequent elevated levels of PIP_3 results in the activation of the serine/threonine kinase known as PDK-1 which in turn phosphorylates AKT-1/2 (Paradis & Ruvkun, 1998). The phosphorylation of DAF-16/FOXO by AKT-1/2 causes its interaction with 14-3-3 proteins known as PAR-5 and FTT-2 which are

responsible for the resulting subcellular localization of DAF-16 (Paradis & Ruvkun, 1998). It is also important to note that the DAF-18/PTEN lipid phosphatase and the serine/threonine phosphatase PPTR-1/PP2A counteract AGE-1/PI3K and AKT-1 signalling respectively (Solari et al., 2005).

Under standard conditions when IIS is active, since the pathway negatively regulates DAF-16, it stays sequestered in the cytoplasm and is unable to translocate into the nucleus to activate stress resistance genes. However, mutations in either *daf-2* or *age-1* have been seen to cause longer life span in *C. elegans* compared to wildtype involving an increase in stress resistance (Kenyon et al., 1993). This is due to a dependence on DAF-16 since AKT-1/2 phosphorylation would decrease and DAF-16 would therefore be free to translocate into the nucleus and activate its target genes. We see an increase in longevity as well when the IIS pathway is not activated, and DAF-16 translocates into the nucleus.

In addition to inhibiting DAF-16, the IIS pathway also inhibits another important transcription factor that plays a role in activating stress response genes, known as SKN-1. AKT-1/2 can phosphorylate SKN-1, as it does to DAF-16, to keep it sequestered in the cytoplasm (Tullet et al., 2008) (Figure 1.4). Therefore, under reduced IIS signalling and increased oxidative stress, this leads to the nuclear localization of SKN-1 to transcriptionally activate important detoxification genes. Hence, it is clear to see that the IIS pathway plays a large role in the determination of the activation of important genes needed for the oxidative stress response.

1.3.2 The MAPK Pathways

Mitogen-activated protein kinase (MAPK) signalling pathways are known as pathways that integrate extracellular signals to internal cellular responses. MAPKs can be activated by various stimuli such as growth factors, cytokines, stress signals or neurotransmitters to ultimately

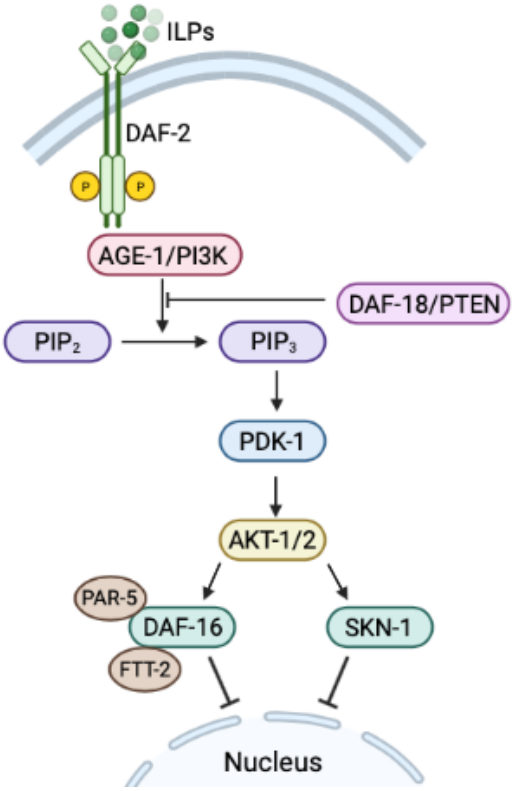

Figure 1.4: The IIS Pathway

Insulin-like peptides (ILPs) bind to the DAF-2 transmembrane receptor which results in its activation by phosphorylation. Once active, DAF-2 recruits and activates the phosphoinositide 3 kinase (AGE-1/PI3K). AGE-1 then goes on to catalyze the conversion of PIP_2 into PIP_3. The subsequent elevated levels of PIP_3 results in the activation of the serine/threonine kinase known as PDK-1 which in turn phosphorylates AKT-1/2. The phosphorylation of DAF-16 by AKT-1/2 causes its interaction with 14-3-3 proteins known as PAR-5 and FTT-2 which keep DAF-16 sequestered in the cytoplasm. AKT-1/2 can also phosphorylate SKN-1 to keep it in the cytoplasm and prevent its nuclear translocation. DAF-18/PTEN lipid phosphatase can antagonize AGE-1/PI3K to prevent subsequent activation events. Figure adapted and modified from Sun et al., 2017.

allow for adaptation to environmental changes or stressful conditions. There are three main MAPK signalling cascades which include: the extracellular signal-regulated kinase (ERK), the c-JUN N-terminal kinase (JNK), and the p38 MAPK (Zhang & Liu, 2002). Each of these pathways are essential for the cell to carry out normal biological processes.

Once an initial extracellular signal is relayed, it gets integrated by the MAPK pathway through the activation of no less than three enzymes in a series: a MAPK kinase kinase (MAPKKK), a MAPK kinase (MAPKK), and a MAP Kinase (MAPK). This ultimately elicits a physiological response such as proliferation, differentiation, development, inflammatory responses or apoptosis (Zhang & Liu, 2002).

The ERK/MAPK Pathway:

The ERK pathway, also known as the Raf-MEK-ERK pathway is known to be one of the best characterized MAPK signalling pathways. This pathway can be involved in multiple different cellular processes such as proliferation, differentiation, apoptosis, and others. When this pathway is activated, an external growth factor (EGF) will bind to a receptor tyrosine kinase (RTK) which will then dimerize and auto phosphorylate (Lemmon & Schlessinger, 2010). Adaptor proteins are then able to bind to the phosphorylated tyrosine residues which in turn recruit the guanine exchange factor (GEF) that activates the small GTPase RAS. Once RAS is activated, it will bind LIN-45 (*C. elegans* ortholog of RAF1) (Karnoub & Weinberg, 2008). Through the aid of scaffold protein KSR, LIN-45 becomes activated and can subsequently phosphorylate and activate MEK-2 (*C. elegans* ortholog of MEK 1/2) (Udell et al., 2011). MEK-2 then phosphorylates and activates MPK-1 (*C. elegans* ortholog of ERK 1/2), which is then able to enter the nucleus and activate transcription factors to promote gene expression (Yoon &

Seger, 2006). Therefore, in this pathway LIN-45 acts as the MAPKKK, MEK-2 acts as the MAPKK, and MPK-1 acts as the MAPK.

One of the main transcription factors that MPK-1 can phosphorylate and activate includes SKN-1. In this way, the ERK/MAPK-mediated signalling pathway promotes longevity as the direct phosphorylation of SKN-1 results in its translocation into the nucleus (Okuyama et al., 2010). Once in the nucleus, SKN-1 is able to transcriptionally activate phase II detoxification genes needed for the oxidative stress response.

The c-Jun N-terminal Kinase (JNK) Pathway:

The JNK pathway is another subgroup of the MAPK superfamily, which can be activated by cytokines but also serves as a molecular sensor for stresses such as ROS and DNA damage (Davis, 2000). This pathway is very important as it has been seen to play roles in multiple biological processes such as development, survival, apoptosis, and cancer. ROS levels that cause oxidative stress can activate JKK-1 (*C. elegans* JNKK ortholog) which in turn activates JNK-1 (*C. elegans* JNK ortholog). Once JNK-1 is activated by phosphorylation, it is able to directly phosphorylate DAF-16 to promote its activation and nuclear translocation (Oh et al., 2005). DAF-16 can subsequently transcriptionally activate important detoxification genes needed for the oxidative stress response and lifespan extension.

In order to fully understand the importance that the JNK pathway holds for *C. elegans,* a study showed that loss-of-function mutations in *jnk-1* and *jkk-1* lead to a significant decrease in lifespan suggesting that this pathway positively regulates longevity (Oh et al., 2005). Studies also found that overexpression of JNK-1 lead to high stress resistance to oxidative stress and resulted in a large amount of DAF-16 nuclear translocation (Oh et al., 2005). It is also important to note that the JNK pathway acts in parallel to the IIS pathway to regulate lifespan by both converging

onto DAF-16 (Oh et al., 2005). Ultimately, JNK signalling antagonizes the IIS pathway as it directly phosphorylates DAF-16 to promote its nuclear translocation while the IIS pathway phosphorylates DAF-16 to keep it sequestered in the cytoplasm.

The p38 MAPK Pathway:

Another known MAPK pathway includes the p38 pathway which plays an important role in adaptation, homeostasis, and stress responses. This pathway becomes activated in response to a variety of different stressors and cytokines. This specifically includes oxidative stress inducing compounds such as arsenite, paraquat and *tert*-Butyl hydroperoxide (Inoue et al., 2005). In this pathway, NYS-1 can phosphorylate and activate SEK-1 which phosphorylates and activates PMK-1 (Inoue et al., 2005). PMK-1 then goes on to phosphorylate SKN-1 specifically at its Ser-74 and Ser-340 residues (Inoue et al., 2005). These phosphorylation events lead to the activation and nuclear translocation of SKN-1 where it can activate detoxification genes needed for the oxidative stress response (Inoue et al., 2005). Therefore, in this signal cascade, NYS-1 acts as the MAPKKK, and SEK-1 acts as the MAPKK, and PMK-1 acts as the MAPK. Each of these pathways play an important role in the activation of both DAF-16 and SKN-1 transcription factors in terms of their activation and subsequent roles in increasing transcriptional levels of phase I and II detoxification genes (Figure 1.5).

1.4 The Role of SKN-1 in the Oxidative Stress Response

The SKN-1 transcription factor remains to be one of the master regulators in *C. elegans* as it performs a wide range of developmental and protective functions. SKN-1 is the ortholog of the mammalian Nrf2 transcription factor as they regulate many of the same gene families. Therefore, studies carried out on SKN-1 hold considerable predictive value into understanding

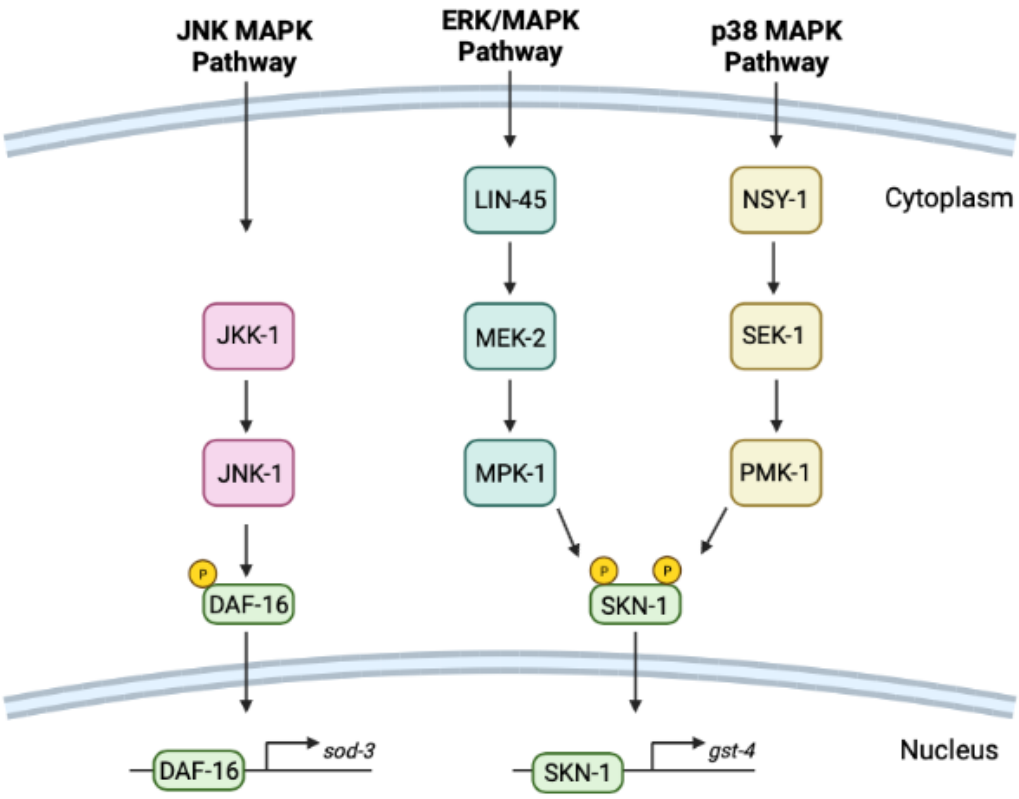

Figure 1.5: The JNK, ERK, and p38 MAP Kinase Pathways Regulate SKN-1 and DAF-16 in the *C. elegans* Oxidative Stress Response

Multiple MAPK pathways play an important role in the *C. elegans* oxidative stress response due to their role in activating both DAF-16 and SKN-1. The JNK MAPK pathway can phosphorylate and activate DAF-16 to allow its translocation into the nucleus. Once in the nucleus, DAF-16 can transcriptionally activate phase I detoxification genes such as *sod-3.* The ERK and p38 MAPK pathways can phosphorylate and activate SKN-1 to allow its translocation into the nucleus. Once in the nucleus, SKN-1 can transcriptionally activate phase II detoxification genes such as *gst-4.* Respective components of the individual MAPK pathways adapted from Blackwell et al., 2015, Inoue et al., 2005, Oh et al., 2005, and Okuyama et al., 2010.

how mammalian Nrf proteins function. Like SKN-1, Nrf2 is known to regulate cellular defenses against toxic and oxidative threats through the activation of genes involved in the oxidative stress response (He et al., 2020). It is encoded by the gene nuclear factor, erythroid 2 like 2 (NFE2L2) and belongs to the Cap'n'Collar (CNC) subfamily of the basic leucine zipper (bZIP) transcription factors comprised of nuclear factor erythroid-derived 2 (NFE2), Nrf1, Nrf2, and Nrf3 (He et al., 2020). Nrf2 is comprised of multiple conserved NRF2-ECH homology (Neh) domains that each carry out different functions needed for Nrf2 transcriptional activity. For example, the bZIP in the Neh1 domain heterodimerizes with small musculoaponeurotic fibrosarcoma proteins (sMAF) as well as other bZIP proteins to recognize antioxidant response elements (ARE) for activation of gene transcription (He et al., 2020). This is essentially what will happen when the cell is under oxidative stress; Nrf2 will translocate into the nucleus and bind to AREs to activate detoxification genes. The Neh2 domain contains motifs that specifically interact with the Kelch domain of Kelch-like-ECH-associated protein 1 (KEAP1) which mediates Nrf2 ubiquitination and degradation (He et al., 2020). This will occur under non-stressful conditions when Nrf2 is not needed in the nucleus to activate detoxification genes.

Although SKN-1 shares remarkable similarities with Nrf2 in terms of function, it has diverged considerably in terms of structure and DNA binding. For example, SKN-1 lacks the ZIP dimerization module and is instead built around a version of the CNC domain that allows it to form a stable helical structure to recognize DNA bases in the minor groove (Blackwell et al., 1994). However, Nrf2 and SKN-1 share a highly conserved 14-residue motif called DIDLID (Figure 1.6). This region in SKN-1 is critical for transcriptional activation and interaction with WDR-23 which targets SKN-1 for proteasomal degradation (Walker et al., 2000).

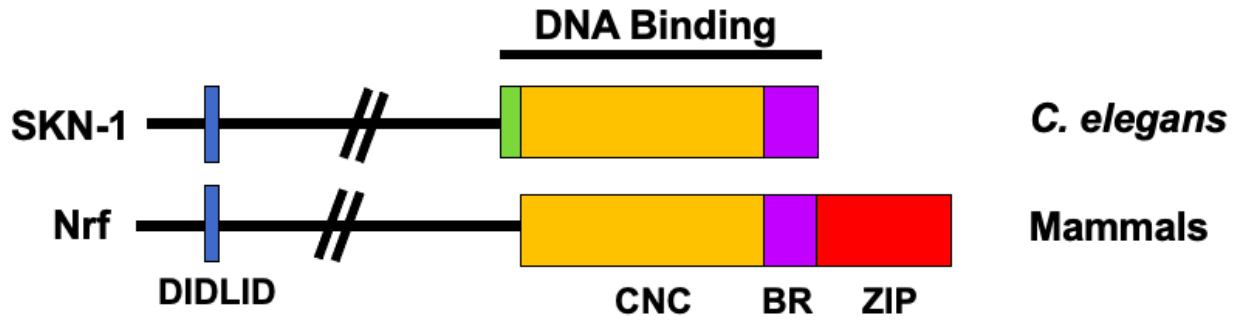

Figure 1.6: SKN-1 is the *C. elegans* Ortholog of the Highly Conserved Mammalian Nrf/CNC Proteins

SKN-1 found in *C. elegans* and Nrf found in mammals share many similarities in terms of their function, however their structures consist of some differences. SKN-1 and Nrf both contain the DIDLID and DNA-binding regions. However, SKN-1 lacks the ZIP domain (red) and instead directly interacts with DNA sequences through the BR (purple) and short element (green) domains in the minor groove. (CNC: conserved Cap'n'Collar domain in orange). Figure adapted from Blackwell et al., 2015.

There are three different protein isoforms of SKN-1 found in *C. elegans* known as SKN-1A, SKN-1B and SKN-1C. SKN-1A is expressed in all tissues, while SKN-1B is expressed in neurons and SKN-1C is expressed in the intestines (Blackwell et al., 2015). Therefore, upon exposure to oxidative stress, the SKN-1C isoform accumulates in the nucleus of cells in the intestine (Blackwell et al., 2015). Overall, SKN-1 remains to hold great importance into our understanding of Nrf2 and the influence it has on mammalian aging and longevity.

1.4.1 SKN-1 Function and Activation

One of the most important functions of SKN-1 is its role in the oxidative stress response as it regulates phase II (PII) detoxification genes. SKN-1 is normally held inactive in the cytoplasm but can become activated and translocate into the nucleus when the cell is under oxidative stress (An & Blackwell, 2003). Depending on the level of ROS present in the cell, this will determine how SKN-1 will be regulated. However, this process is not simple as SKN-1 can be regulated by multiple different pathways. Therefore, it is important to understand how these pathways work in order to provide further insight into the specific factors that may influence disease states overall.

SKN-1 activation can be achieved through the ERK/MAPK pathway as well as the p38/MAPK pathway as they serve as positive regulators of SKN-1. When the ERK/MAPK pathway becomes activated, MEK-2 becomes activated which in turn phosphorylates MPK-1. MPK-1 is then able to phosphorylate SKN-1 to promote its activation (Okuyama et al., 2010). Also, when the p38/MAPK pathway becomes activated, this results in PMK-1 activation which then goes on to phosphorylate SKN-1 specifically at its Ser-74 and Ser-340 residues (Inoue et al., 2005). These phosphorylation events lead to the activation and nuclear translocation of SKN-1 however, some signalling pathways can lead to its inhibition instead (Figure 1.7). For example,

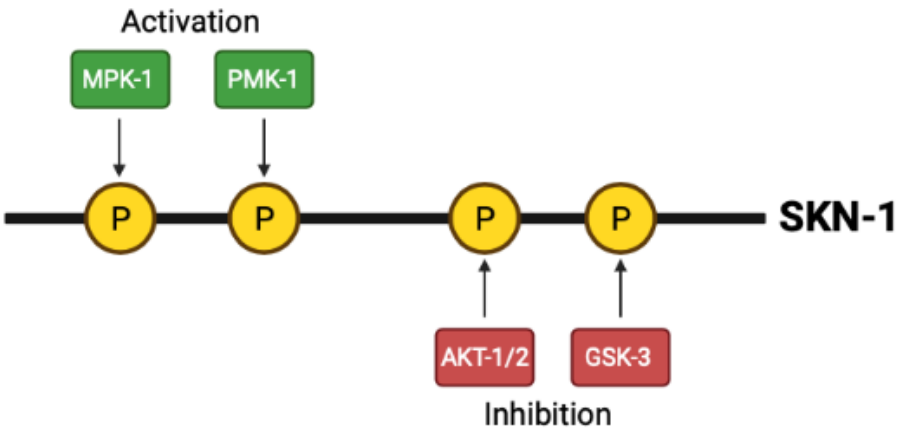

Figure 1.7: SKN-1 Activation and Inhibition Phosphorylation Events

SKN-1 can get phosphorylated to become activated, allowing its translocation into the nucleus, or phosphorylated to become inhibited which results in its sequestration in the cytoplasm. Phosphorylation by MPK-1 from the ERK/MAPK pathway or PMK-1 from the p38/MAPK pathway results in SKN-1 activation. However, phosphorylation by AKT-1/2 from the IIS pathway, or GSK-3 results in SKN-1 inhibition. Figure adapted and modified from Blackwell et al., 2015.

the IIS pathway serves as a main negative regulator of SKN-1. When this pathway becomes activated, AKT-1/2 phosphorylates SKN-1 to inhibit it and keep it sequestered in the cytoplasm (Blackwell et al., 2015). In addition to this, GSK-3, which also plays a large role in WNT signalling, has been seen to be a negative regulator of SKN-1. GSK-3 can phosphorylate SKN-1 to inhibit it and therefore prevent its translocation into the nucleus to activate detoxification genes (An et al., 2005). SKN-1 contains specific GSK-3 phosphorylation sites which are seen to be conserved in mammalian Nrf proteins indicating the possibility that GSK-3 phosphorylation may also be involved in Nrf protein regulation (An et al., 2005).

Another main repressor of SKN-1 involves the WD40 repeat protein known as WDR-23. WDR-23 is a direct repressor of SKN-1 as it is a ubiquitin ligase adaptor protein that will form a complex with CUL-4 and DDB-1 and bind to SKN-1 to trigger ubiquitylation and subsequent protein degradation (Choe et al., 2009). SKN-1 can be targeted by different ubiquitin ligases that function in different areas of the cell, however this specific proteasomal degradation occurs in the nucleus. When the cell is under oxidative stress, SKN-1 will be released from WDR-23 repression, and it will be able to subsequently accumulate in the nucleus to activate specific detoxification genes such as *gst-4* and *gcs-1*. These detoxification enzymes are then subsequently able to act in the stress response and decrease the amount of ROS in the cell. It has been observed that loss of function mutations of *wdr-23* leads to the activation of *gst-4* and upregulation of *gcs-1* which ultimately promotes longevity and stress resistance (Hasegawa & Miwa, 2010). It is clear to see the strong effect WDR-23 has on SKN-1 and the importance of its regulation on SKN-1-mediated activation of detoxification genes. However, sometimes the way in which transcription factors are regulated are not as directly understood or laid out. This is why it is important to keep in mind that transcription factors can also be regulated indirectly.

1.5 BRAP2 as a Cytoplasmic Retention Protein

When the cell is under a high yet manageable amount of oxidative stress, it will activate pathways that involve detoxification enzymes that may induce cell cycle arrest to ensure cell survival. BRAP2 and BRCA1 in mammalian cells include two important cytoplasmic proteins that are involved in regulating these pathways. For example, BRCA1 is involved in many different cell functions such as regulating cell cycle progression, responding to DNA damage, and preventing cancer development (Somasundaram et al., 1997; Thompson et al., 2002). More specifically, BRCA1 translocates into the nucleus during oxidative stress-inducing conditions and activates a cyclin kinase inhibitor to promote cell cycle arrest. However, when oxidative stress is minimal, BRCA1 does not need to induce cell cycle arrest. Therefore, during these specific conditions, the BRAP2 cytoplasmic retention protein will bind to the nuclear localization signal (NLS) of BRCA1 and prevent its translocation into the nucleus (Li et al., 1998).

1.5.1 The Role of BRAP-2 in the Oxidative Stress Response

BRAP2 has also been seen to serve as a negative regulator of the RAS/MAPK pathway. Part of the RAS/MAPK signalling cascade includes the KSR scaffold protein which couples Raf to its substrate MEK (Matheny et al., 2004). However, when this pathway is not activated, BRAP2 can inhibit KSR which ultimately uncouples Raf from MEK and affects subsequent downstream cellular responses (Matheny et al., 2004). When RAS becomes activated however, this causes activation of BRAP2 to become ubiquitinated and auto degraded by its ubiquitin ligase activity which will ultimately release its inhibition on KSR (Matheny et al., 2004). This will allow for Raf and MEK coupling, and the signalling cascade will proceed to downstream events (Figure 1.8).

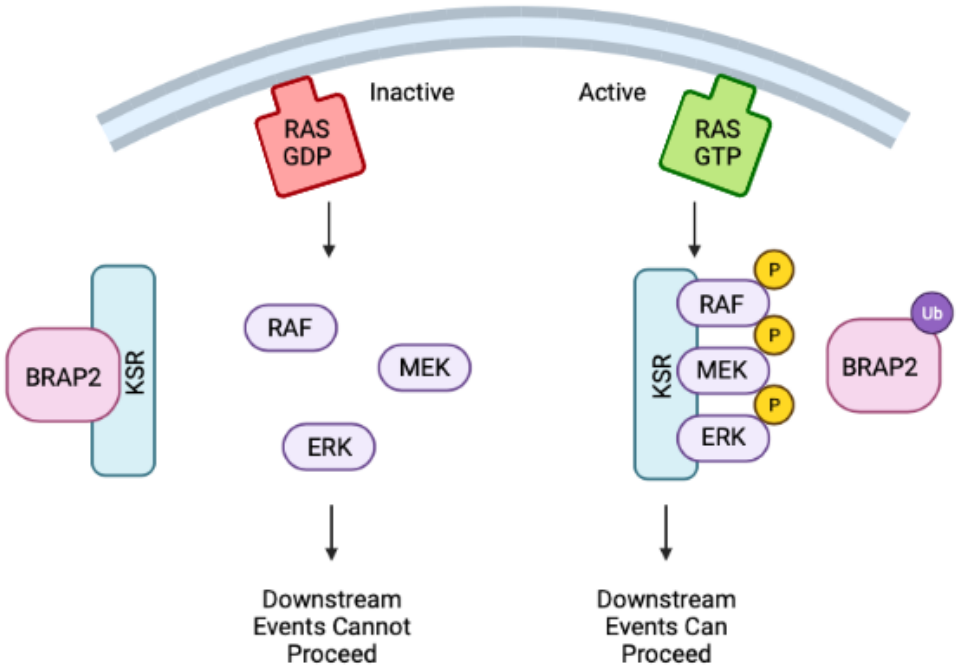

Figure 1.8: BRAP2 Acts as a Cytoplasmic Retention Protein in the RAS/MAPK Pathway

BRAP2 serves as a negative regulator of the RAS/MAPK pathway through sequestration of the KSR scaffold protein. KSR plays a crucial role in the RAS pathway, as it brings RAF, MEK and ERK together to allow the signalling cascade to occur. However, when RAS is inactive, BRAP2 can retain KSR and bring it away from its targets therefore preventing the signal transduction from proceeding. When RAS turns into its active state, BRAP2 will instead become ubiquitinated and the KSR scaffold protein will be free to bring RAF, MEK and ERK together therefore allowing downstream events to proceed. Respective components of RAS pathway adapted from Matheny et al., 2004.

In *C. elegans*, the BRAP2 ortholog known as BRAP-2 has been hypothesized to play a major role in regulating the nuclear localization of SKN-1 through the p38/MAPK pathway, rendering worms highly sensitive to oxidative stress (Hu et al., 2017). Specifically, BRAP-2 may indirectly render SKN-1 in the cytoplasm and prevent its nuclear translocation which negatively regulates expression levels of phase II detoxification enzymes (Hu et al., 2017). *brap-2* mutant worms (deleted Zinc-Finger Ubiquitin Binding Domain and leucine heptad repeats) have been seen to show elevated expression levels of SKN-1 dependent PII detoxification enzymes that specifically fall under the regulation of PMK-1 from the p38/MAPK pathway. With *brap-2* mutated, a 1.4-fold increase in phosphorylated PMK-1 levels were seen and measured through Western blot analysis which gave indication of an increase in activated PMK-1 levels (Hu et al., 2017). This gives further indication that in the absence of BRAP-2, PMK-1 would be free to phosphorylate SKN-1 and allow its translocation into the nucleus for subsequent activation of PII detoxification genes. Whether this inhibition is due to a direct interaction between BRAP-2 and PMK-1, or an indirect mechanism of activation remains to be unclear. Regardless, this information presents great insight into the affect BRAP-2 may have on the oxidative stress response.

Although SKN-1 remains to be a prominent and important regulator of detoxification genes needed for the stress response, it is important to consider that SKN-1 likely does not work alone in completing this task. Therefore, our lab previously conducted an RNAi screen on *brap-2(ok1492)* deletion mutants (which showed an increase in *gst-4*) to find other transcription factors that may play a role in also influencing expression levels. It was observed that RNAi of *fkh-9* caused a decrease in expression levels of *gst-4* compared to *brap-2(ok1492)* mutants

without this knockdown. This ultimately suggested a role that FKH-9 may play in the cell's oxidative stress response, potentially through interaction with SKN-1.

1.6 The Role of DAF-16 in the Oxidative Stress Response

Another master regulator of the *C. elegans* oxidative stress response includes the DAF-16 transcription factor. The mammalian ortholog of DAF-16 includes the FOXO transcription factor family which belongs to the class O of the Forkhead transcription factors (Zečić & Braeckman, 2020). These transcription factors are characterized based on their unique winged helix Forkhead box DNA-binding domain (Kaestner et al., 2000). In mammals specifically, there are four FOXO genes known as FOXO1, FOXO3, FOXO4 and FOXO6 (Albert et al., 1981). *C. elegans* however, only possess one FOXO gene known as *daf-16* which was named off the initial finding of the isolated dauer defective phenotype when mutated. *daf-16* encodes eight different transcripts from *daf-16a* to *daf-16h,* with *daf-16a* and *daf-16d/f/h* being the major isoforms involved in dauer arrest and aging (Riddle et al., 1981).

Both FOXO and DAF-16 share a lot of similarities in their function, pathways, and DNA binding domain sequences. For example, they both play important roles in aging, development, longevity, nutrient deprivation, and oxidative stress. They are also both regulated by specific pathways involved in aging and longevity such as AMPK, JNK, mTOR and IIS. Both of their Forkhead binding domains also share highly similar sequences. For example, DAF-16A contains the same RxRxxS/T phosphorylation motif with three FOXOs (Kwon et al., 2010). The *C. elegans* DAF-16 also contains a DNA binding domain that recognizes TTGTTTAC known as the DAF-16 Binding Element (DBE) (Murphy et al., 2003). This is a core consensus sequence found at numerous phase I (PI) genes, therefore being a key regulator in the oxidative stress response.

1.6.1 DAF-16 Function and Activation

Since DAF-16 is responsible for activating genes involved in aging, longevity, and oxidative stress, it can be regulated by multiple different cellular signalling pathways. Certain pathways in the cell negatively regulate DAF-16, hindering it inactive in the cytoplasm. However, others can positively regulate it therefore activating DAF-16 and allowing its translocation into the nucleus to transcriptionally activate specific PI genes.

In terms of DAF-16 inhibition, the IIS pathway is the main pathway that can keep DAF-16 sequestered in the cytoplasm. When ILPS bind and activate DAF-2, DAF-16 will become phosphorylated by AKT-1/2 to antagonize it and negatively regulate longevity (Paradis & Ruvkun, 1998). Due to this, mutations in this pathway such as in *daf-2* or any signal transducers within the pathway such as *akt-1/2* have portrayed long-lived phenotypes compared to WT. Another pathway involved with DAF-16 inhibition includes target of rapamycin (TOR). If *C. elegans* exhibit caloric or dietary restriction, this pathway will become inactivated to promote activation of DAF-16 and subsequent lifespan extension (Robida-Stubbs et al., 2012). In this pathway, the TORC1 complex can negatively regulate DAF-16, as the inhibition of TORC1 results in increased transcription of *daf-16* and nuclear translocation of DAF-16 (Robida-Stubbs et al., 2012).

In terms of DAF-16 activation, the AMP-Activated Protein Kinase (AMPK) pathway is an energy-sensing pathway that positively regulates DAF-16. AMPK was seen to directly phosphorylate DAF-16 to promote its nuclear translocation (Greer et al., 2007). In-turn, DAF-16 has been seen to be a direct transcriptional activator of *aakg-4,* which encodes the regulatory subunit of AMPK (Greer et al., 2007). This suggests a positive feedback loop that further activates DAF-16 and its target genes. This has been additionally supported through upregulation

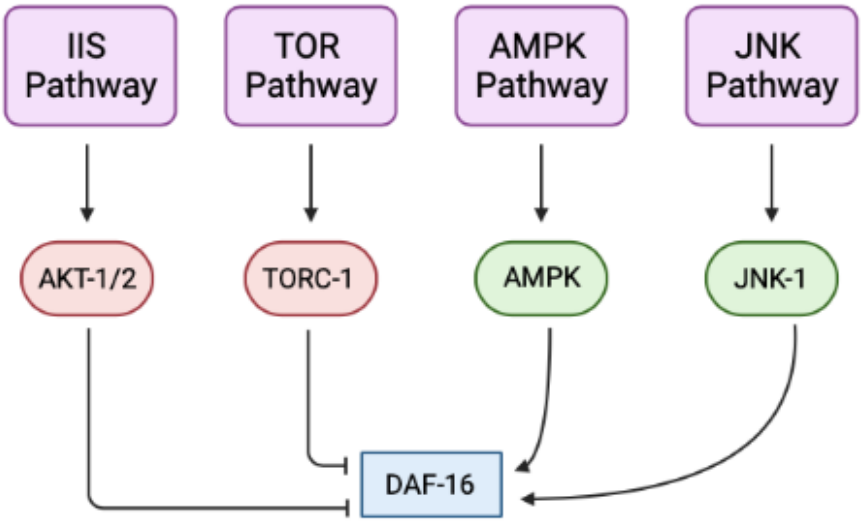

Figure 1.9: The Regulation of DAF-16

DAF-16 is an important transcription factor that functions in the *C. elegans* oxidative stress response. Due to this, DAF-16 can be regulated by multiple different pathways that will either inhibit it to keep it sequestered in the cytoplasm or activate it to allow its translocation into the nucleus. For example, AKT-1/2 from the IIS pathway and TORC-1 from the TOR pathway will inhibit DAF-16. However, AMPK from the AMPK pathway and JNK-1 from the JNK pathway will activate DAF-16. Respective components of individual pathways adapted from Sun et al., 2017.

of *aakg-4* in *daf-2* mutants and lifespan shortening of *daf-2* due to *aakg-4* RNAi or mutation (Greer et al., 2007). When the cell is under oxidative stress, DAF-16 can also be activated by the JNK pathway. ROS can activate the JNK pathway which causes activation of JNK-1 and this goes on to phosphorylate DAF-16 and promote its translocation into the nucleus (Oh et al., 2005). Overexpression of JNK/increased JNK activity showed lifespan extension through increased DAF-16 phosphorylation (Oh et al., 2005) (Figure 1.9).

Once in the nucleus, DAF-16 acts as a transcriptional activator of genes that promote stress resistance and prolong lifespan. For example, when DAF-16 responds to stressors it can activate genes such as *sod-3, dod-3,* and *mtl-1* (Senchuk et al., 2018). SOD-3 in particular, is an important PI detoxification enzyme that heavily functions in the act of reducing ROS levels in the cell. Overall, it is clear to see the crucial regulatory functions DAF-16 possesses in terms of aging and longevity through the activation of detoxification genes.

1.7 Current Understanding of Transcription Factor FKH-9

When our lab previously conducted the RNAi screen on *brap-2(ok1492)* mutants, we aimed to also identify specific transcription factors involved in the *C. elegans* oxidative stress response. RNAi of *fkh-9* resulted in a decrease of *gst-4* expression levels which indicated a potential role that FKH-9 may play in the oxidative stress response. Due to this, the FKH-9 transcription factor was selected to be examined in further detail.

The FKH-9 transcription factor in *C. elegans* corresponds to the Forkhead box (FOX) transcription factor family in mammals. The *forkhead (fkh)* gene was originally discovered in a random mutagenesis screen performed in *Drosophila melanogaster* (Weigel et al., 1989). This initial study showed that *fkh* is required for normal gut development, and that its absence results in a ‘fork head’ appearance as the foregut transforms into a head structure. Following this

finding, multiple different FOX genes were identified in organisms ranging from yeast to humans. All FOX proteins share a winged-helix DNA binding domain termed the 'forkhead box.' However, FOX proteins still differ in features and functions. For example, different FOX genes regulate different biological processes such as: regulation of gastrulation, stem cell maintenance, regulation of metabolism and cell cycle control, the differentiation and proper functioning of tissues, and DNA repair and aging (Hannenhalli & Kaestner, 2009). Humans contain 44 FOX genes, while *C. elegans* have 11 (Golson & Kaestner, 2016). The FOX gene family has been subcategorized into four groups based on their functions: FOXA, FOXM1, FOXP and FOXO (Golson & Kaestner, 2016). The FOXO group is known to play a role in regulating metabolism and longevity. DAF-16 remains to be the sole FOXO ortholog in *C. elegans.* Mutations in FOX genes are associated with human disease, which is why animal models continue to be used to study the function of these transcription factors.

In literature, the biological role of FKH-9 in *C. elegans* is scarce as not much is known about this specific protein or its functions, especially in terms of the oxidative stress response. However, a few recent studies within the past 5 years have examined FKH-9 in some detail and its potential roles have been discovered.

1.7.1 The Role of FKH-9 in Axon Regeneration

Kaletsky et al., (2016) examined the role of FKH-9 in mechanosensory neurons of *C. elegans* and discovered that it is required for axon regeneration, short-term associative memory, and lifespan. More specifically, a direct link was observed between FKH-9 and DAF-2/DAF-16. The authors identified mechanosensory genes regulated by neuronal IIS/FOXO to find *daf-2/daf-16*-dependent candidates. FKH-9 is known to be a neuronal IIS/FOXO target and is expressed in mechanosensory neurons which made it a potential candidate for the authors to further examine.

With chromatin immunoprecipitation experiments and quantitative PCR (ChIP-qPCR), it was confirmed that DAF-16 occupied the *fkh-9* promoter (Kaletsky et al., 2016).

Using FKH-9 tagged with GFP, Kaletsky et al., (2016) observed that FKH-9-GFP localized to the nucleus and that the neurons were the primary site of differential expression levels in *daf-16* mutants. This ultimately helped suggest a role for FKH-9 in *daf-16*-mediated neuronal function.

Short term memory was also seen to be affected by FKH-9, as *fkh-9* RNAi in adult *daf-2* mutants impaired their extended short term auditory memory (STAM). This therefore portrayed that FKH-9 is important in maintaining adult enhanced memory. Following this, *daf-2;fkh-9* double mutants were seen to be defective in STAM and also learning, however neuronal re-expression of *fkh-9* was able to rescue these defects (Kaletsky et al., 2016). This therefore portrayed FKH-9 requirement for extended memory and neuronal development in the *daf-2* mutants.

FKH-9 was also seen to play a role in the lifespan of the *daf-2* mutant worms. *fkh-9* knockdown in adult mutant worms significantly shortened their lifespan, but neuronal re-expression of *fkh-9* did not rescue it (Kaletsky et al., 2016). This suggested that FKH-9 regulates lifespan by acting in non-neuronal tissues which will need further examination. Overall, Kaletsky et al., (2016) provides an excellent study on the importance of the FKH-9 transcription factor for *C. elegans* adult axon regeneration, memory, and lifespan.

1.7.2 The Role of FKH-9 in Intestinal Gene Expression

FKH-9 has also been seen to have an important function in *C. elegans* intestines. Goszczynski et al., (2016) examined the *vit-2* vitellogenin gene which is intestine-specific and hermaphrodite-specific, therefore not transcribed in males. Specifically, the authors examined

how the enhancer of this specific gene is directly activated by FKH-9. After confirming that FKH-9 functioned in the intestine, they examined the effects of *fkh-9* RNAi on GFP expression with different *vit-2*-GFP reporter constructs. With a strain known as DZ28 (includes a 0.25 kb *vit-2* promoter), *fkh-9* RNAi had a low but still detectable effect on the GFP expression (Goszczynski et al., 2016). With another strain known as JM180 (includes the full 2.7 kb *vit-2* promoter), the authors could not detect lowered GFP expression caused by the *fkh-9* RNAi (Goszczynski et al., 2016). Therefore, they suspected that FKH-9 activates the *vit-2* enhancer but only makes a small contribution to the activity of the full promoter. To verify this, Goszczynski et al., (2016) used qRT-PCR to measure endogenous levels of *vit-2* transcripts with strain OLB11 which includes intestine only RNAi. With this *fkh-9* RNAi performed on the worms, the *vit-2* transcript levels were decreased compared to control therefore further supporting FKH-9's role in the intestinal activation of the *vit-2* gene.

Goszczynski et al., (2016) also performed electrophoretic mobility shift assays to show that FKH-9 bound to the *vit-2* enhancer oligonucleotide. Binding was inefficiently competed off the oligonucleotide when two, three or five base pairs in FKH-9 were mutated. The authors then constructed transgenic strains with a five base pair mutation in the *vit-2* enhancer which abolished FKH-9 binding. This enhancer was constructed to drive GFP expression and in 15 transgenic lines produced, GFP reporter expression was undetectable. Overall, Goszczynski et al. (2016) were able to conclude that FKH-9 is a direct transcriptional activator of the *vit-2* enhancer.

In relation to the previous study mentioned by Kaletsky et al., (2016), Goszczynski et al., (2016) also found a link between FKH-9 and DAF-16 as they saw that while FKH-9 activated *vit-2*, DAF-16 repressed it in a *daf-2* dependent manner. It was seen that both transcription

factors bound to the same DNA sequence within the *vit-2* enhancer. Therefore, the positive activity of FKH-9 could potentially compete with the negative influence of DAF-16 under the conditions where DAF-16 enters intestinal nuclei. Overall, Goszczynski et al., (2016) provides an excellent study into examining the function of FKH-9 as activating the enhancer of the *vit-2* gene in the intestines of hermaphrodite worms.

1.7.3 The Role of FKH-9 in Endoplasmic Reticulum Homeostasis

The FKH-9 transcription factor has also been seen to modulate *C. elegans* endoplasmic reticulum (ER) homeostasis during infection. Tillman et al., (2018) examined the unfolded protein response (UPR) conserved pathway which helps sense and respond to misfolded proteins in the ER lumen. Specifically, the IRE-1-XBP-1 branch of the UPR is required to maintain *C. elegans* ER homeostasis during larval development against pathogenic *Pseudomonas aeruginosa* (Tillman et al., 2018). FKH-9 is one transcription factor that helps suppress the larval lethality when XBP-1 is mutated caused by immune activation in response to infection by pathogenic bacteria (Tillman et al., 2018). The authors specifically examined loss-of-function mutations in FKH-9 and also determined that the loss of FKH-9 enhanced resistance to an ER toxin and resulted in enhanced ER-associated degradation (ERAD). Increased ERAD of *fkh-9* loss-of-function mutants was accompanied by the inability to degrade cytosolic proteasomal substrates as well as increased sensitivity to the proteasomal inhibitor bortezomib.

Mutated XBP-1 resulted in a loss of rough ER and a decrease in visible cisternae in the presence of the *Pseudomonas aeruginosa* pathogen. However, Tillman et al., (2018) observed that with loss of *fkh-9,* these ER structural changes were suppressed and resulted in preserved ER homeostasis. Due to this, the authors wanted to investigate the role of FKH-9 in further detail as they were also motivated by the Kaletsky et al., (2016) study previously mentioned. Due to the

fkh-9 mutations resulting in restoration of ER architecture in XBP-1 mutants, the authors hypothesized that the main site of FKH-9 activity is in the intestines. Tillman et al., (2018) generated GFP-tagged *fkh-9* using CRISPR/CAS9 and observed FKH-9 expression in both neurons and intestinal nuclei.

Proteasome function in the cytosol was also examined in terms of impairment with *fkh-9* mutants. Tillman et al., (2018) generated reporter strains with a transgene including GFP fused to a ubiquitin mutant that could not be cleaved off. This ubiquitinated GFP is usually degraded by the proteasome, however RNAi of the *hecd-1* gene which encodes an E3 ubiquitin ligase, caused an accumulation of Ubv::GFP. The *fkh-9* mutation was therefore seen to contribute to this increase in accumulation which supports proteasome dysfunction. Ultimately, Tillman et al., (2018) show that *fkh-9* loss enhanced the removal of misfolded proteins from the ER lumen with proteasomal degradation in the cytosol. This role that FKH-9 plays in balancing proteostasis may also coincide with the Kaletsky et al., (2016) study in its role of enhancing axonal regeneration in adult worms. Overall, Tillman et al., (2018) provides an excellent study into examining the role of FKH-9 in *C. elegans* endoplasmic reticulum homeostasis.

1.8 Rationale, Objectives and Hypothesis of Thesis

Although some information resides in the literature about the roles and functions of FKH-9 in *C. elegans,* its specific role in the oxidative stress response remains largely unknown. Due to the indirect inhibitory effect that BRAP-2 may have on SKN-1 and subsequent *gst-4* expression levels, the lab previously conducted an RNAi screen on *brap-2(ok1492)* mutants using *C. elegans* that contained a GFP coding region fused to the *gst-4* promoter (*gst-4p::gfp).* In this RNAi screen, multiple different transcription factors were knocked down to monitor changes in *gst-4* expression through confocal microscopy and further quantification. When RNAi was done

on *fkh-9* specifically, this knockdown resulted in lowered *gst-4* expression levels due to lowered GFP levels observed.

This RNAi screen presented an indication that FKH-9 may have activator-like functions in the *C. elegans* oxidative stress response. Therefore, the main objective of my project was to aid in expanding our understanding of the stress response pathways by investigating the role of FKH-9. I hypothesize that FKH-9 plays an important role in the GST-4/SKN-1 signalling pathway particularly through activator-like mechanisms. I also hypothesize that the absence of FKH-9 will hinder *C. elegans* biological performance by causing shortened survival in oxidative stress inducing environments as well as shortened lifespan overall.

CHAPTER 2: MATERIALS AND METHODS

2.0 Materials and Methods:

2.1 The Maintenance and Genetics of *C. elegans* Strains

All the *C. elegans* strains used in this project were obtained from the *Caenorhabditis* Genetics Center (The University of Minnesota) and the National Bioresource Project (Tokyo, Japan). The strains were maintained under standard conditions according to the protocol designed by Sydney Brenner (Brenner, 1974). All experiments were performed using N2 as the wild type at a temperature of 20 degrees Celsius unless specified otherwise. The following strains of *C. elegans* were used in this project: YF123 [*fkh-9(ok1709)*], DR466 [(*him-5(e1490)*], CL2166 [*dvIs19(gst- 4p::gfp)*], YF221 [*fkh-9(ok1709);dvIs19(gst-4p::gfp)*], YF15 [*brap-2(ok1492)*], YF124 [*brap-2(ok1492);fkh-9(ok1709)*], YF67 [*brap-2(ok1492);dvIs19(gst-4p::gfp)*], CF1553[*muls84(sod-3p::gfp)*], and YF225 [*fkh-9(ok1709);muls84(sod-3p::gfp)*]. Please also refer to Table 7 in the appendix for list of strains used in this project.

2.2 Generation of Transgenic Worms

The YF221 [*fkh-9(ok1709)*] and CL2166 [*dvIs19(gst-4p::gfp)*] strains were used to generate the transgenic worm strain [*fkh-9(ok1709);dvIs19(gst-4p::gfp)*]. The YF221 [*fkh-9(ok1709)*] and CF1553[*muls84(sod-3p::gfp)*] strains were used to generate the transgenic worm strain YF225 [*fkh-9(ok1709);muls84(sod-3p::gfp)*].

In order to generate the *fkh-9(ok1709);dvIs19(gst-4p::gfp)* transgenic worm line, *him-5(e1490)* male mutant worms were crossed with *dvIs19(gst-4p::gfp)* hermaphrodites at the L3/L4 stage. As a result of this cross, green males expressing *dvIs19(gst-4p::gfp)* were collected using fluorescence microscopy and were crossed with *fkh-9(ok1709)* hermaphrodites. These worms were considered the Parental worms, or P1. The green hermaphrodites produced as a result of this cross were considered F1. Once these F1 worms hatched and grew to the L3/L4 stage, they

were individually plated onto separate NGM plates to lay eggs. These progenies were considered F2. The genotype of the individual F1 worms was determined by SW-PCR (Single Worm Polymerase Chain Reaction) with primers specific for the *fkh-9(ok1709)* deleted region. F1 worms that were homozygous for the *fkh-9(ok1709)* deletion mutation were selected and their F2 progenies were screened by SW-PCR to confirm all worms were homozygous for the *fkh-9(ok1709)* gene deletion and also expressed *dvIs19(gst-4p::gfp).* F3 and subsequent generations were maintained on NGM plates after genotyping.

Similar approaches were done to generate the *fkh-9(ok1709);muls84(sod-3p::gfp)* transgenic worm line. First, *him-5(e1490)* male mutant worms were crossed with *muls84(sod-3p::gfp)* hermaphrodites at L3/L4 stage. As a result of this cross, green males expressing *muls84(sod-3p::gfp)* were collected using fluorescence microscopy and were crossed with *fkh-9(ok1709)* hermaphrodites. These worms were considered the Parental worms, or P1. The green hermaphrodites produced as a result of this cross were considered F1. Once these F1 worms hatched and grew to the L3/L4 stage, they were individually plated onto separate NGM plates to lay eggs. These progenies were considered F2. The genotype of the individual F1 worms was determined by SW-PCR (Single Worm Polymerase Chain Reaction) with primers specific for the *fkh-9(ok1709)* deleted region. F1 worms that were homozygous for the *fkh-9(ok1709)* mutation were selected and their F2 progenies were screened by SW-PCR to confirm all worms were homozygous for the *fkh-9(ok1709)* gene deletion and also expressed *muls84(sod-3p::gfp).* F3 and subsequent generations were maintained on NGM plates after genotyping.

2.3 Single Worm – Polymerase Chain Reaction

A single worm was picked and placed into a 20 µl PCR tube containing 4 µl of Single Worm Lysis buffer which was prepared by mixing 10x thermopol buffer (NEB E50000S),

Proteinase K (NEB P8107S) and sterile filtered water. The PCR tube was then stored at -80 °C overnight. The following day the PCR tube was placed in the Thermocycler (Biometra T Personal Thermocycler) for a Proteinase K reaction (1 hr at 65°C followed by 15 mins at 95°C). After this reaction was completed, a PCR master mix was prepared by mixing 20 µl of 10x thermopol buffer (NEB E50000S), 20 µl of 2 mM dNTPs (NEB E50000S), 1 µl of 100 µM forward primer, 1 µl of 100 µM reverse primer, 1 µl of Taq Polymerase (NEB E50000S) and 157 µl of nuclease-free H_2O (Bioshop WAT222). 20 µl of this PCR master mix was then added to the PCR tube and placed back into the Thermocycler for a second reaction of CT PCR (DNA denaturation at 95°C, primer annealing at 47°C and primer extension at 68°C). Once completed, a 1% agarose gel was made with 0.4g of Agarose (Sigma A9539-50G) and 40 mL of 1X TAE (Tris(hydroxymethyl)aminomethane Acetic acid Ethylenediaminetetraacetic acid) buffer. 6X loading dye was mixed with the contents of the PCR tube and added into the gel. Gel electrophoresis was then carried out to examine the results from the PCR tube. The bands were then examined by UV light using Alphaimager software to detect either a WT or mutant genotype.

2.4 Worm Synchronization

Adult L4 worms (12-15 sample size) were picked and placed on NGM plates seeded with OP-50 (*E. coli* food source). The worms were left to lay eggs for 4-6 hours and were then picked and placed back onto their original plates. The eggs were maintained under standard conditions for 48-72 hours. After about 48 hours, the worms from these hatched eggs had reached the L4 adult stage. These L4 synchronized worms were used for further experiments.

2.5 Fluorescence Microscopy and GFP Quantification

About 10-12 worms of *gst-4p::gfp, fkh-9(ok1709);gst-4p::gfp, sod-3p::gfp* and *fkh-9(ok1709);sod-3p::gfp* were picked and placed on separate microscope slides to observe with confocal microscopy. A bed of 2% agarose gel was placed on the glass slide first, followed by 2mM of Levamisole to help paralyze the worms and prevent movement. The worms were then mounted onto the slide followed by placement of a coverslip on top. The fluorescent worms were then observed under the Zeiss Observer Z1 Spinning Disk Confocal Microscope. Images were captured using both the tiling and Z-stack features of the microscope and subsequently analyzed with ZEN 2.6 Software®. Image J software was used to quantify whole worm fluorescence.

2.6 RNA Extraction and qRT-PCR

Worms were first synchronized to the L4 adult stage and were then washed off the 6cm NGM plate using 1.5 mL of M9 buffer. The mix was transferred to a 1.5 mL microfuge tube and was centrifuged at 10,000 x g for 30 seconds. The supernatant was aspirated and 1 mL of M9 buffer was added to the microfuge tube to be centrifuged again. This was repeated three more times. Once all washes were complete, the remaining worm pellet (~200 µl) was stored overnight at -80 °C. The next day, RNA extraction was carried out by first thawing the microfuge tube containing the worm pellet and adding 250 µl of TRI reagent (Sigma 93289). The microfuge tube was then briefly vortexed for ~5 seconds and then placed on a 4 °C vortex shaker for 15 minutes. Following this, 250 µl of absolute ethanol was added to the microfuge tube which was again briefly vortexed for ~5 seconds. The full contents of the tube were then transferred to a Zymo-spin IC column (Zymo R2060) and RNA extraction was carried out by following the manufacturer's protocol. Once the protocol was fully carried out, the total RNA concentration was measured using the Fisher Thermo NanoDrop2000. The RNA samples were

then stored overnight at -80 °C. The following day, the RNA sample was used to synthesize cDNA using the OneScript® Plus or the AdvanTech cDNA synthesis kit according to the manufacturer's protocol. Following this, quantification of mRNA expression levels of various genes was measured by qRT-PCR by using specific gene primers, BlasTaq™ 2X qPCR MasterMix (abm G891) and the Qiagen Roto-Gene Q System. The ΔΔCT method was used to analyze all data using results obtained from three independent trials. The mRNA expression levels of all experimental strains were always normalized to the N2 wildtype (WT) strain. Housekeeping genes known as *tba-1* and *cdc-42* were used as the endogenous control genes. Please refer to Table 6 in the appendix for list of forward and reverse primers used in this project.

2.7 RNAi (RNA interference)

The transcription factor RNAi library used to perform RNAi was generated by the Walhout lab. NGM plates were prepared with different ingredients to perform the RNAi. These include: 0.4 mM IPTG, 100 μg/mL Ampicillin and 12.5 μg/mL Tetracycline. The plates were then seeded with transformed HT115 *Escherichia coli* (*E. coli*) expressing double-stranded RNA (dsRNA) from pL4440 control plasmids or plasmids containing the homologous sequence to the target gene. Worms were placed and left on these plates to feed off the *E. coli* and were allowed to reach the L4 adult stage. The adult worms were then collected and used under the confocal microscope for GFP quantification.

2.8 Oxidative Stress Assays

Two different oxidative stress assays were performed, using two different types of reagents such as: sodium arsenite (As) and *tert*-butyl hydrogen peroxide (tBHP). All worms used were raised and synchronized to the L4 adult stage at 20°C.

For the sodium arsenite assay, N2 WT and *fkh-9(ok1709)* mutant worms were picked and transferred to a 24-well plate with M9 buffer (for the control group) and 5mM sodium As (for the experimental group). M9 buffer was prepared by mixing 3.0 g KH_2PO_4, 6.0 g Na_2HPO_4, 0.5 g NaCl, and 1.0 g NH_4Cl in 1 L of H_2O. After the worms were placed in the wells, they were monitored every hour and the number of live worms were scored. Worms that did not respond to prodding by a worm pick were considered dead. For analysis, data was collected from three independent trials.

For the tBHP assay, 7.7 mM tBHP agar plates were made the day before conducting the experiment. Both N2 WT and *fkh-9(ok1709)* mutant worms were picked and placed on regular unseeded NGM plates (for the control group) and on unseeded tBHP plates (for the experimental group). All worms were then monitored every hour and the number of live worms were scored. Worms that did not respond to prodding by a worm pick were considered dead. For analysis, data was collected from three independent trials.

2.9 ER Stress Assay

All worms used were raised and synchronized to the L4 adult stage at 20 °C. 10mM Dithiothreitol (DTT) agar plates were made the day before conducting the experiment. Both N2 WT and *fkh-9(ok1709)* mutant worms were picked and placed on regular unseeded NGM plates (for the control group) and on unseeded DTT plates (for the experimental group). All worms were then monitored every hour and the number of live worms were scored. Worms that did not respond to prodding by a worm pick were considered dead. For analysis, data was collected from three independent trials.

2.10 Longevity Assay

All worms used were raised and synchronized to the L4 adult stage at 20 °C. Both N2 WT and *fkh-9(ok1709)* mutant worms were allowed to lay eggs for 4-6 hours and were then transferred back to their original NGM plates. Once the eggs hatched, L4 adult worms from each strain were picked to follow overtime to assess in terms of length of lifespan. In order to follow these original L4 adult worms picked, and to also prevent crowding and starvation, they were regularly transferred to fresh plates with a fresh supply of food. Worms that did not respond to prodding by a worm pick were considered dead. For analysis, data was collected from three independent trials.

2.11 Cell Culture and Luciferase Assay

The effects of specific *C. elegans* transcription factors were examined through luciferase activity of firefly luciferase which was under the control of specific promoters. This was examined using Human Embryonic Kidney Cells (HEK293T cells) which were cultured in GibcoTM Dulbecco's Modified Eagle's Medium (DMEM) (Fisher Scientific 11995065) supplemented with 10% Fetal Bovine Serum (FBS). Cells were maintained at 37°C with 5% CO_2 levels and passaged using GibcoTM Trypsin-EDTA (0.25%) (Fisher Scientific 25200056). Once the HEK293T cells reached 70-90% confluency on 10cm treated petri dishes, they were ready to be used for luciferase assay experimentation.

The HEK293T cells were transferred to a 24-well plate which were incubated overnight at 37°C. The following day the cells were co-transfected with Opti-MEM, Lipofectamine 3000 (Invitrogen L3000001) and all DNA constructs (1 μg of DNA used for each construct in each transfection) based on manufacturer's protocol. The transfected cells were incubated overnight at 37°C. The following day, cells were lysed and transferred to a 96-well plate to be prepared for

luminescence readings using the Firefly & *Renilla* Luciferase Single Tube Assay Kit (Biotium 300811) based on the manufacturer's guidelines. Luminescence was quantified using the Synergy™ H4 Hybrid Multi-Mode Microplate Reader (BioTek). Data was analyzed using results from three independent trials.

2.12 Primer Design

All primers used for this project were designed using the Primer3 and BLAST (NCBI) programs using the *C. elegans* genome to ensure primer pair specificity. Primer pairs were chosen based on optimal T_m, GC% and self-complementarity and were validated to ensure there were no off-targets hits. Primers TK133, TK135, and TK139 were used to genotype *fkh-9(ok1709)* deletion mutants. Please also refer to Table 8 in the appendix for list of primers used for genotyping the *fkh-9(ok1709)* mutation.

2.13 Statistical Analysis

GraphPad Prism 8 Software was utilized to generate graphs and analyze data. Statistical methods, Multiple *t*-tests, Two-tailed Unpaired Student's *t*-test or One Way ANOVA was used to establish statistical significance. Log-rank (Mantel-Cox) method was used to calculate the statistical significance of survival and longevity assays. Data showing P values below 0.05 were considered statistically significant. Error bars represent the +/- standard error of the mean.

CHAPTER 3: RESULTS

3.0 Results:

3.1 *fkh-9* is Required for Induced Expression Levels of *gst-4* in *brap-2(ok1492)* Mutant Worms and Under Oxidative Stress-Inducing Conditions

My initial interest in the *C. elegans* FKH-9 transcription factor stemmed from an RNAi screen that the lab previously carried out. This screen was performed on a *brap-2(ok1492)* mutant strain that contained a GFP coding region fused to the *gst-4* promoter (*gst-4p::gfp*). With this screen, the lab was able to knockdown a library of transcription factors and subsequently monitor the changes in *gst-4* expression through GFP fluorescence. With knockdown of *fkh-9(ok1709)* specifically, reduced expression of *gst-4* was observed therefore suggesting it may be a positive regulator of *gst-4.* To begin my investigation to further test this result, an *fkh-9(ok1709)* mutant strain was obtained from *Caenorhabditis* Genetics Center (CGC) which I used for my experimentation.

I first generated a transgenic worm line carrying the *fkh-9(ok1709)* deletion mutation along with the *gst-4p::gfp* reporter construct known as *fkh-9(ok1709);gst-4p::gfp.* This was done in order to visualize *gst-4* expression using confocal microscopy in comparison with WT *gst-4p::gfp* worms. I first examined basal *gst-4* levels in both strains with a 2-hour M9 buffer treatment, and there was not a significant difference seen in *gst-4* expression as it was minimal in both strains. However, I also examined induced *gst-4* levels with a with a 2-hour sodium arsenite (As) treatment. Both the WT *gst-4p::gfp* and *fkh-9(ok1709);gst-4p::gfp* mutant strain exhibited much higher *gst-4* expression levels compared to when treated with M9 buffer. This was expected since As creates an oxidative stressful environment for the worms. Compared to M9 buffer, the WT appeared 4.61 x brighter when treated with As, and the *fkh-9(ok1709);gst-4p::gfp* strain appeared 4.66 x brighter when treated with As compared to M9 buffer. However, there

was no significant difference seen in GFP fluorescence between the two strains when treated with As. (Figure 3.1 A, B).

To examine this further, I performed qRT-PCR on both N2 WT and *fkh-9(ok1709)* mutants with and without As treatment to examine *gst-4* expression levels. The qRT-PCR results were consistent with previous confocal imaging results, as both N2 WT and *fkh-9(ok1709)* mutants had low basal *gst-4* mRNA levels. However, they portrayed much high expression levels when induced with As (Figure 3.2). With N2 WT, there is a significant 8.8-fold difference seen between basal and induced *gst-4* mRNA expression levels, with a large increase with As treatment. With the *fkh-9(ok1709)* mutants there was a 6.7-fold difference seen between basal and induced *gst-4* mRNA expression levels with a large increase with As treatment as well. However, there was not a significant difference in *gst-4* mRNA levels seen between the two strains when treated with As. These results were normalized to the *tba-1* housekeeping gene and were obtained from 3 independent trials. Taken together, these results suggest that FKH-9 may function to increase the expression of induced *gst-4* levels specifically, while most likely not playing a major role in terms of basal expression levels.

In order to examine this idea of FKH-9's role in induced *gst-4* levels specifically, I decided to examine this in another way by validating the preliminary results obtained from the RNAi screen. Therefore, I first performed *fkh-9* RNAi on *brap-2(ok1492);gst-4p::gfp* worms and used the pL4440 vector as a control with comparison of GFP fluorescence levels to the WT *gst-4p::gfp* strain. As expected, the *gst-4p::gfp* worms showed very similar *gst-4* expression levels when treated with either the pL4440 control vector or *fkh-9* RNAi as there was no significant difference seen. However, in terms of the *brap-2(ok1492);gst-4p::gfp* strain, due to the *brap-2(ok1492)* mutation causing induced *gst-4* expression levels, these worms appeared very bright

when treated with the pL4440 control vector. However, when treated with the *fkh-9* RNAi, the fluorescence decreased by 1.60 x (Figure 3.3 A, B).

To examine this further, I performed qRT-PCR on N2 WT, *fkh-9(ok1709), brap-2(ok1492)* and *brap-2(ok1492);fkh-9(ok1709)* mutants with and without As treatment to examine *gst-4* expression levels. The qRT-PCR results were consistent with previous confocal imaging results as the *brap-2(ok1492)* mutant worms showed a large increase in *gst-4* expression compared to the *brap-2(ok1492);fkh-9(ok1709)* double mutant worms. This was seen both with and without As treatment. Without As treatment, normalized to the *tba-1* housekeeping gene, *brap-2(ok1492);fkh-9(ok1709)* showed a 4.6-fold significant decrease in *gst-4* mRNA expression levels and a 1.2-fold significant decrease when normalized to the *cdc-42* housekeeping gene compared to *brap-2(ok1492)* (Figure 3.4 A). With As treatment, normalized to the *tba-1* housekeeping gene, *brap-2(ok1492);fkh-9(ok1709)* showed a 1.5-fold significant decrease in *gst-4* mRNA expression levels and a 1.1-fold decrease when normalized to the *cdc-42* housekeeping gene compared to *brap-2(ok1492)* (Figure 3.4 B). Both results were obtained from 3 independent trails. These results help confirm the notion that FKH-9 most likely plays a role in increasing induced expression levels of the *gst-4* PII detoxification gene specifically.

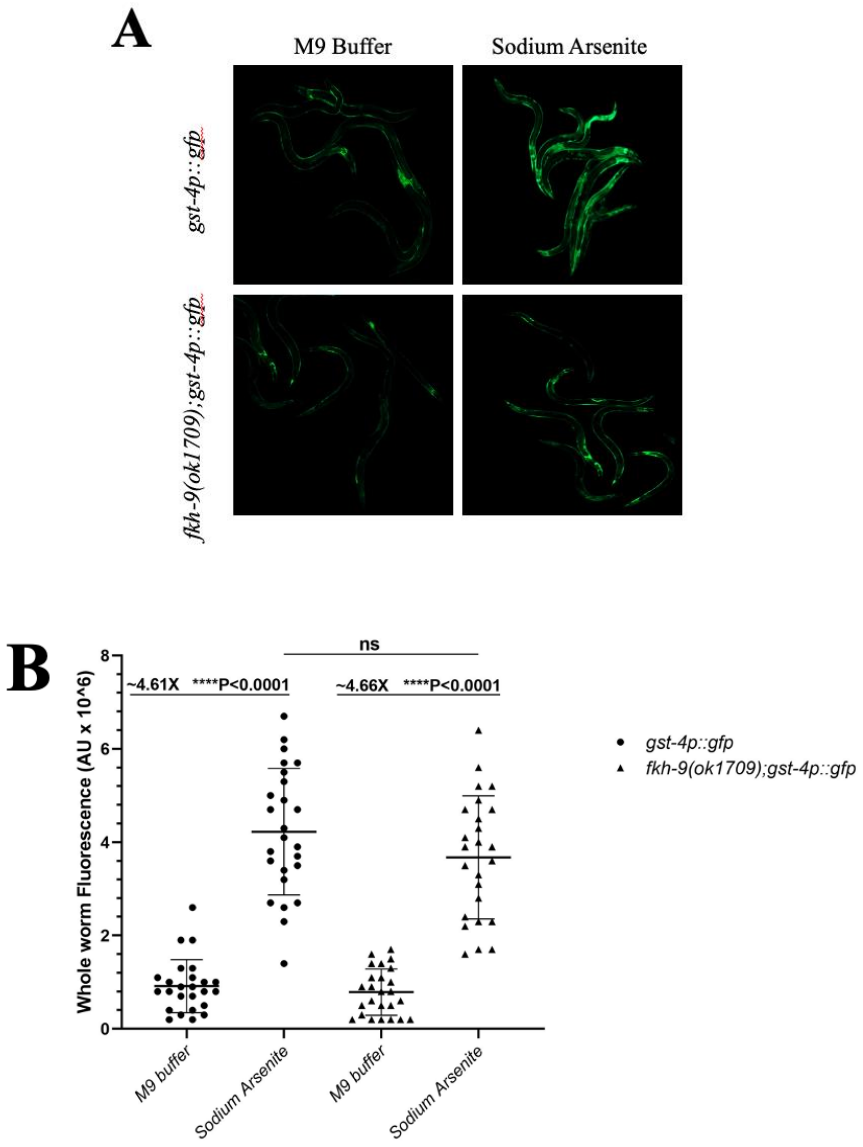

Figure 3.1: *fkh-9(ok1709)* Mutants and *gst-4::gfp* WT Exhibit Higher Expression Levels of *gst-4* with Sodium Arsenite Treatment

(A) Whole worm GFP fluorescence was visualized in the *gst-4p::gfp* and *fkh-9(ok1709);gst-4p::gfp* strains with and without As treatment. Fluorescence was captured using the Zeiss Observer Z1 Spinning Disk Confocal Microscope under 20X magnification. **(B)** Fluorescence intensity was quantified using ImageJ Software. Results for n=25 worms are shown as individual points as the difference between the intensity reading per worm minus the background fluorescence. The mean fluorescence intensity is displayed as a solid black line for each worm strain. GFP levels in *gst-4p::gfp* worms treated with As were ~ 4.61 x brighter than when treated with M9 buffer. GFP levels in *fkh-9(ok1709);gst-4p::gfp* worms treated with As were ~ 4.66 x brighter than when treated with M9 buffer. The difference in fluorescence between both strains treated with As was not significant. Statistical analyses were performed using the Two-tailed Unpaired Student's *t*-test; **** $P < 0.0001$.

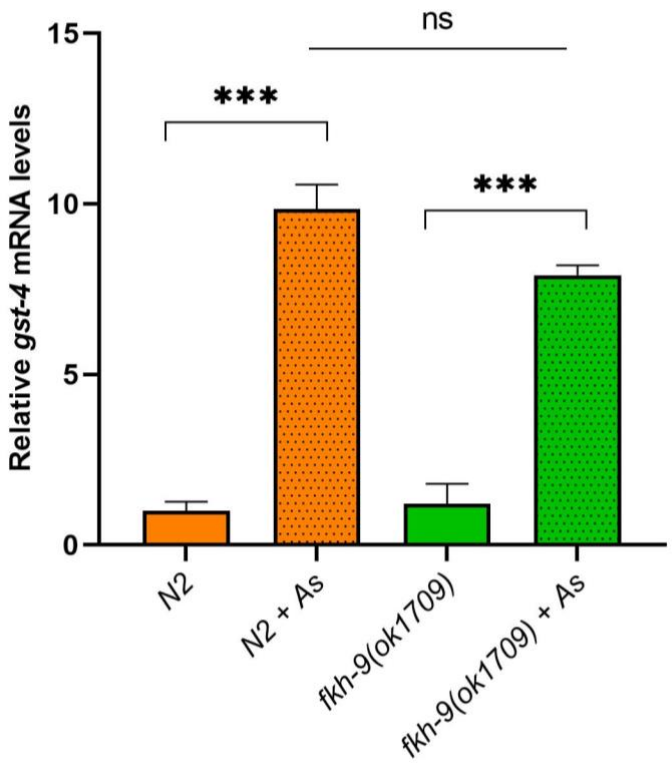

Figure 3.2: *fkh-9(ok1709)* Mutants and WT Show Elevated *gst-4* mRNA Levels with Sodium Arsenite Treatment

qRT-PCR was done to measure the mRNA levels of the PII detoxification gene *gst-4* in both N2 WT and *fkh-9(ok1709)* mutant worms with and without As treatment. *gst-4* mRNA levels were significantly enhanced in both N2 WT and *fkh-9(ok1709)* mutants when treated with sodium arsenite. The difference in *gst-4* mRNA levels was not significant between both strains treated with sodium arsenite. Results were derived from 3 independent trials and normalized to the *tba-1* housekeeping gene. Statistical analysis was carried out using Multiple *t*-tests. Error bars represent ± SEM; *** $P < 0.001$.

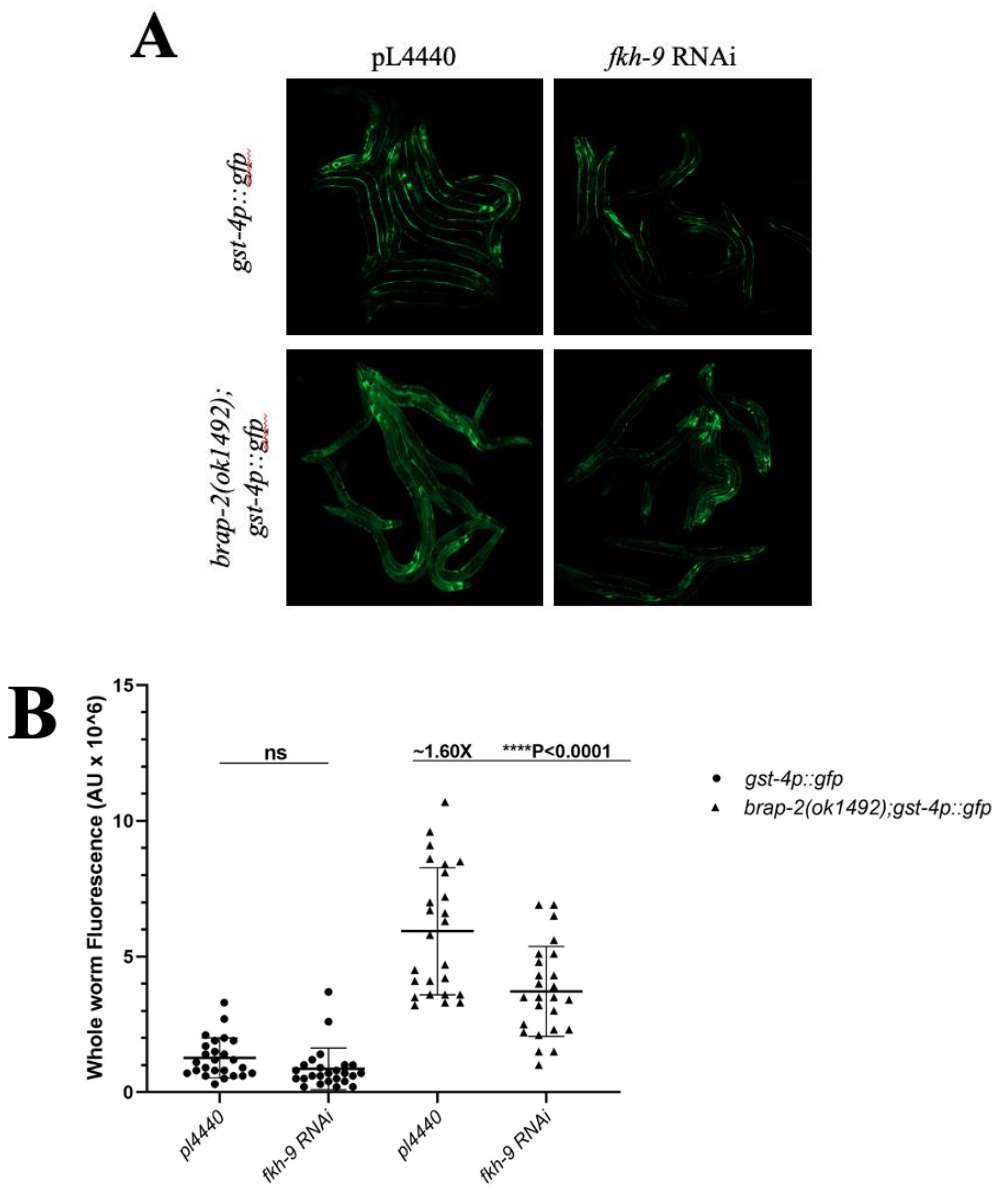

Figure 3.3: *brap-2(ok1492)* Mutants Show Lower Expression of *gst-4* with *fkh-9* RNAi Compared to the pL4440 Control Vector

(A) Whole worm GFP fluorescence was visualized in the *gst-4p::gfp* and *brap-2(ok1492);fkh-9(ok1709)* strains with and without *fkh-9* RNAi. Fluorescence was captured using the Zeiss Observer Z1 Spinning Disk Confocal Microscope under 20X magnification. **(B)** Fluorescence intensity was quantified using ImageJ Software. Results for n=25 worms are shown as individual points as the difference between the intensity reading per worm minus the background fluorescence. The mean fluorescence intensity is displayed as a solid black line for each worm strain. GFP levels in *gst-4p::gfp* worms with and without the *fkh-9* RNAi were not significantly different. GFP levels in *brap-2(ok1492);fkh-9(ok1709* worms treated with the *fkh-9* RNAi were ~ 1.60 x less bright than when treated with the control pL4440 control vector. Statistical analysis was performed using the Two-tailed Unpaired Student's *t*-test; **** $P < 0.0001$.

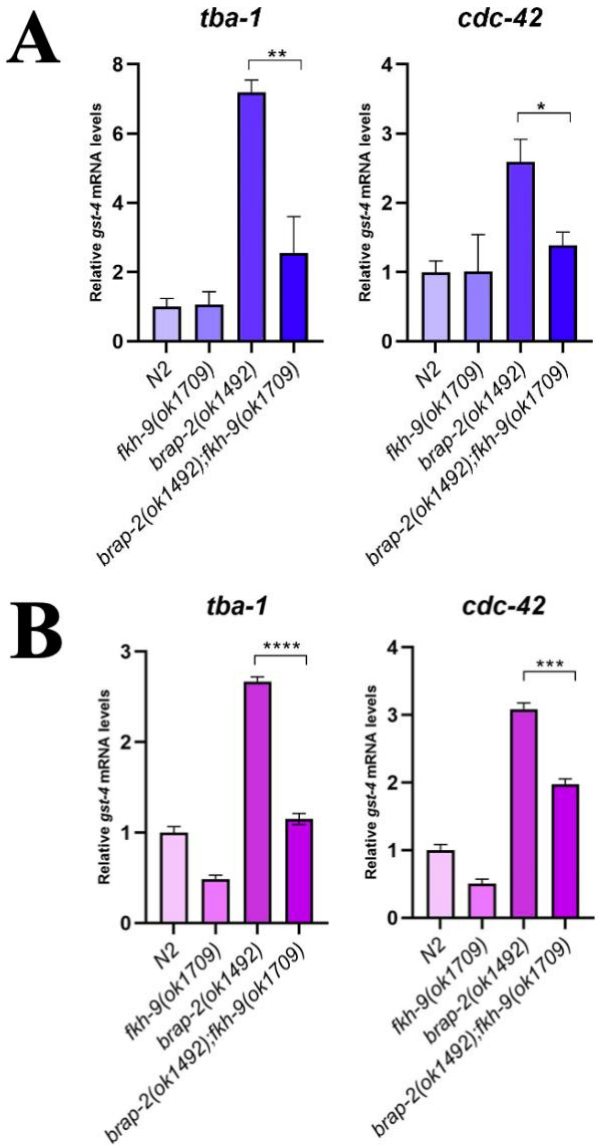

Figure 3.4: *brap-2(ok1492);fkh-9(ok1709)* Double Mutants Show Lower *gst-4* mRNA Levels With and Without Sodium Arsenite Treatment Compared to *brap-2(ok1492)* Mutants

qRT-PCR was done to measure the mRNA levels of the PII detoxification gene *gst-4* in N2 WT, *fkh-9(ok1709)* mutant, *brap-2(ok1492)* mutant and *brap-2(ok1492);fkh-9(ok1709)* double mutant worms with **(B)** and without **(A)** As treatment. **(A)** *gst-4* mRNA levels were significantly enhanced in *brap-2(ok1492)* mutant worms compared to *brap-2(ok1492);fkh-9(ok1709)* double mutant worms when normalized to both the *tba-1* and *cdc-42* housekeeping genes. **(B)** With As treatment, *gst-4* mRNA levels were significantly enhanced in *brap-2(ok1492)* mutant worms compared to *brap-2(ok1492);fkh-9(ok1709)* double mutant worms when normalized to both the *tba-1* and *cdc-42* housekeeping genes. Results were derived from 3 independent trials. Statistical analysis was carried out using Multiple *t*-tests. Error bars represent ± SEM; **** $P < 0.0001$, *** $P < 0.001$, ** $P < 0.01$, * $P < 0.05$.

3.2 *fkh-9* is Required for Basal Expression Levels of Phase II Detoxification Genes

After learning that FKH-9 may positively regulate induced *gst-4* expression through both transgenesis and qRT-PCR experimentation, I was curious to see if FKH-9 would influence the expression of other PII detoxification genes. Therefore, I used qRT-PCR to measure the mRNA expression levels of *ugt-13, gsto-2, dhs-8* and *sdz-8* in both N2 WT and *fkh-9(ok1709)* mutants. The purpose of this experiment was to go outside the box of only examining *gst-4* and to see if FKH-9 has a general effect on PII genes. I examined these 4 genes with and without As treatment and normalized the data to both the *tba-1* and *cdc-42* housekeeping genes.

Without As treatment, there is less mRNA expression seen in the *fkh-9(ok1709)* mutants for majority of the genes. Specifically, when normalized to the *cdc-42* housekeeping gene, there is a significant difference in mRNA expression levels of *dhs-8* and *sdz-8.* There is a 0.5-fold difference in expression in *dhs-8* and a 0.6-fold difference in *sdz-8* expression in the *fkh-9(ok1709)* mutants compared to N2 WT. This is not evident when normalized to the *tba-1* housekeeping gene (Figure 3.5 A). These results were obtained from 3 independent trials.

Examining these genes with As treatment, the complete opposite was observed between N2 WT and *fkh-9(ok1709)* mutants. For majority of the genes, there is more mRNA expression seen in the *fkh-9(ok1709)* mutants compared to WT. Specifically, when normalized to the *tba-1* housekeeping gene there is a significant difference in *dhs-8* with a 1.1-fold difference in mRNA expression seen in the *fkh-9(ok1709)* mutants (Figure 3.5 B). These results were obtained from 3 independent trials. Overall, these results help suggest that FKH-9 may be required for basal expression levels of these PII detoxification genes (*dhs-8* and *sdz-8* specifically) but may play a repressive role in induced levels (*dhs-8* specifically).

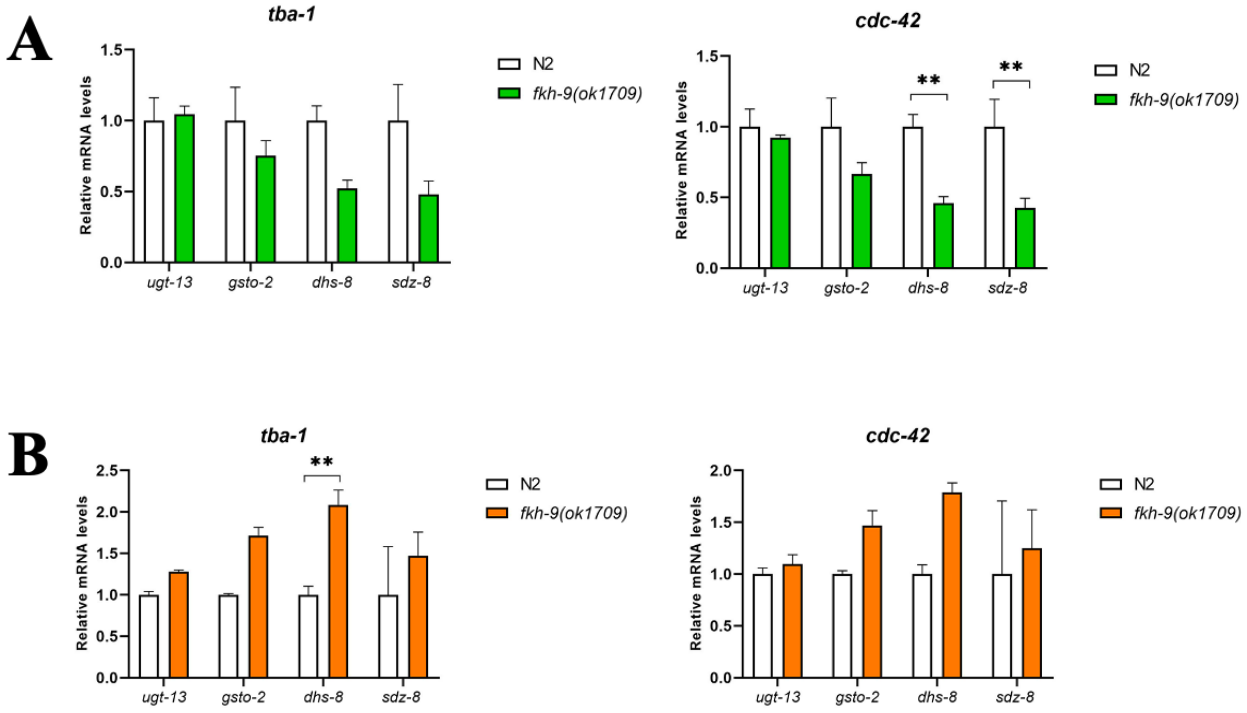

Figure 3.5: *fkh-9(ok1709)* Mutation Influences Basal and Induced Expression Levels of Other Phase II Detoxification Genes

qRT-PCR was done to measure the mRNA levels of other PII detoxification genes in both N2 WT and *fkh-9(ok1709)* mutant worms with **(B)** and without **(A)** As treatment. **(A)** *dhs-8* and *sdz-8* mRNA levels were significantly lowered in *fkh-9(ok1709)* mutant worms compared to N2 WT when normalized to the *cdc-42* housekeeping gene. **(B)** With As treatment, *dhs-8* mRNA levels were significantly enhanced in the *fkh-9(ok1709)* mutant worms compared to N2 WT when normalized to the *tba-1* housekeeping gene. Results were derived from 3 independent trials. Statistical analysis was carried out using Multiple *t*-tests. Error bars represent ± SEM; ** P < 0.01.

3.3 Loss of *fkh-9* Positively Influences Induced Expression Levels of *sod-3*

After examining the influence FKH-9 has on *gst-4* expression and other PII detoxification genes, I wanted to explore the effect it may have on PI detoxification genes as well. I started with examining *sod-3* and *daf-16* mRNA levels with qRT-PCR. I grouped *daf-16* along with *sod-3* in this case since DAF-16 is known to be a transcriptional activator of *sod-3.* I examined mRNA levels in both N2 WT and *fkh-9(ok1709)* mutants with and without As treatment and normalized the data to both the *tba-1* and *cdc-42* housekeeping genes.

Without As treatment, there is no significant difference seen in mRNA levels for either *sod-3* or *daf-16* when normalized to either the *tba-1* or *cdc-42* housekeeping gene. There is a slight increase in levels in the *fkh-9(ok1709)* mutants, however this difference is not significant (Figure 3.6 A). Therefore, FKH-9 most likely does not have an influence on basal *sod-3* mRNA expression levels. However, when examining *sod-3* and *daf-16* mRNA levels with As treatment, there is a significant difference seen with a 4.0-fold increase in mRNA levels when normalized to the *tba-1* housekeeping gene and a 3.9-fold increase in mRNA levels when normalized to the *cdc-42* housekeeping gene in the *fkh-9(ok1709)* mutants (Figure 3.6 B). These results were obtained from 3 independent trials. Overall, this helps portray that FKH-9 may play a repressive role in induced *sod-3* expression.

To examine this further, I wanted to observe a visual aid as well (just as when examining *gst-4* expression levels) so I generated another transgenic worm line known as *fkh-9(ok1709);sod-3p::gfp* carrying the *fkh-9(ok1709)* deletion mutation along with the *sod-3p::gfp* reporter construct. This was carried out to visualize *sod-3* expression using the confocal microscope in comparison with WT *sod-3p::gfp* worms. I first examined basal *sod-3* levels in both strains with a 2-hour M9 buffer treatment, and there was not a significant difference seen in

sod-3 expression as it was low in both strains. However, I also examined induced *sod-3* levels with a 2-hour As treatment. The *sod-3p::gfp* strain appeared 1.88 x brighter than when treated with M9 buffer and the *fkh-9(ok1709);sod-3p::gfp* strain appeared 3.01 x brighter than when treated with M9 buffer. However, comparing both strains treated with As, the *fkh-9(ok1709);sod-3p::gfp* mutants appeared 1.41 x brighter than the WT (Figure 3.7 A, B). These results were consistent with previous qRT-PCR results carried out, with the *fkh-9(ok1709)* mutants exhibiting an increase in *sod-3* expression. Overall, this helps confirm that FKH-9 may play a repressive role in *sod-3* expression levels potentially through DAF-16.

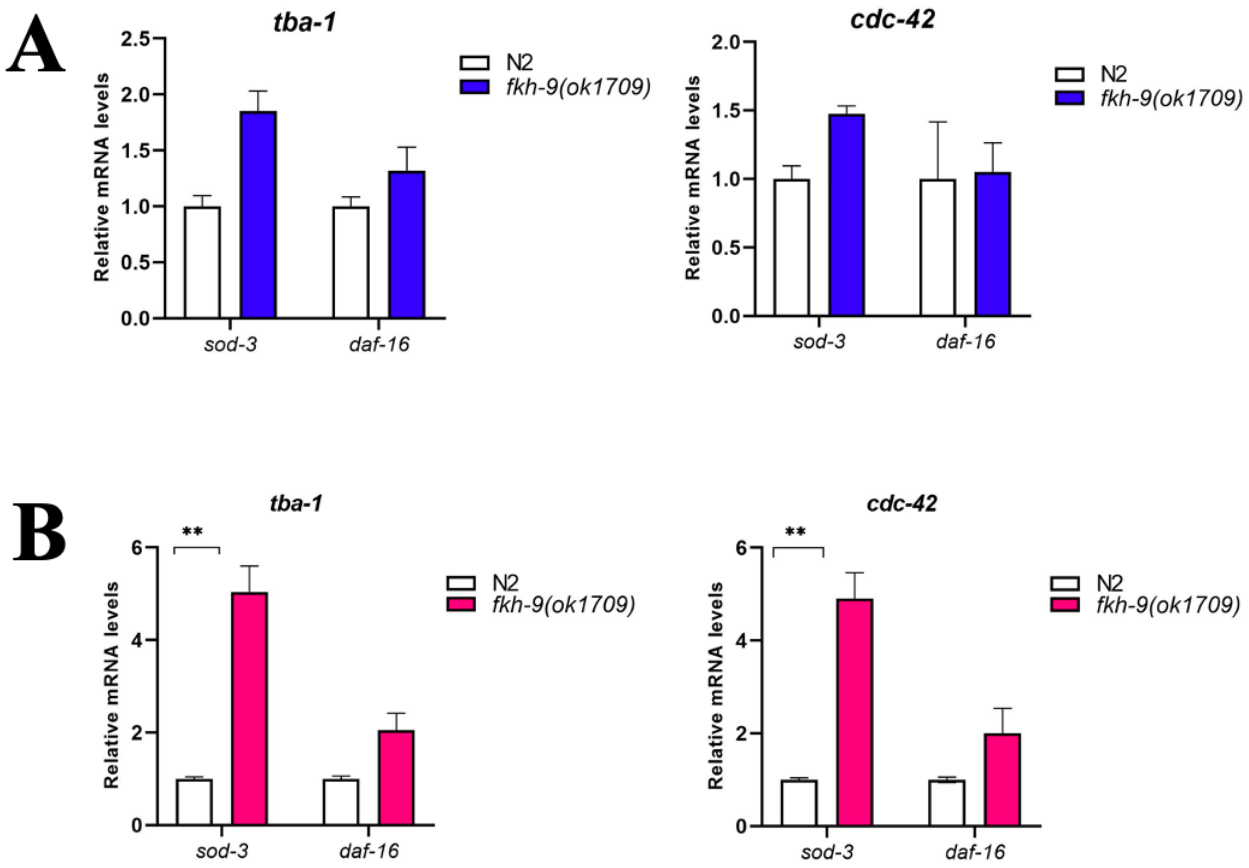

Figure 3.6: *fkh-9(ok1709)* Mutants Show Elevated Levels of *sod-3* with Sodium Arsenite Treatment

qRT-PCR was done to measure the mRNA levels of the PI gene *sod-3* and its transcriptional activator *daf-16* in both N2 WT and *fkh-9(ok1709)* mutant worms with **(B)** and without **(A)** As treatment. **(A)** No significant difference seen in mRNA levels between N2 WT and *fkh-9(ok1709)* mutant worms when normalized to either the *tba-1* or *cdc-42* housekeeping gene. **(B)** With As treatment, *sod-3* mRNA levels were significantly enhanced in the *fkh-9(ok1709)* mutant worms compared to N2 WT when normalized to either the *tba-1* or *cdc-42* housekeeping genes. Results were derived from 3 independent trials. Statistical analysis was carried out using Multiple *t*-tests. Error bars represent ± SEM; ** $P < 0.01$.

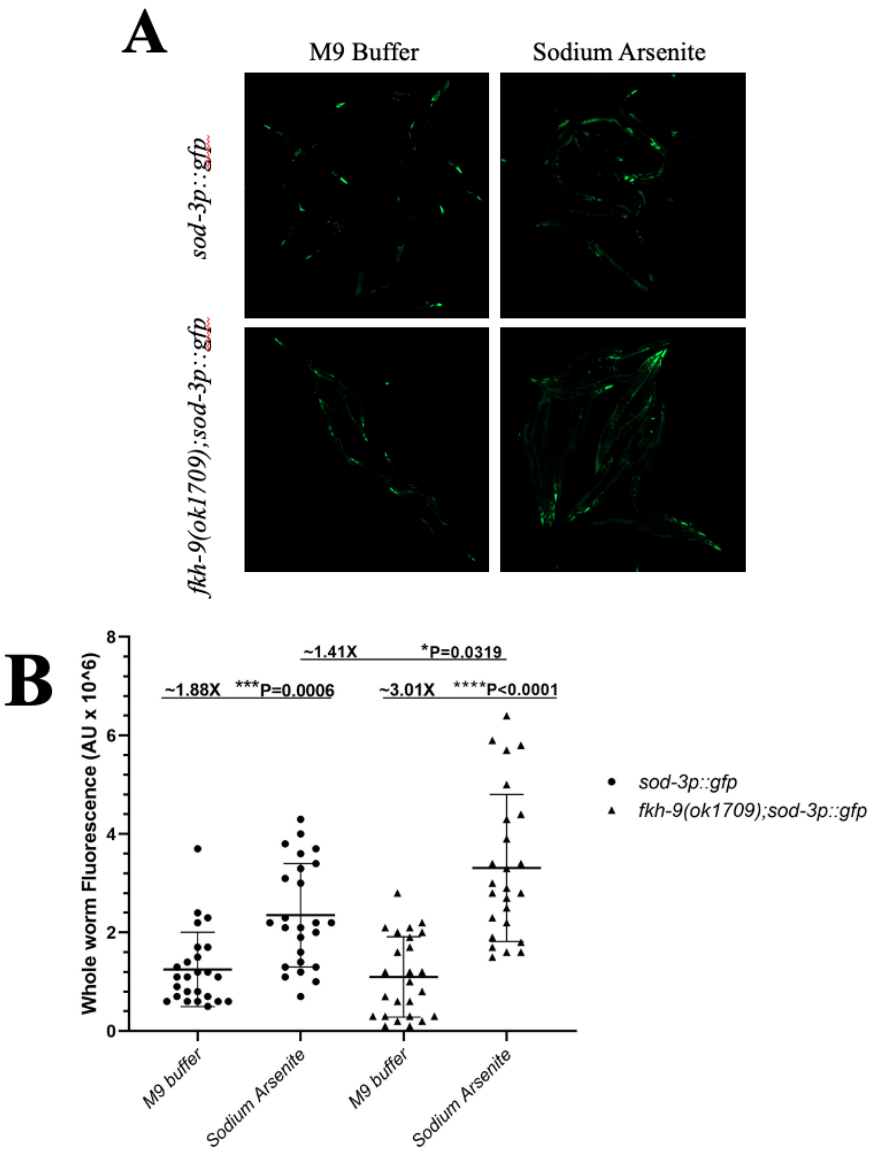

Figure 3.7: *fkh-9(ok1709)* Mutants Show Higher Expression of *sod-3* Compared to WT with Sodium Arsenite Treatment

(A) Whole worm GFP fluorescence was visualized in the *sod-3p::gfp* and *fkh-9(ok1709);sod-3p::gfp* strains with and without As treatment. Fluorescence was captured using the Zeiss Observer Z1 Spinning Disk Confocal Microscope under 20X magnification. **(B)** Fluorescence intensity was quantified using ImageJ Software. Results for n=25 worms are shown as individual points as the difference between the intensity reading per worm minus the background fluorescence. The mean fluorescence intensity is displayed as a solid black line for each worm strain. GFP levels in *sod-3p::gfp* worms treated with As were ~ 1.88 x brighter than when treated with M9 buffer. GFP levels in *fkh-9(ok1709);sod-3p::gfp* worms treated with As were ~ 3.1 x brighter than when treated with M9 buffer. The *fkh-9(ok1709);sod-3p::gfp* worms were ~ 1.41 x brighter than *sod-3p::gfp* when treated with As. Statistical analyses were performed using the Two-tailed Unpaired Student's *t*-test; **** $P < 0.0001$, *** $P < 0.001$, * $P < 0.05$.

3.4 Loss of *fkh-9* Influences Basal and Induced Expression Levels of Non-Phase II Detoxification Genes from the *fmo* Gene Family

After learning that FKH-9 may negatively regulate induced *sod-3* expression through both transgenesis and qRT-PCR, I was curious to see if FKH-9 would influence the expression of other non-phase II detoxification genes. Therefore, I used qRT-PCR to measure the mRNA expression levels of other SOD gene family members (*sod-1, sod*-2), FMO gene family members (*fmo-1, fmo-2, fmo*-3) and *hsp-4* in both N2 WT and *fkh-9(ok1709)* mutants. The purpose of this experiment was to go outside the box of only examining *sod-3* and to see if FKH-9 has a general effect on non-PII genes. I examined these 6 genes with and without As treatment and normalized the data to the *tba-1* housekeeping gene.

Without As treatment, there is a significant difference seen in mRNA levels in *fmo-2* and *fmo-3* specifically. To start with *fmo-2,* there is a significant decrease in expression seen in the *fkh-9(ok1709)* mutants compared to WT without As treatment with a 0.5-fold decrease in expression. However, when treated with As the *fkh-9(ok1709)* mutants exhibit higher mRNA expression levels of *fmo-2,* but still less than WT with a 0.5-fold decrease in expression. Interestingly, when examining *fmo-3* mRNA levels in WT without As treatment, there is a significant 0.9-fold decrease in mRNA expression levels when treated with As. However, similar to *fmo-2,* there is a 0.85-fold decrease in *fkh-9(ok1709)* mutants compared to WT without As treatment, but a 0.7-fold increase in mRNA expression levels in the *fkh-9(ok1709)* mutants compared to WT when treated with As. These results were obtained from 3 independent trials. Overall, FKH-9 seems to be required for basal expression levels of *fmo-2* and *fmo-3* but seems to have repressor-like functions for induced levels of *fmo-2* and activator-like functions for induced levels of *fmo-3.*

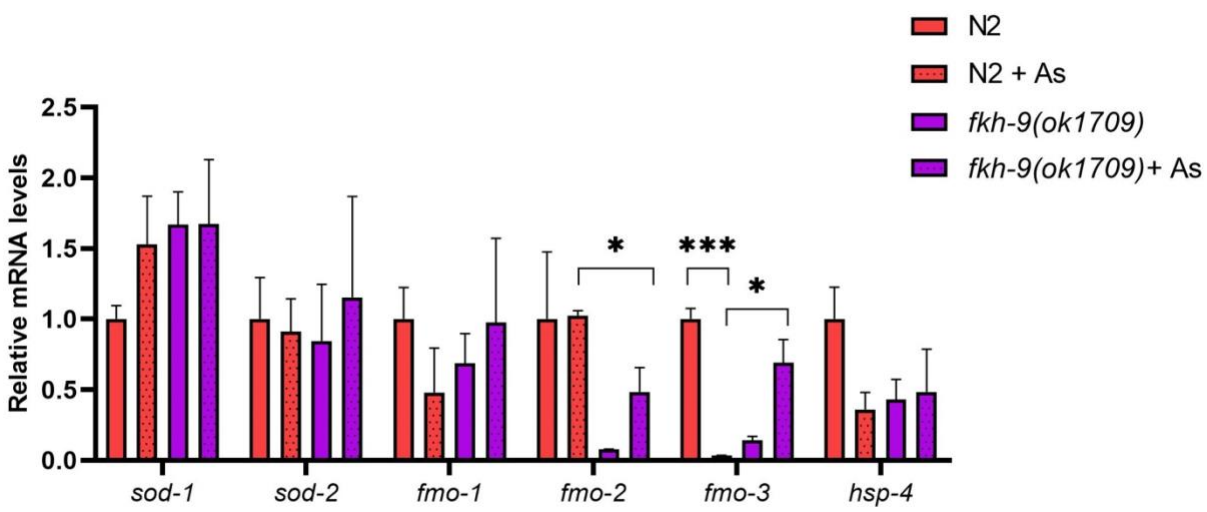

Figure 3.8: *fkh-9(ok1709)* Mutants Show Decreased Levels of *fmo-2* and Increased Levels of *fmo-3* with Sodium Arsenite Treatment

qRT-PCR was done to measure the mRNA levels of non-PII detoxification genes in both N2 WT and *fkh-9(ok1709)* mutant worms with and without As treatment. *fmo-2* mRNA levels were significantly decreased in the *fkh-9(ok1709)* mutants compared to N2 WT when treated with As. *fmo-3* mRNA levels were significantly increased in the *fkh-9(ok1709)* mutants compared to N2 WT when treated with As. Results were derived from 3 independent trials and normalized to the *tba-1* housekeeping gene. Statistical analysis was carried out using Multiple *t*-tests. Error bars represent ± SEM; * $P < 0.05$.

3.5 Loss of *fkh-9* Positively Influences Induced Expression Levels of Mediator *mdt-15*

The SKN-1 transcription factor plays a large role in the cellular signalling pathway that becomes activated during the oxidative stress response as it is the transcriptional activator of the PII detoxification gene *gst-4.* Due to this, I thought it was important to also examine *skn-1* mRNA expression levels as well as SKN-1-associated genes such as *gcs-1* and *mdt-15. gcs-1* is another PII detoxification gene transcriptionally activated by SKN-1. *mdt-15* is part of a mediator complex that is hypothesized to interact with SKN-1 and aid in SKN-1 mediated transcriptional activation. I examined these mRNA levels using qRT-PCR in both N2 WT worms and *fkh-9(ok1709)* mutants with and without As treatment and normalized the results to both the *tba-1* and *cdc-42* housekeeping genes.

Without As treatment, there is no significant difference seen between WT and *fkh-9(ok1709)* mutants when normalized to either housekeeping gene (Figure 3.9 A). Therefore, when the worms are not under oxidative stress, the *fkh-9(ok1709)* mutation does not heavily influence basal mRNA expression levels. However, when the WT and *fkh-9(ok1709)* mutants were treated with As, there was a significant difference seen in mRNA expression levels in *mdt-15* specifically (Figure 3.9 B). There is a 3.3-fold increase in expression seen in the *fkh-9(ok1709)* mutants when normalized to the *tba-1* housekeeping gene and a 3.2-fold increase when normalized to the *cdc-42* housekeeping gene. These results were obtained from 3 independent trials. Overall, these results help suggest that loss of FKH-9 during the oxidative stress response results in an increase in *mdt-15* mRNA expression levels.

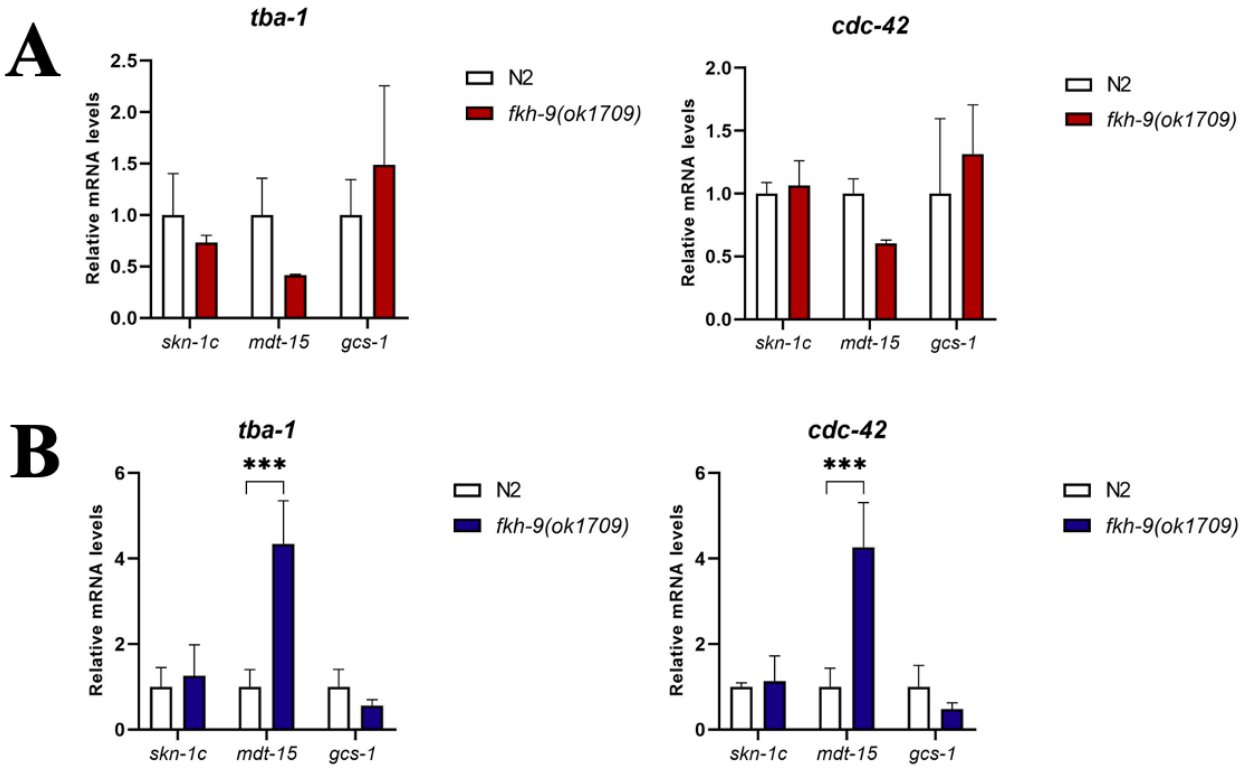

Figure 3.9: *fkh-9(ok1709)* Mutants Show Elevated Levels of *mdt-15* with Sodium Arsenite Treatment

qRT-PCR was done to measure the mRNA levels of *skn-1c* and associated genes in both N2 WT and *fkh-9(ok1709)* mutant worms with **(B)** and without **(A)** As treatment. **(A)** No significant difference was seen in mRNA levels between N2 WT and *fkh-9(ok1709)* mutant worms when normalized to either the *tba-1* or *cdc-42* housekeeping gene. **(B)** With As treatment, *mdt-15* mRNA levels were significantly enhanced in *fkh-9(ok1709)* mutant worms compared to N2 WT when normalized to either the *tba-1* or *cdc-42* housekeeping genes. Results were derived from 3 independent trials. Statistical analysis was carried out using Multiple *t*-tests. Error bars represent ± SEM; *** $P < 0.001$.

3.6 *fkh-9* Expression Levels are not Altered in *brap-2(ok1492)* Mutant Worms

After examining the expression of multiple different genes in *fkh-9(ok1709)* mutants related to the oxidative stress response, it is clear to see that FKH-9 most likely plays a role in induced expression levels of genes specifically. This was seen with As treated worms and also in *brap-2(ok1492)* mutants. Due to this, I wanted to examine *fkh-9* mRNA expression levels in both N2 WT and *brap-2(ok1492)* mutants with and without As treatment.

I hypothesized that one of the reasons as to why the *fkh-9(ok1709)* mutation caused a decrease in *gst-4* expression levels specifically in *brap-2(ok1492)* mutants was because *fkh-9* mRNA expression levels may be elevated in the *brap-2(ok1492)* mutants, especially during the oxidative stress response to aid in the needed expression of *gst-4.* This would help us to understand how and why when *fkh-9* is mutated in the *brap-2(ok1492)* mutants, there is not as much *gst-4* expression. However, when I examined *fkh-9* mRNA expression levels in both N2 WT and *brap-2(ok1492)* mutants with and without As treatment, I did not see a significant difference (Figure 3.10). There is an increase in *fkh-9* mRNA expression levels seen in WT and *brap-2(ok1492)* mutants when treated with As. Even though this difference is not significant, it portrays a trend in both strains with more *fkh-9* expression in oxidative stressful conditions from these 3 independent trials alone. Therefore, this finding requires further investigation to fully examine the effects of induced *fkh-9* mRNA expression levels in both WT and *brap-2(ok1492)* mutant worms.

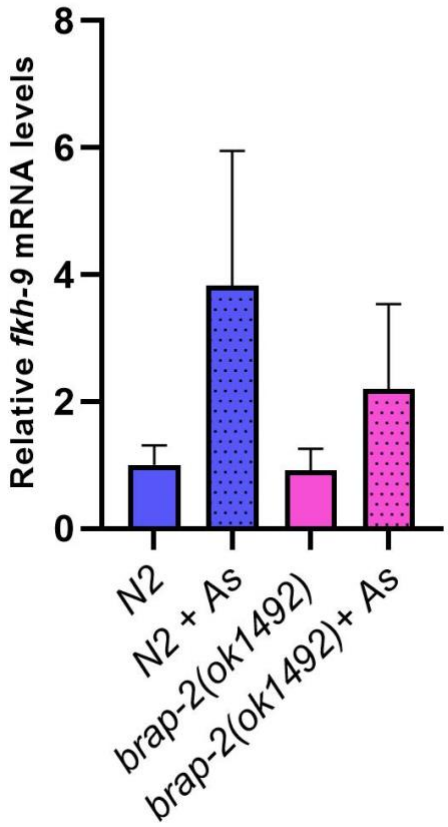

Figure 3.10: *fkh-9* Basal or Induced mRNA Expression Levels are not Altered in WT or *brap-2(ok1492)* Mutant Worms

qRT-PCR was done to measure the mRNA levels of *fkh-9* in both N2 WT and *brap-2(ok1492)* mutant worms with and without As treatment. The difference in *fkh-9* mRNA levels with or without As treatment was not significant in either strain. Results were derived from 3 independent trials and normalized to the *tba-1* housekeeping gene. Statistical analysis was carried out using Multiple *t*-tests. Error bars represent ± SEM.

3.7 FKH-9 Enhances SKN-1 Mediated *skn-1c* Promoter Activation

After conducting past experiments and investigating how FKH-9 affects PI and PII detoxification genes, I wanted to explore where and how FKH-9 may function in the cellular signalling pathway during the oxidative stress response. This tempted me to conduct luciferase assays examining both the *gst-4* (*gst-4p*) and *skn-1c* (*skn-1cp*) promoters.

I first sought to investigate if FKH-9 plays a role at the *gst-4p,* possibly through interaction with SKN-1 to help activate *gst-4* transcription levels. I transfected Human Embryonic Kidney (HEK) 293T cells with a luciferase reporter construct fused to the *gst-4p* along with SKN-1, FKH-9 and both SKN-1 and FKH-9 together. As expected, since SKN-1 is a transcriptional activator of *gst-4,* there was a 380.9-fold increase in luciferase activity compared to the *gst-4p* alone. When I transfected the cells with FKH-9 alone, it was unable to activate the *gst-4p.* Therefore, to test for a possible interaction between SKN-1 and FKH-9 at the *gst-4p,* I transfected them together with the *gst-4p,* but the luciferase activity was not as robustly enhanced as it was when transfected with SKN-1 alone (Figure 3.11 A). These results were obtained from 3 independent trials. Overall, this suggests that FKH-9 most likely does not have a synergistic effect with SKN-1 in activating the PII *gst-4* detoxification gene.

Due to these previous results, I decided to perform another set of luciferase assays, this time to examine the *skn-1cp* and test if FKH-9 possibly acts here instead. I decided to include both SKN-1 and FKH-9 in this luciferase assay, as well as DAF-16 to investigate if DAF-16 would be able to also work in promoting *skn-1cp* activity. I transfected the HEK293T cells with multiple different combinations of the *skn-1cp* and expression plasmids. When transfected with FKH-9 alone, there was no difference in luciferase activity compared to the *skn-1cp* alone. Based on the finding that SKN-1 transactivates itself through binding to the *skn-1cp,* this was observed,

as there was an increase in luciferase activity when transfected with SKN-1 alone. However, compared to this, when transfected with both SKN-1 and FKH-9 there was a 25.6-fold increase in luciferase activity (Figure 3.11 B). This portrayed the highest luciferase activity than any other combination of transfected expression plasmids. SKN-1 and FKH-9 together portrayed a 40.7-fold increase compared to SKN-1 and DAF-16, a 47.2-fold increase compared to FKH-9 and DAF-16, and a 43.5-fold increase compared to SKN-1, FKH-9, and DAF-16. These results were obtained from 3 independent trials. Overall, these results suggest that SKN-1 and FKH-9 may produce a synergistic effect in activating the *skn-1cp*. Figure 3.11C presents a schematic view of showing the reporter gene luciferase expression cassettes along with the interactions at the *skn-1cp*.

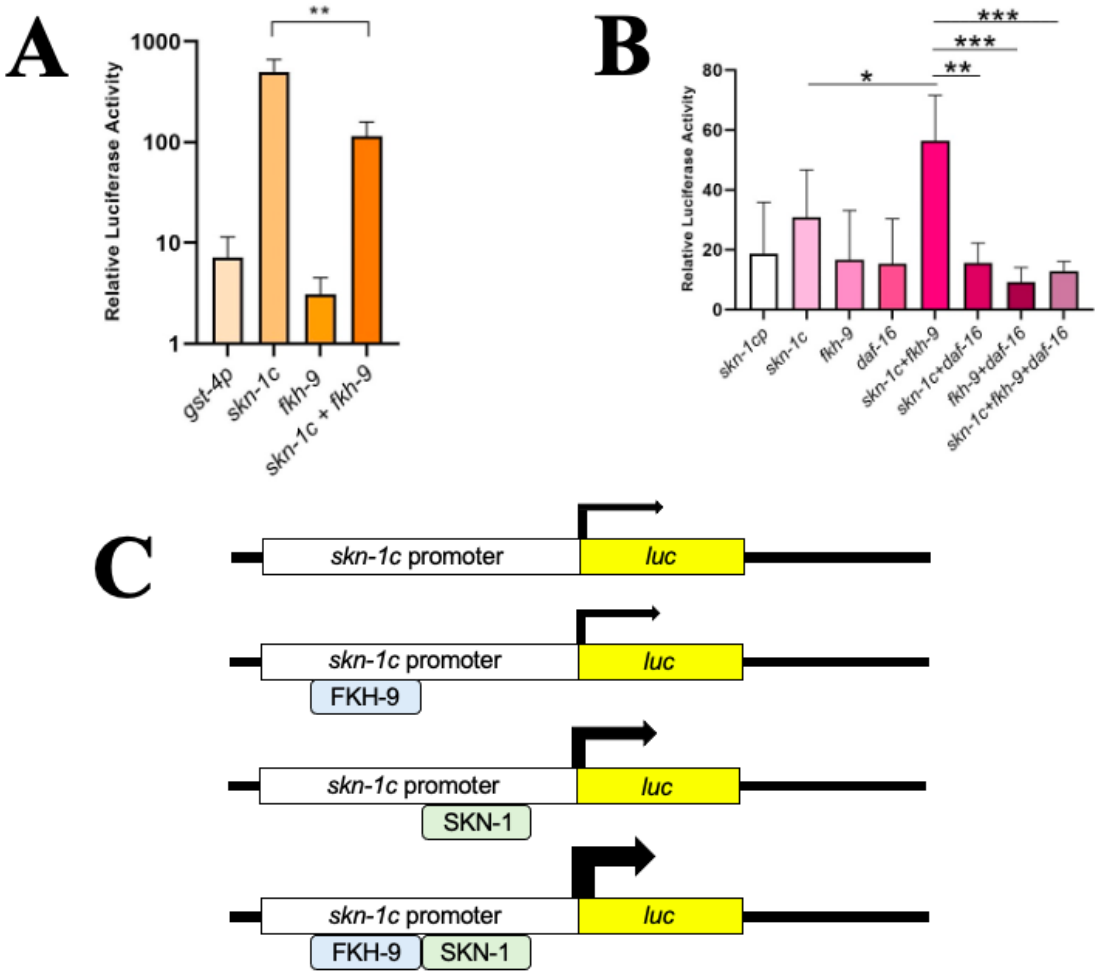

Figure 3.11: Activity of the *skn-1c* Promoter was Robustly Enhanced in the Presence of Both SKN-1 and FKH-9 Suggesting a Synergistic Activating Effect

(A) Results for the Firefly/*Renilla* Dual Luciferase detection assay of the *gst-4* promoter represented as Relative Luciferase Activity. HEK293T cells were co-transfected with either the *gst-4p-luc* plasmid alone, or along with the expression plasmid for SKN-1, FKH-9, or both. SKN-1 significantly enhanced the promoter activity compared to SKN-1 and FKH-9 together. The data was derived from 3 independent trials. Statistical analysis was done using One-way ANOVA; ** $P < 0.01$. **(B)** Results for the Firefly/*Renilla* Dual Luciferase detection assay of the *skn-1c* promoter represented as Relative Luciferase Activity. HEK293T cells were co-transfected with either the *skn-1cp-luc* plasmid alone, or along with the expression plasmid for SKN-1, FKH-9, DAF-16 in multiple combinations. SKN-1 with FKH-9 significantly enhanced the promoter activity compared to SKN-1 alone, SKN-1 with DAF-16, FKH-9 with DAF-16, or SKN-1 with FKH-9 and DAF-16. The data was derived from 3 independent trials. Statistical analysis was done using One-way ANOVA; *** $P < 0.001$, ** $P < 0.01$, * $P < 0.05$. **(C)** Schematic representation of the reporter gene luciferase expression cassettes. Expression of the *luc* gene driven by the *skn-1c* promoter was very low in the absence of the SKN-1 protein but robustly increased in the presence of both SKN-1 and FKH-9 proteins. Thickness of arrows are indicator of robustness at the promoter.

3.8 *fkh-9* Mutants are More Susceptible to Oxidative and ER Stress-Inducing Conditions and Do Not Survive as Long as Wildtype

After examining how PI and PII detoxification genes are affected in the absence of FKH-9, I wanted to determine if there was also a phenotypic difference between *fkh-9(ok1709)* mutants and N2 WT when exposed to different kinds of oxidative stressors. Therefore, I conducted two different oxidative stress assays as well as one ER stress assay to examine the biological role FKH-9 may play in *C. elegans.*

I first conducted an oxidative stress assay using an As solution. A 5mM solution of As was prepared and added to a 24-well plate where 6 wells contained the 5mM As solution; 3 contained the *fkh-9(ok1709)* mutants and 3 contained the WT worms. M9 buffer was used as the control. Worms were scored every hour and the ones that did not respond to prodding were considered dead. Three trials in total were carried out; Figure 3.12A portrays a Kaplan-Meier survival plot for one trial between the *fkh-9(ok1709)* mutants and N2 WT (solid blue and pink lines respectively). There was a significant difference seen in the survivability between the two strains, with WT worms surviving longer in the As solution than the *fkh-9(ok1709)* mutants. The WT population reached 100% mortality by the 12th hour while the *fkh-9(ok1709)* mutants reached 100% mortality by the 9th hour (Figure 3.12A). All worms in the M9 buffer stayed alive over the course of the experiment.

The next oxidative stress assay I conducted included a *tert*-butyl hydroperoxide (tBHP) assay. I poured agar plates containing 7.7 mM tBHP and placed *fkh-9(ok1709)* mutants and N2 WT worms on these unseeded plates. Worms were scored every hour and the ones that did not respond to prodding were considered dead. Three trials in total were carried out; Figure 3.12B portrays a Kaplan-Meier survival plot for one trial between the *fkh-9(ok1709)* mutants and N2 WT (solid purple and red lines respectively). As time started to progress, it was very clear to see

the effect that the tBHP had on the worms as they became much slower and less active almost as if they were paralyzed. There was a significant difference seen in the survivability of the two strains, with WT surviving longer on the tBHP plates than the *fkh-9(ok1709)* mutants. The WT population reached 100% mortality by the 9th hour while the *fkh-9(ok1709)* mutants reached 100% mortality by the 6th hour (Figure 3.12B). NGM plates were used as a control and the worms on these plates stayed alive for the duration of the experiment.

Following this experiment, I decided to carry out an ER stress assay as well using dithiothreitol (DTT). I poured agar plates containing 10 mM DTT and placed *fkh-9(ok1709)* mutants and N2 WT worms on these unseeded plates. Worms were scored every hour and the ones that did not respond to prodding were considered dead. Three trials in total were carried out; Figure 3.12C portrays a Kaplan-Meier survival plot for one trial between the *fkh-9(ok1709)* mutants and N2 WT (solid blue and orange lines respectively). As time started to progress, it was very clear to see the effect that the DTT had on the worms as they not only heavily slowed down but also became stubby and shrunken and would explode at the touch of the wormpick. There was a significant difference seen in the survivability of the two strains, with WT surviving longer on the DTT plates than the *fkh-9(ok1709)* mutants. Although both strains started dying off at the same rate, by the 4th hour the *fkh-9(ok1709)* mutants started dying off in much larger numbers compared to WT. The WT population reached 100% mortality by the 10th hour while the *fkh-9(ok1709)* mutants reached 100% mortality by the 7th hour (Figure 3.12C). NGM plates were used as a control and the worms on these plates stayed alive for the duration of the experiment. Statistical calculations for all three trials of all three assays can be found in Tables 1, 2 and 3 respectively in the appendix.

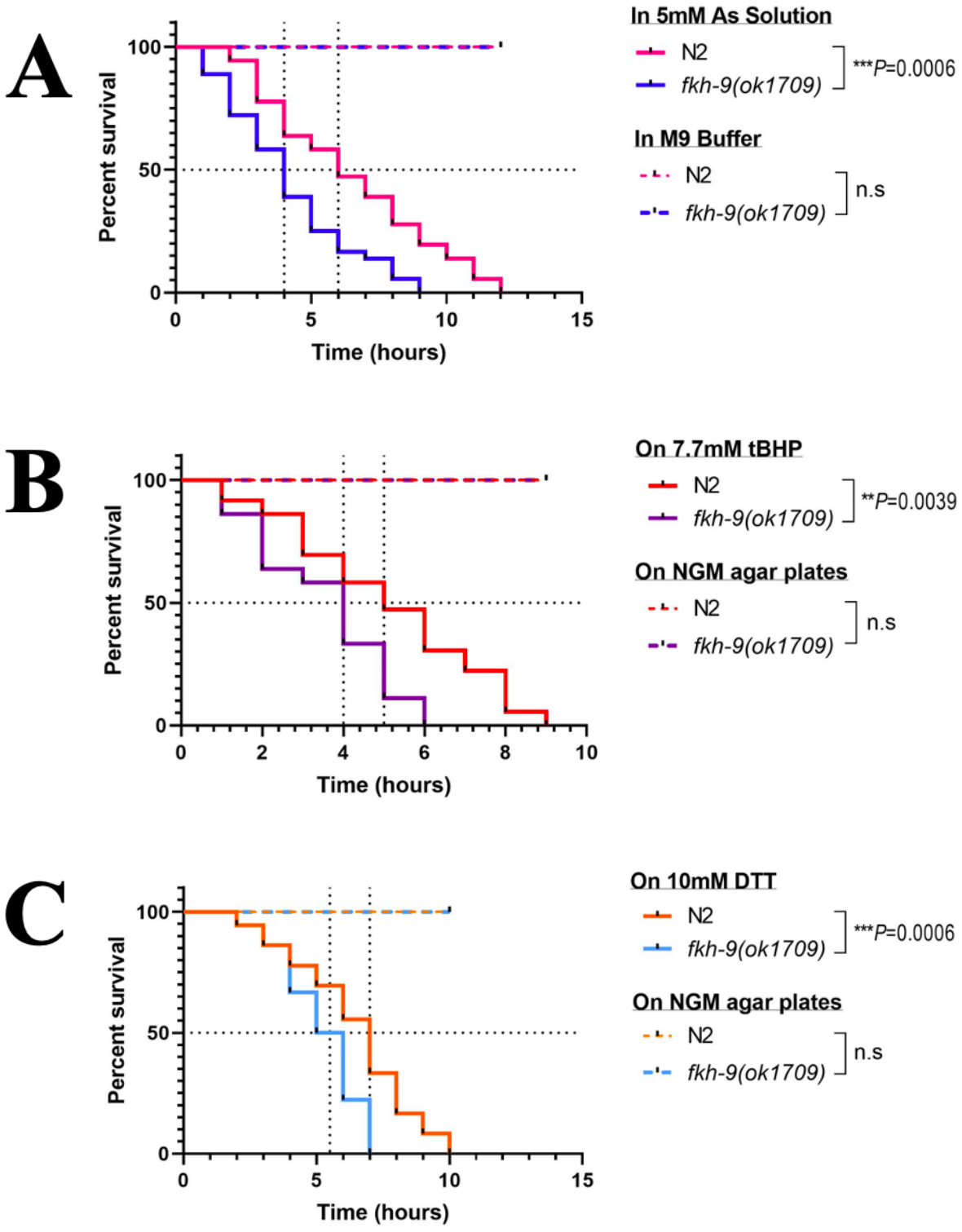

Figure 3.12: *fkh-9(ok1709)* Mutants Exhibited Lower Resistance during Oxidative and ER Stress Assays Compared to WT

See figure caption on next page.

(A) Survival plot of the As-assay comparing *fkh-9(ok1709)* mutants (blue line) to N2 WT worms (pink line) in 5 mM As solution. M9 buffer served as a control. Three independent trials were performed with a sample size of 36 worms for each strain (n=36). N2 median survival was 6 hours and survived 12 hours total. *fkh-9(ok1709)* mutant median survival was 4 hours and survived 9 hours total. For statistical details please refer to Table 1 in the appendix. **(B)** Survival plot of the tBHP-assay comparing *fkh-9(ok1709)* mutants (purple line) to N2 WT (red line) on 7.7 mM tBHP agar plates. Regular NGM plates were used as a control. Three independent trials were performed with a sample size of 36 worms for each strain (n=36). N2 median survival was 5 hours and survived 9 hours total. *fkh-9(ok1709)* mutant median survival was 4 hours and survived 6 hours total. For statistical details please refer to Table 2 in the appendix. **(C)** Survival plot of the DTT-assay comparing *fkh-9(ok1709)* mutants (blue line) to N2 WT (orange line) on 10 mM DTT agar plates. Regular NGM plates were used as a control. Three independent trials were performed with a sample size of 36 worms for each strain (n=36). N2 median survival was 7 hours and survived 10 hours total. *fkh-9(ok1709)* mutant median survival was 5.5 hours and survived 7 hours total. For statistical details please refer to Table 3 in the appendix. For all assays, the survival functions are calculated using the Kaplan-Meier method and the Log-rank (Mantel-Cox) test was used to calculate significance and P-values; *** $P < 0.001$, ** $P < 0.01$. Data represents one trial for each and was analyzed using the online survival analysis program OASIS®.

3.9 *fkh-9* Mutation Shortens Lifespan and Cannot Live as Long as Wildtype

To further explore the biological role that FKH-9 may play in *C. elegans,* I also conducted longevity assays to see how long *fkh-9(ok1709)* mutants can live compared to N2 WT worms. Worms were scored every day and the ones that did not respond to prodding were considered dead. Worms were regularly transferred to fresh NGM plates to avoid crowding and starvation until they stopped laying eggs. Three trials in total were carried out; Figure 3.13 portrays a Kaplan-Meier survival plot for one trial between the *fkh-9(ok1709)* mutants and N2 WT (purple and green lines respectively). There was a significant difference seen in the longevity of the two strains, with WT living longer than the *fkh-9(ok1709)* mutants. The WT population reached 100% mortality by day 40 while the *fkh-9(ok1709)* mutants reached 100% mortality by day 27 (Figure 3.13C). Statistical calculations for all three trials can be found in Table 4 in the appendix.

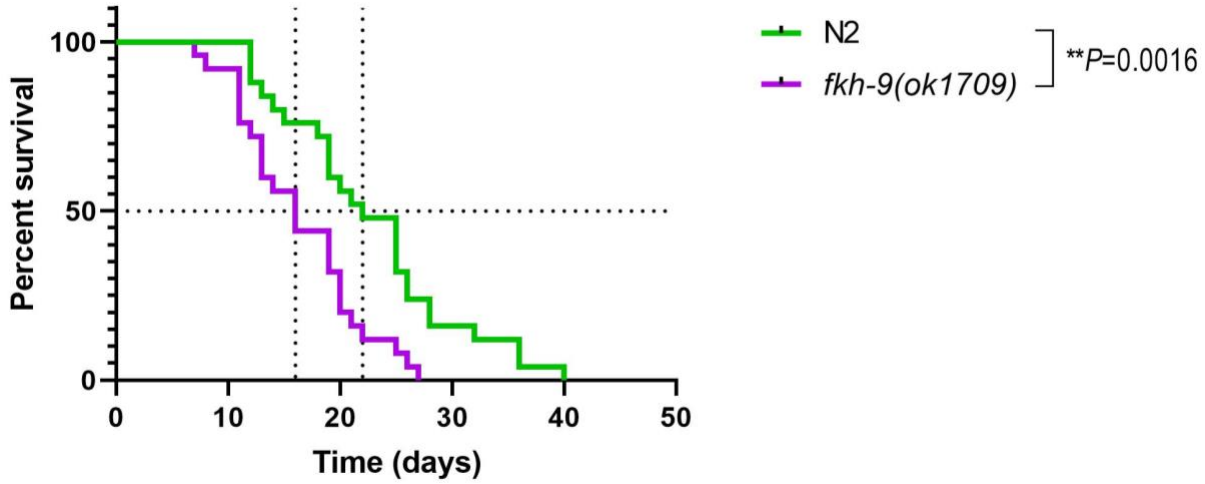

Figure 3.13: *fkh-9(ok1709)* Mutants Do Not Live as Long as WT

Survival plot representing the lifespan of *fkh-9(ok1709)* mutants (purple line) and N2 WT worms (green line). Three independent trials were performed with a sample size of 25 worms for each strain (n=25). N2 median lifespan was 22 days and lived until day 40. *fkh-9(ok1709)* mutant median lifespan was 16 days and lived until day 27. For statistical details please refer to Table 4 in the appendix. The estimates of the longevity functions are calculated using the Kaplan-Meier method whereas the Log-rank (Mantel-Cox) test was used to calculate significance and P-values. ** $P < 0.01$. Data represents one trial and was analyzed using the online survival analysis program OASIS®.

CHAPTER 4: DISCUSSION

4.0 Discussion:

4.1 Summary

The main purpose of this project was to determine the role of FKH-9 in the *C. elegans* oxidative stress response and how vital it is for *C. elegans* survival against oxidative stress and lifespan. In order to investigate this, I used various methods to examine different areas such as GFP fluorescence imaging, qRT-PCR, luciferase assays and various biological assays. I have thus gathered valuable information providing initial insight into the potential role of the FKH-9 transcription factor. Throughout this project, I have learned that FKH-9 positively regulates induced expression levels of *gst-4* in *brap-2(ok1492)* deletion mutants. The way in which FKH-9 achieves this effect is potentially through interaction with SKN-1 at the *skn-1c* promoter to help enhance expression. I have also learned that FKH-9 negatively regulates induced expression levels of *sod-3,* and generally regulates expression levels of other PI and PII detoxification genes as well. In addition to this, I learned about the biological role of FKH-9 using survival and longevity assays. The *fkh-9(ok1709)* deletion mutation causes a decrease in survivability against multiple stress-inducing agents and causes shortened lifespan overall. Therefore, this chapter will involve an in-depth and thorough discussion about all results found in an attempt to gain a better understanding of FKH-9's mechanism of action in the *C. elegans* oxidative stress response.

4.2 FKH-9 as a Transcription Factor that Positively Regulates Induced Expression Levels of *gst-4* in *brap-2(ok1492)* Mutants Potentially through the Enhancement of SKN-1 Mediated *skn-1c* Promoter Activation

The aim of our lab is to elucidate cellular mechanisms that contribute too and play an overall role in the oxidative stress response. It is critical for all organisms to have an efficient ROS detoxification system for healthy aging and longevity. Therefore, we use *C. elegans* as a model organism, to help us understand and identify as many factors involved in combating

oxidative stress. Various and complex cellular signaling pathways are known to be involved and regulated during the oxidative stress response. Transcription factors specifically are known to be a part of these pathways, often being able to regulate biological processes through their interaction with DNA. Therefore, by investigating their roles it helps us to uncover new regulatory mechanisms that aid in our understanding of how transcription factors function in relation to cellular mechanisms. Our lab aims to identify novel candidates involved in stress responses and the underlying genetics of oxidative stress, aging, and longevity. We aim to form genetic links between novel transcription factors and well-known major players involved in ROS detoxification. In accordance with this, I aimed to identify the role of transcription factor FKH-9 in relation to the cytoplasmic retention protein BRAP-2, the transcription factor SKN-1 and the PII detoxification enzyme GST-4.

As previously mentioned, BRAP2 (BRCA1 binding protein) in mammals has been characterized as a Ras effector protein due to its ability to inhibit the KSR scaffold protein and prevent the signal cascade from occurring (Matheny et al., 2004). On the other hand, the Nrf2 transcription factor has been reported to regulate phase II detoxification enzymes via nuclear translocation under the control of the Ras signaling pathway (He et al., 2020). Since BRAP-2 is the *C. elegans* ortholog of the mammalian BRAP2 and SKN-1 is the *C. elegans* ortholog of mammalian Nrf2, it is hypothesized that BRAP-2 may regulate SKN-1 nuclear localization through similar mechanisms as it does in mammalian cells. Our lab previously demonstrated a genetic interaction between *brap-2* and *skn-1*. In *brap-2(ok1492)* mutants, there is a high presence of nuclear-localized SKN-1 along with elevated expression levels of SKN-1 target genes. This ultimately illustrates that BRAP-2 can down-regulate expression levels of SKN-1 target genes by negatively regulating SKN-1 nuclear localization (Hu et al., 2017).

Among the PII detoxification enzymes, expression levels of *gst-4* were most affected by *brap-2* mutations in *C. elegans.* This makes sense as SKN-1 is a main transcriptional activator of *gst-4.* PII detoxification enzymes exert major protective roles against both endogenously and exogenously produced toxins, and GSTS specifically have one of the most prominent roles in neutralizing ROS damage. Due to this, the lab previously conducted a transcription factor RNAi screen on *brap-2(ok1492)* mutants and observed that with the knockdown of *fkh-9, gst-4* expression levels were reduced. Thus, this gave an initial suggestion that FKH-9 may be involved in the SKN-1 mediated regulation of *gst-4.* To begin my investigation into this initial finding, I started by examining *gst-4p::gfp* levels in WT and *fkh-9(ok1709);gst-4p::gfp* transgenic worms to see if the *fkh-9(ok1709)* mutation had an effect on *gst-4* levels (subsequently examined through GFP fluorescence).

I examined these two worm strains first with a 2-hour treatment in M9 buffer as a control, and then with a 2-hour treatment with sodium arsenite (As). I did this first before working with *brap-2(ok1492)* mutants directly simply as another means to examine induced *gst-4* expression; As exposure causes oxidative stress to the worms by generating ROS. Specifically, As causes the BLI-3/NADPH oxidase complex to produce ROS at the ER or through the mitochondria. Subsequent sulfenylation at a cysteine site within the IRE-1 kinase activation loop induces SKN-1 activation (Hourihan et al., 2016). This therefore alters the expression of genes related to the stress response and antioxidant activities. Throughout this project, I used As multiple times as a way to evaluate induced gene expression, as this created an oxidative stressful environment for the worms compared to no treatment (basal gene expression).

With M9 buffer treatment, the *gst-4p::gfp* levels in both the WT and *fkh-9(ok1709);gst-4p::gfp* mutant strain were low (Figure 3.1 A, B). This was expected as worms treated with M9

buffer would exhibit basal expression levels of detoxification genes since the worms are not under oxidative stress and these enzymes are therefore not needed. However, when examining induced levels of *gst-4* with As treatment, the GFP fluorescence levels in both strains significantly increased (Figure 3.1 A, B). This was expected since As causes oxidative stress to the worms. However, the *fkh-9(ok1492)* mutation alone did not hinder *gst-4* expression significantly. The *fkh-9(ok1709);gst-4p::gfp* strain does portray a slight decrease in GFP fluorescence, however this difference is not significant (Figure 3.1 B). To examine this further, I then performed qRT-PCR on both N2 WT and *fkh-9(ok1492)* mutants with and without As treatment to examine *gst-4* mRNA expression levels. The results obtained here matched up to the confocal imaging of the *gst-4p::gfp* fluorescence levels. As expected, basal *gst-4* levels in WT and *fkh-9(ok1492)* mutants were low but significantly increased when treated with As. Although the *fkh-9(ok1492)* mutants portrayed a slight decrease in *gst-4* mRNA expression, it is not significant compared to WT (Figure 3.2 A, B).

I started my research project in this way, by simply examining the effects that the *fkh-9(ok1709)* mutation would possibly have on *gst-4* expression. This was done to see if this mutation was strong enough alone to have a significant impact on this PII detoxification gene. After not seeing a significant difference between the *fkh-9(ok1709)* mutants and WT, I decided to confirm the previous RNAi screening results the lab performed on the *brap-2(ok1492)* mutants to see the effect FKH-9 would have on *gst-4* expression. I started with examining the *gst-4p::gfp* levels in WT and *brap-2(ok1492);gst-4p::gfp* strains with and without *fkh-9* RNAi (using the pL4440 vector as a control). When first examining the *gst-4p::gfp* WT strain, basal *gst-4* levels (treated with pL4440) were low, which was expected. Following this, I then treated the worms with the *fkh-9* RNAi. This was another way to examine FKH-9 manipulation and its

effect on *gst-4* expression levels to coincide with the creation of the *fkh-9(ok1709);gst-4p::gfp* transgenic line. It was interesting to examine the GFP fluorescence with *fkh-9* mutated and then again with *fkh-9* knocked down. Again as expected, the *gst-4p::gfp* strain with the *fkh-9* RNAi portrayed very low GFP fluorescence similar to the control vector (Figure 3.3 A, B). This was also seen when examining basal (M9 buffer treatment) GFP fluorescence in the *fkh-9(ok1709);gst-4p::gfp* mutant strain; having FKH-9 essentially non-functional alone does not seem to drastically affect *gst-4* levels. However, examining the *brap-2(ok1492);gst-4p::gfp* strain showed a significant difference between treatment with the pL4440 control vector and the *fkh-9* RNAi. As already known, the *brap-2(ok1492)* mutation causes an increase in *gst-4* expression levels which was observed, as GFP fluorescence greatly increased. However, when treated with the *fkh-9* RNAi, the GFP fluorescence levels significantly decreased (Figure 3.3 B). Ultimately, with the *fkh-9* knockdown there is not as much *gst-4* expression seen compared to when *brap-2(ok1492)* is mutated alone and treated with the pL4440 control vector. This helps indicate that *fkh-9* is required for the *brap-2(ok1492)* mutants to keep their *gst-4* expression levels elevated.

Once I had the previous RNAi screen confirmed, I wanted to examine this further and in a different way by looking at the *gst-4* mRNA expression levels. Using qRT-PCR, I examined this in the *brap-2(ok1492)* mutants and the *brap-2(ok1492);fkh-9(ok1709)* double mutants with and without As treatment. When normalized to either the *tba-1* or *cdc-42* housekeeping gene, the *gst-4* mRNA expression levels increase significantly in the *brap-2(ok1492)* mutants, which again was expected. However, the main takeaway from this experiment was the difference seen between the *brap-2(ok1492)* mutants and the *brap-2(ok1492);fkh-9(ok1709)* double mutants. The *gst-4* mRNA expression levels decrease significantly with *fkh-9* mutated along with *brap-*

2(ok1492) (Figure 3.4 A). This was also seen with As treatment, normalized to either the *tba-1* or *cdc-42* housekeeping gene (Figure 3.4 B). This result matched up with the GFP fluorescence images and illustrates that *fkh-9* is an essential gene for *brap-2(ok1492)* mutants to express elevated/induced levels of *gst-4* mRNA.

Although the RNAi experiments and qRT-PCR portrayed the same trend in results with how manipulation of *fkh-9* can affect *gst-4* levels, it is still important to understand why they do not portray the exact same data. There is a difference between a gene knockdown and a gene knockout. Mutations can permanently prevent the expression of target genes while RNAi achieves complete silence of gene expression or partial reduction of gene expression (Han, 2018). In the case of the *fkh-9* RNAi treatment, it induces a partial reduction in expression levels of *fkh-9* in *C. elegans*. This is of course different from a homozygous *fkh-9(ok1709)* mutation, as with the RNAi there is still some *fkh-9* expression. Therefore, examining knockouts with qRT-PCR and knockdowns with RNAi are two great methods for examining the effect that the manipulation of a specific gene may have, but overall may not show the exact same results to the same degree.

After seeing the effects that *fkh-9* had on *gst-4* expression in the *brap-2(ok1492)* mutants, I wanted to try and understand why this occurred and what role FKH-9 may be playing in the oxidative stress response. Due to the results seen on how the mutation or knockdown of *fkh-9* can hinder expression of *gst-4* in *brap-2(ok1492)* mutants, this indicated that when FKH-9 is fully functional in the *brap-2(ok1492)* mutants, it plays a role in helping to induce *gst-4* expression levels. One possible explanation for this could be an upregulation of *fkh-9* in *brap-2(ok1492)* mutants that subsequently leads to the upregulation of *gst-4* levels. For example, recent literature has shown *skn-1* and its subsequent target genes to be upregulated during the

oxidative stress response (Park et al., 2009). To examine if this was the possible case with *fkh-9* as well, I examined *fkh-9* mRNA expression levels in *brap-2(ok1492)* mutants along with N2 WT both with and without As treatment (Figure 3.10). In this way, I was able to examine both basal and induced expression levels of *fkh-9.* However, my results did not indicate an upregulation of *fkh-9* mRNA levels as no significant difference was seen. Even though this difference is not significant, there is a trend in both strains with more *fkh-9* expression in oxidative stressful conditions from the As treatment. Therefore, this finding requires further investigation to fully examine induced *fkh-9* mRNA expression levels.

Previous studies have shown that the *brap-2(ok1492)* mutation increases SKN-1 localization into intestinal nuclei and subsequent expression of PII detoxification genes, revealing BRAP-2 as a negative regulator of SKN-1 (Hu et al., 2017). Specifically, Hu et al., 2017 revealed that SKN-1 recognizes the *gst-4* promoter and enhances promoter activity through work with luciferase assays. Hu et al., 2017 was also able to discover that the transcription factor known as ELT-3 upregulates expression levels of *gst-4* and dimerizes with SKN-1 to enhance SKN-1 mediated regulation of *gst-4*. Therefore, in *brap-2(ok1492)* mutants the main explanation for why *gst-4* levels increase significantly could be due to SKN-1's translocation into the nucleus and subsequent activation of PII detoxification genes. Due to this, I wanted to examine if FKH-9 possibly has an interactive role with SKN-1 at the *gst-4* promoter. I performed luciferase assays and found that SKN-1 could enhance the *gst-4* promoter significantly (Figure 3.11 A). However, with FKH-9 added along with SKN-1, there is a significant drop in *gst-4p* luciferase activity. Due to this, this gave an indication that FKH-9 most likely does not work with SKN-1 at the *gst-4* promoter to enhance *gst-4* expression. Therefore, I moved on to examining the *skn-1c* promoter. As previously mentioned, SKN-1 has isoforms and SKN-1C is the main transcription

factor that regulates the oxidative stress response. Recent findings have shown that SKN-1 can transactivate its own promoter activity (Blackwell et al., 2015). Just as I tested the effect of SKN-1 + FKH-9 at the *gst-4* promoter, I did the same with the *skn-1c* promoter. Using luciferase assays, I found that FKH-9 synergistically enhances SKN-1 mediated *skn-1c* promoter activity. In other words, the *skn-1c* promoter activity significantly increased with SKN-1 + FKH-9 transfected together rather than with SKN-1 transfected alone (Figure 3.11 B). This finding indicates that FKH-9 is potentially involved in regulating the expression of *skn-1c* which subsequently goes on to regulate the expression of PII detoxification genes. However, when performing this luciferase assay, I decided to incorporate not only SKN-1 and FKH-9, but also DAF-16 to see if I could find another link between all three transcription factors. DAF-16, like SKN-1, is a very important transcription factor that acts during oxidative stress to transcriptionally activate PI genes such as *sod-3* for example (Senchuk et al., 2018). Various links between SKN-1 and DAF-16 have also been discovered in recent literature. For example, constitutive activation of SKN-1 or *skn-1* gain of function mutations have been seen to suppress DAF-16, however SKN-1 inhibition was also found to activate DAF-16 (Deng et al., 2020). This suggests that SKN-1 has dual roles as an activator of oxidative stress resistance genes but also as a possible negative regulator of DAF-16. Recent literature has also shown a parallel with SKN-1 and DAF-16 in terms of the IIS signaling pathway. The IIS kinases, AKT-1/2 are able to phosphorylate DAF-16 to keep it sequestered in the cytoplasm, but also phosphorylates SKN-1 to prevent its nuclear accumulation and subsequent target gene activation (Tullet et al., 2008). Due to this, I was curious to see if there was a link between SKN-1 and DAF-16 with FKH-9 at the *skn-1c* promoter. However, my results did not indicate a synergistic effect between these

transcription factors, indicating that DAF-16 most likely does not promote *skn-1c* transcriptional activation.

The luciferase assay is a great tool to use to examine if a protein can activate the expression of a target gene using luciferase as a reporter protein. Using this assay, I was able to observe a synergistic effect between SKN-1 and FKH-9 at the *skn-1c* promoter. This ultimately gives great indication and understanding of the role FKH-9 may play in the oxidative stress response. Due to this, I also decided to examine the mRNA expression levels of *skn-1* and SKN-1-associated genes in both N2 WT and *fkh-9(ok1492)* mutants. Therefore, along with *skn-1*, I examined mRNA expression levels of *gcs-1* and *mdt-15. gcs-1* is another important PII detoxification gene that is known to be transcriptionally activated by *skn-1* (Inoue et al., 2005). MDT-15 is part of a conserved mediator complex which is required for oxidative stress responses in *C. elegans*. Recent literature has shown that *mdt-15* is required for the expression of genes in a SKN-1 dependent manner as there is a significant overlap in SKN-1 and MDT-15-dependant genes where several genes respond similarly to both *skn-1* and *mdt-15* depletion (Goh et al., 2014). Specifically, MDT-15 primarily affects *gcs-1* and *gst-4* expression levels like SKN-1 does (Goh et al., 2014). This suggests that MDT-15 and SKN-1 directly coregulate some detoxification genes. Following this, using the yeast-two-hybrid system, a domain in MDT-15 was seen to bind to SKN-1 strongly and specifically (Goh et al., 2014). I examined these three genes both with and without As treatment. Without As treatment, there was no significant difference seen in gene expression between WT and *fkh-9(ok1492)* mutants (Figure 3.9 A). However, with As treatment *mdt-15* mRNA expression levels significantly increased in *fkh-9(ok1492)* mutants (Figure 3.9 B). As previously seen with the luciferase assays, FKH-9 may work synergistically with SKN-1 to increase *skn-1c* transcriptional levels. SKN-1 is of course

needed when the cell is under oxidative stress to transcriptionally activate PII detoxification genes. Since MDT-15 possibly works with SKN-1 to aid in this transcriptional activation of its target genes, the reason for the large increase in *mdt-15* mRNA expression levels in the *fkh-9(ok1492)* mutants could be due to a feedback mechanism. With *fkh-9* mutated, there may not be as much SKN-1 present in the cell and therefore *mdt-15* expression levels may increase to make up for this and aid in SKN-1 mediated activation of PII genes to help reduce levels of ROS.

4.3 FKH-9 as a Transcription Factor that Negatively Regulates Induced Expression Levels of *sod-3*

After investigating the role of FKH-9 in the *brap-2(ok1709)* mutants in terms of *gst-4* expression, I wanted to explore if FKH-9 also influenced PI detoxification genes. PI enzymes are involved in the first step of the detoxification process as they work before the PII enzymes. For example, PI enzymes can act to break down xenobiotics in the liver, but this results in a by-product of ROS (Aronica et al., 2022). Ultimately, PI enzymes can solubilize targets by oxygen molecule transfer but then PII enzymes must work to catalyze the conjugation on the targets to neutralize ROS reactivities. PIII of the detoxification process simply involves the elimination phase in which ROS molecules are now able to be pumped out of the cell and excreted from the body. An important family of PI detoxification enzymes include SODs known as superoxide dismutase. SODs can detoxify superoxide, which is one form of ROS and are therefore crucial players in the *C. elegans* oxidative stress response. *C. elegans* possess many different *sod* genes, and an important gene from this family includes *sod-3* that is usually found in the mitochondrial matrix. As previously mentioned, *sod-3* is an important antioxidant gene that gets transcriptionally activated by DAF-16. DAF-16 is a target of the IIS signaling pathway in which ILS and cytokines can activate the *daf-2* receptor which leads to the phosphorylation of DAF-16 by AKT-1/2 and results in DAF-16 sequestration in the cytoplasm. However, when the cell is

under oxidative stress, DAF-16 will get phosphorylated to translocate into the nucleus where it will transcriptionally activate important detoxification genes such as *sod-3.* Due to this, SOD-3 is another detoxification enzyme that the lab studies along with GST-4.

I wanted to test whether FKH-9 would have any effect on *sod-3* expression the way it did with *gst-4* expression. Therefore, I started by examining the mRNA expression levels of both *sod-3* and *daf-16* in N2 WT and *fkh-9(ok1492)* mutants with and without As treatment. Without As treatment, there was no significant difference seen in mRNA expression levels as expected (Figure 3.6 A). However, very interestingly, with As treatment the levels of *daf-16* increased in the *fkh-9(ok1492)* mutants while the *sod-3* expression levels significantly increased compared to WT (Figure 3.6 B). Since DAF-16 is the transcriptional activator of *sod-3* it makes sense that an increase in *daf-16* causes an increase in *sod-3.* Due to this finding, I wanted to examine this further through a visual aid. Therefore, I created another transgenic line *fkh-9(ok1709);sod-3p::gfp* and examined the GFP fluorescence in comparison to WT both with and without As treatment. I examined these two worm strains first with a 2-hour treatment in M9 buffer as a control, and then with a 2-hour treatment in As just as I did in previous experiments. It is important to note that when examining *sod-3p::gfp* in *C. elegans*, we see the fluorescence at the head and tail region. This is because SOD-3 is mainly expressed in the pharynx in the head and in the tail, however expression still occurs in the intestine and muscle (Zhao et al., 2016). When treated with M9 buffer, both strains portrayed relatively low GFP fluorescence which was expected since the worms were not under oxidative stress. However, when treated with As the GFP fluorescence increased significantly in the WT strain but increased even more in the *fkh-9(ok1709);sod-3p::gfp* mutant strain (Figure 3.7 A, B). This matched up with the qRT-PCR results seen in terms of increased expression of *sod-3* in the *fkh-9(ok1709)* mutants.

This finding was very fascinating due to the opposite effect it has here compared to on *gst-4.* The *fkh-9(ok1709)* mutation in *brap-2(ok1492)* mutants caused a decrease in *gst-4* expression, while the *fkh-9(ok1709)* mutation alone caused an increase in *sod-3* expression with sodium arsenite treatment. This tells me that the FKH-9 transcription factor may serve as both an activator and repressor in terms of PI and PII detoxification genes, therefore exhibiting a dual role overall. My initial thought into how FKH-9 may repress *sod-3* expression is through its role in working with SKN-1 to increase *skn-1c* levels. For example, as previously mentioned SKN-1 has been seen to be a negative regulator of DAF-16, but if FKH-9 is mutated and there is not as much SKN-1 being transcriptionally activated, then DAF-16 would become highly active and able to transcriptionally activate *sod-3.* Another possible explanation could be that FKH-9 plays a role in the IIS signaling pathway since this is one pathway that regulates DAF-16. FKH-9 could cause the inhibition of DAF-16 and its subsequent sequestration in the cytoplasm, preventing *sod-3* expression. For example, recent literature has identified a *C. elegans* protein known as EAK-7 that inhibits DAF-16 and is therefore a FoxO regulator (Alam et al., 2010). A mutation in *eak-7* increases nuclear DAF-16 activity and in this case, *eak-7* mutants also exhibited increased levels of *sod-3* mRNA (Alam et al., 2010). It is possible that FKH-9 may act in a similar manner. However, it is also possible that FKH-9 may not affect DAF-16 and instead target *sod-3* directly. FKH-9 may act as a transcriptional repressor to decrease transcriptional activation of *sod-3*, resulting in less SOD-3 expression overall. This would help explain why the *fkh-9(ok1709)* mutation resulted in significantly higher expression levels of *sod-3*, seen with both qRT-PCR and GFP fluorescence imaging. Overall, further investigation is needed to fully understand the repressive role FKH-9 may play in DAF-16 and SOD-3 expression.

4.4 Initial Insight into the Role of FKH-9 on Expression Levels of Other Phase I and Phase II Detoxification Genes

After examining the effects that FKH-9 has on two major detoxification enzymes (GST-4 and SOD-3), I decided to also investigate the effects that FKH-9 may have on other PI and PII detoxification genes. Therefore, qRT-PCR was carried out to examine the mRNA expression levels in N2 WT and *fkh-9(ok1709)* mutants with and without As treatment as an act to gain initial insight on the possible effects FKH-9 may have on detoxification genes overall. To start off, I examined other PII detoxification genes such as *ugt-13, gsto-2, dhs-8,* and *sdz-8.* UGT-13 is another important PII detoxification enzyme that conjugates a reduced form of UDP to ROS to form glucuronides and thus reduce ROS overall (Blackwell et al., 2015). In this way, it works very similarly to *gst-4* by removing free radicals through conjugation. While GST-4 and UGT-13 work on the radicals directly through conjugation to remove ROS, GSTO-2 does not work in this same way. GSTO1 is the mammalian ortholog of GSTO-2 and GSTO1 detoxifies As in the human body. In order to metabolize As in the body, a series of reduction reactions must occur along with methylation events. GSTO1 reduces MMA^{V} (MonoMethylArsonic acid) to MMA^{III} (MonoMethylArsonous acid) which are then excreted through urine (Rodrigues et al., 2012). Therefore, if GSTO-2 works on ROS by reducing the amount of toxic MMA^{V} in *C. elegans*, then this means it focusses on removing As itself rather than the free radicals. I also examined *dhs-8* mRNA expression levels which is the mammalian WWOX ortholog. WWOX enzymes are WW domain-containing oxidoreductases that have been seen to have a relation to mitochondria and ROS (O'Keefe et al., 2011). Specifically, WWOX is needed to prevent mitochondrial dysfunction and remove free radicals. This means that it may play a role in removing ROS specifically generated from mitochondrial dysfunction instead of ROS generated from As. SDZ-8 is the *C. elegans* ortholog of CBR3 which is an NADPH (Reduced form of Nicotinamide

Adenine Dinucleotide Phosphate) dependent reductase. CBR3 catalyzes the reduction of carbonyl substrates using NADPH and H^+ (López De Cerain et al., 1999). It is also important to note that CRB3 is under the control of Nrf2 which upregulates expression levels of CRB3 during As-induced oxidative stress. Therefore, SDZ-8 is most likely SKN-1-dependant and may resolve oxidative stress by catalyzing the reduction of carbonyl substrates using NADPH and free radicals produced by As.

When I examined these genes without As treatment, mRNA expression levels were fairly low as was expected. Specifically, when the data was normalized to the *cdc-42* housekeeping gene, there was significantly lower expression of *dhs-8* and *sdz-8* in the *fkh-9(ok1709)* mutants (Figure 3.5 A). This shows that FKH-9 may be required for basal expression levels of these two detoxification genes specifically. However, with As treatment there is a significant increase in *dhs-8* mRNA expression levels when normalized to the *tba-1* housekeeping gene with higher expression seen in the *fkh-9(ok1709)* mutants (Figure 3.5 B). Therefore, when the cell is under oxidative stress FKH-9 may play a repressive role in *dhs-8* mRNA expression specifically. This again shows the duality of FKH-9, that it may act as both an activator and a repressor during different cellular conditions. It is also interesting to note that *sdz-8* acts on As-induced ROS and is SKN-1 dependent, just as *gst-4* is; we see FKH-9 as an activator for this gene just as we do with *gst-4.* However, *dhs-8* acts on ROS created by mitochondrial dysfunction specifically, instead of from As. In this case we see FKH-9 act as a possible repressor for this gene. Therefore, it is possible that FKH-9 may take on more of an activator role for PII detoxification enzymes that directly work on free radicals generated from As instead of the ones generated from mitochondrial dysfunction. However, this is just a postulated hypothesis based on these three trials completed of qRT-PCR. Regardless, this

experiment provides an initial suggestion that FKH-9 may affect PII detoxification genes and is not specific to only *gst-4.* Much further investigation is needed in order to fully understand the possible role FKH-9 may take on in terms of the expression of these PII genes. For example, I think it would be necessary to examine the mRNA expression levels of these genes in *brap-2(ok1492);fkh-9(ok1709)* mutants specifically. This is because we really see the effect of FKH-9 come to life in terms of *gst-4* expression when examining *fkh-9* manipulation along with the *brap-2(ok1492)* mutation. Therefore, with *brap-2* mutated as well, FKH-9 may have a larger/stronger effect on these PII detoxification genes which will bring further insight and understanding to the role of FKH-9 in the *C. elegans* oxidative stress response.

After examining the mRNA expression levels of these other PII detoxification genes, I also wanted to look at some other PI/non-PII genes due to the previous interesting find with *sod-3* and *daf-16.* Therefore, qRT-PCR was carried out to examine the mRNA expression levels in N2 WT and *fkh-9(ok1709)* mutants with and without As treatment. Specifically, I examined other genes from the SOD family such as *sod-1* and *sod-2* followed by genes from the FMO family such as *fmo-1, fmo-2,* and *fmo-3* and I also included the *hsp-4* gene. To start off with SOD-1 and SOD-2, they are part of the SOD family and therefore work similarly to SOD-3 but are found in different areas of the cell. SOD-2 is found in the mitochondrial matrix like SOD-3, but SOD-1 is found in the cytoplasm (Yang et al., 2007). FMO-1/2/3 are part of the FMO family which are the flavin-containing monooxygenases. These enzymes are specifically xenobiotic-metabolizing enzymes that oxygenate substrates by adding a molecule of oxygen to nitrogen, sulfur, or other nucleophilic atoms to increase the solubility of xenobiotics (Huang et al., 2021). In *C. elegans, fmo-1 and fmo-2* are expressed in the intestines while *fmo-3* is expressed in the hypodermis. *fmo-2* specifically is known to be a longevity gene that is induced in the intestine

and needed for lifespan extension (Huang et al., 2021). Following this, I also examined *hsp-4* mRNA expression levels which is a heat shock protein and plays a role in ER stress through the UPR (Ient et al., 2012). It therefore plays a role in the cytoprotective response and longevity overall.

There was not a significant difference seen in mRNA expression levels of *sod-1* and *sod-2* between WT and *fkh-9(ok1709)* mutants. This shows that FKH-9 likely does not influence these SOD genes as it does with *sod-3,* and the main reason for this could most likely be that *sod-3* is under the transcriptional regulation of DAF-16. Therefore, FKH-9 may act as a repressor for *sod-3* specifically and no other SOD family gene members. Furthermore, since the *fkh-9(ok1709)* mutation causes a large increase in *sod-3* mRNA expression levels when treated with As, this may be enough to help combat the elevated ROS levels, so the cell does not feel the need to compensate with elevated expression levels of *sod-1* and *sod-2* as well. However, when examining the *fmo* genes there was a significant difference in mRNA expression levels of *fmo-2* and *fmo-3* specifically. When treated with As, the *fkh-9(ok1709)* mutants portrayed a decrease in *fmo-2* expression with an increase in *fmo-3* expression compared to WT (Figure 3.8). This could potentially show that FKH-9 may act as an activator of FMO-2 and a repressor of FMO-3 during the oxidative stress response. However, the N2 WT mRNA expression levels of *fmo-3* specifically, were significantly lower when treated with As compared to no treatment (Figure 3.8). This was very interesting to see, so further investigation is needed to evaluate WT *fmo-3* induced expression levels. It is important to keep in mind however, that the FMO gene family does not work on ROS generated from As, but instead targets xenobiotics directly. Therefore, a possible explanation as to why *fmo-3* mRNA expression levels were so low in WT when treated with As is because As would not induce the expression of these genes to the degree that

xenobiotics would. Also, As mainly targets the gut of *C. elegans* and creates majority of the ROS in this area (Wang et al., 2007), but *fmo-3* is mainly expressed in the hypodermis of *C. elegans.* Since FMOs work in a completely different way from other PI and PII detoxification genes, further investigation (possibly with xenobiotic metabolism) is needed to fully understand the role FKH-9 may play in terms of this gene expression. There also was not a significant difference seen in mRNA expression levels of *hsp-4* between N2 WT and the *fkh-9(ok1709)* mutants with or without As treatment. Again, the main reason for this could be that HSP-4 does not respond to ROS generated from As, but instead has been seen to play a role in the UPR. Therefore, further investigation is needed to examine the role of FKH-9 in terms of *hsp-4* expression levels. However, it is important to note that recent literature has shown that the HSP-4 protein may not play as much of a role in the UPR as previously thought and is instead activated by the *C. elegans* developmental program. HSP-4 has been seen to be induced by a specific developmental program, the dauer program/L4 stage to adult transition (Zha et al., 2019). With this new role of HSP-4 being investigated currently in the literature, further investigation will be needed to investigate any possible connection between FKH-9 and HSP-4.

4.5 The Biological Role of FKH-9

The biological role of FKH-9 was also examined through survival assays, ER stress assays and longevity assays. After examining induced gene expression in *fkh-9(ok1709)* mutants in terms of PI and PII detoxification enzymes, I wanted to test if this would have an impact on how well *fkh-9(ok1709)* mutants can survive in oxidative stressful environments.

I started by conducting a sodium arsenite (As) survival assay. As previously mentioned, As exposure causes oxidative stress to the worms by generating ROS. Specifically, As causes the BLI-3/NADPH oxidase complex to produce ROS at the ER or through the mitochondria.

Subsequent sulfenylation at a cysteine site within the IRE-1 kinase activation loop induces SKN-1 activation (Hourihan et al., 2016). This therefore alters the expression of genes related to the stress response and antioxidant activities. When I conducted the As survival assay, the *fkh-9(ok1709)* mutants were not able to survive as long as the N2 WT could, and died off significantly sooner (Figure 3.12). The main reason for this could be that the absence of FKH-9 resulted in less SKN-1 expression and subsequent lowered levels of GST-4 to help combat the ROS. Even though *fkh-9(ok1709)* mutants portray an increase in *sod-3* mRNA expression levels, *sod-3* is mainly expressed in the head and tail region of *C. elegans* while As targets the gut. Therefore, the main area of ROS generation would be the intestines and would require GST-4 to help combat the elevated levels. Also, it was previously seen that the *fkh-9(ok1709)* mutants exhibited lower mRNA expression levels of the *fmo-2* gene when treated with As (Figure 3.8). Huang et al., 2021 demonstrated that FMOs can improve stress resistance to oxidative stress in *C. elegans.* Specifically, *fmo-2* overexpressing worms were seen to be more resistant to mitochondrial oxidative stress from ROS. Therefore, this could be another contributor as to why the *fkh-9(ok1709)* mutants were not able to survive as long as WT in the As dilution. However, further investigation is needed as it is possible that FKH-9 may be involved in regulating various processes during oxidative stress and the integration of signals from multiple pathways.

I conducted another survival assay using *tert*-Butyl Hydroperoxide (tBHP). tBHP works differently from As, as it attacks proteins and lipids therefore having broader effects on the worms than As does (Oliveira et al., 2009). Specifically, tBHP causes the accumulation of lipid peroxides which in turn increases needed *gst-4* expression levels. Lipid peroxidation also results in altered lipid metabolism, membrane structure integrity and a redox imbalance. When I conducted the tBHP survival assay, the *fkh-9(ok1709)* mutants were not able to survive as long

as the WT could and died off significantly sooner (Figure 3.12). The expression of almost all detoxification genes in response to As depends on SKN-1, whereas the induction of several genes upon tBHP treatment can be SKN-1-dependent but also SKN-1-independant, suggesting the activation of other oxidative stress response transcription factors (Oliveira et al., 2009). Since tBHP can cause such a large array of attacks to the cell, through multiple different pathways, the loss of *fkh-9* could have other implications that have yet to be determined.

I then conducted another type of survival assay known as an ER stress assay using dithiothreitol (DTT). DTT is a reducing agent that breaks down protein disulfide bonds or prevents disulfide bond formation of proteins in the ER (Braakman et al., 1992). When I conducted the DTT survival assay, the *fkh-9(ok1709)* mutants were not able to survive as long as the WT could and died off significantly sooner (Figure 3.12). In the study by Tillman et al., (2018) previously reviewed, the *Pseudomonas aeruginosa* pathogen targets the ER and causes an increase in misfolded proteins, similar to how the DTT toxin functions. They studied mutated XBP-1 that with loss of *fkh-9* exhibited ER structural changes that were suppressed and resulted in preserved ER homeostasis. They saw that FKH-9 is one transcription factor that helps suppress the larval lethality when XBP-1 is mutated caused by immune activation in response to infection by pathogenic bacteria (Tillman et al., 2018). They also determined that the loss of FKH-9 enhanced resistance to an ER toxin and resulted in enhanced ER-associated degradation (ERAD). During my ER stress assay, the *fkh-9(ok1709)* mutants were not able to survive as long as WT and this could possibly be due to a link with XBP-1. Without XBP-1 mutated, the loss of FKH-9 was not able to enhance resistance to the DTT ER toxin as it was to the pathogen. Regardless, this is simply one postulated hypothesis as the loss of *fkh-9* could have many other implications that have yet to be determined in terms of ER stress.

I also conducted a longevity assay to determine how well the *C. elegans* could live with *fkh-9* mutated. The *fkh-9(ok1709)* mutants were not able to live as long as the WT could and died off significantly sooner (Figure 3.13). There could be many possibilities as to why the *fkh-9(ok1709)* mutants were not able to live as long as the WT. For example, as previously seen in Figure 3.8, *fkh-9(ok1709)* mutants have very low mRNA expression levels of *fmo-2,* and this gene also acts as a longevity gene. However, the loss of *fkh-9* could have other implications that have yet to be determined such as a role in dauer formation, DNA repair systems, or cell death/senescence. Regardless, further investigation is needed in terms of all survival and longevity assays. This could include performing these assays with *brap-2(ok1492);fkh-9(ok1709)* double mutants to see the effect of the *fkh-9* mutation when *brap-2(ok1492)* is mutated as well.

4.6 Future Work to Further Investigate the Role of FKH-9 in *C. elegans*

This project has successfully revealed an important role of FKH-9 in the *C. elegans* oxidative stress response. In *brap-2(ok1492)* mutated worms, we see the importance of FKH-9 to induce *gst-4* expression levels. We also see the potential of FKH-9 to be a repressor of DAF-16/SOD-3 expression through qRT-PCR experimentation. Furthermore, we see the potential regulation of FKH-9 on other PI and PII detoxification genes with an overall biological role in terms of survival and longevity. However, much further investigation can be done to get closer into fully understanding the role of FKH-9 in the oxidative stress response.

With the use of luciferase assays, I presented a role that FKH-9 may play in increasing SKN-1 mediated activation of the *skn-1c* promoter. Although we see an initial indication between FKH-9 and SKN-1 here, it is not clear whether this interaction is direct or indirect with the promoter. To address this, ChIP (Chromatin Immunoprecipitation sequencing analysis) can be done to capture the protein to DNA interaction and identify FKH-9 binding sites. Further

understanding of where FKH-9 interacts with the chromatin will help us understand what exactly is happening at the promoter region and identify other molecular players that may be involved in FKH-9 transcriptional activation or repression of detoxification genes. Also, I think it would be a good idea to confirm that FKH-9 and SKN-1 directly interact at the *skn-1c* promoter by performing Co-IP (Co-immunoprecipitation) experimentation. This will help further our understanding of the conditions needed for FKH-9 and SKN-1 interaction, such as if the interaction between FKH-9 and SKN-1 require the promoter as a platform to interact with each other. To go even further into the analyzation of this possible interaction, we could test how exactly these two proteins interact (such as if by dimerization) by using a native SDS-page gel. Native gels allow us to analyze proteins that are still in their folded state and therefore not denatured. The shift we observe then depends on the physical shape and size of the protein. By comparing this to the individual shifts of FKH-9 and SKN-1, we can try to observe the differences in size and overall hypothesize their interaction.

Another possible experiment for further investigation would be to examine *fkh-9::gfp* levels in *brap-2(ok1492)* mutated worms. This would help present a visual aid of where FKH-9 localizes in the cells when *brap-2* is mutated. It would help confirm that FKH-9 most likely localizes in the nucleus to help activate *skn-1c* levels to subsequently activate *gst-4* levels. It would also help us understand where FKH-9 is mainly found in the worms. Based on other findings reviewed previously in the literature, I would postulate that majority of FKH-9 activation and localization would occur in the cells of the intestines of the worms. Therefore, GFP fluorescence imaging would help us confirm this notion.

Due to the qRT-PCR results found on how the *fkh-9(ok1709)* mutation affected *daf-16* and *sod-3* mRNA expression levels, further experimentation should be done to examine the

repressive role FKH-9 may play in terms of *sod-3* expression. One possible way to examine this would be to conduct luciferase assays with the HEK293T cells looking at the *sod-3* promoter. The cells could be co-transfected with DAF-16, FKH-9 and then also with DAF-16 + FKH-9 to then measure the relative luciferase activity of the *sod-3* promoter. This would give indication if FKH-9 works directly at the promoter to repress *sod-3* expression levels. This could also be done with the *daf-16* promoter to test if FKH-9 represses *daf-16* expression levels which would subsequently lead to lowered *sod-3* levels. Besides luciferase assays, to see if FKH-9 plays an upstream role in the IIS pathway instead of directly at the *sod-3* promoter, we can generate double mutants with the *fkh-9(ok1709)* deletion along with *age-1, pdk-1* or *akt-1/2* genes. The aim here would be to determine precisely what FKH-9 may affect in this pathway that subsequently effects DAF-16 and *sod-3* activation. In addition, RNA-sequencing or microarray analysis can be done to determine other genes that are either upregulated or downregulated by the loss of *fkh-9.* This will help identify potential candidates that may be involved in the oxidative stress response when *fkh-9* is mutated/knocked down.

Lastly, I think it would be beneficial to perform more survival assays with different stress-inducing agents. I examined the survival of *fkh-9(ok1492)* mutants treated with sodium arsenite, *tert*-Butyl Hydroperoxide, and dithiothreitol. However, other stress-inducing reagents may also affect the survival of the mutants. This could include chemicals such as paraquat (PQ) or acrylamide (Ac) for example as these chemicals effect cells in different ways. For example, PQ produces hydrogen peroxide through the NADPH mediated PQ redox cycle which involves the reduction of PQ by NADPH-cytochrome c reductase and oxidation of the reduced PQ by NADPH-cytochrome P-450 (Clejan & Cederbaum, 1989). The subsequent interaction between the reduced PQ and NADPH-cytochrome P-450 results in the production of hydrogen peroxide.

Ac is also linked to P-450 as it metabolizes Ac and converts it into GA (GlycidAmide) which is a reactive epoxide (Calleman et al., 1990). GA is then able to bind to nucleophiles such as GSH for consumption (Yousef & El-Demerdash, 2006). GSH is needed to balance the ROS and therefore this inhibition by GA contributes to elevated ROS levels. Therefore, further studies could include survival assays using these chemicals to identify more biological roles FKH-9 may play in *C. elegans.*

5.0 Conclusion:

Our lab is interested in studying the oxidative stress response since multiple human diseases are linked to cellular damages caused by ROS. Decades of research has brought us closer in our understanding of oxidative stress, the damage it causes and how organisms manage it to protect themselves from harm. However, there is still much unknown about all factors and mechanisms involved in this stress due to the multitude of complex signaling pathways that play roles in protecting the cell from serious harm and damage. Therefore, our lab uses *C. elegans* as a model organism to study oxidative stress *in vivo* as our studies using this organism have continued to bring us valuable insight into stress, aging, and longevity.

BRAP-2 is a cytoplasmic retention protein in *C. elegans* that has been hypothesized to indirectly hold SKN-1 in the cytoplasm and prevent its translocation into the nucleus to activate important phase II detoxification enzymes such as *gst-4.* This project has revealed that loss of *fkh-9* in *brap-2(ok1492)* mutants causes a decrease in *gst-4* expression levels. FKH-9 may potentially interact with SKN-1 at the *skn-1c* promoter to help increase *skn-1c* levels and subsequently increase phase II detoxification genes (Figure 5.1). Although an activator in this regard, this project has also shown that FKH-9 may act as a repressor for the phase I gene *sod-3* (Figure 5.2), while also regulating an array of other stress/longevity genes. Furthermore, this

project has revealed FKH-9 to be a major biological player needed for survival and lifespan. Regardless, more work is required to determine the full mechanism of action in which FKH-9 is regulated by signaling pathways especially in connection to SKN-1 and DAF-16. Overall, the work presented here has identified a new role of FKH-9 in the *C. elegans* oxidative stress response and has brought us one step closer to understanding the profound effects that transcription factors can achieve in the cell.

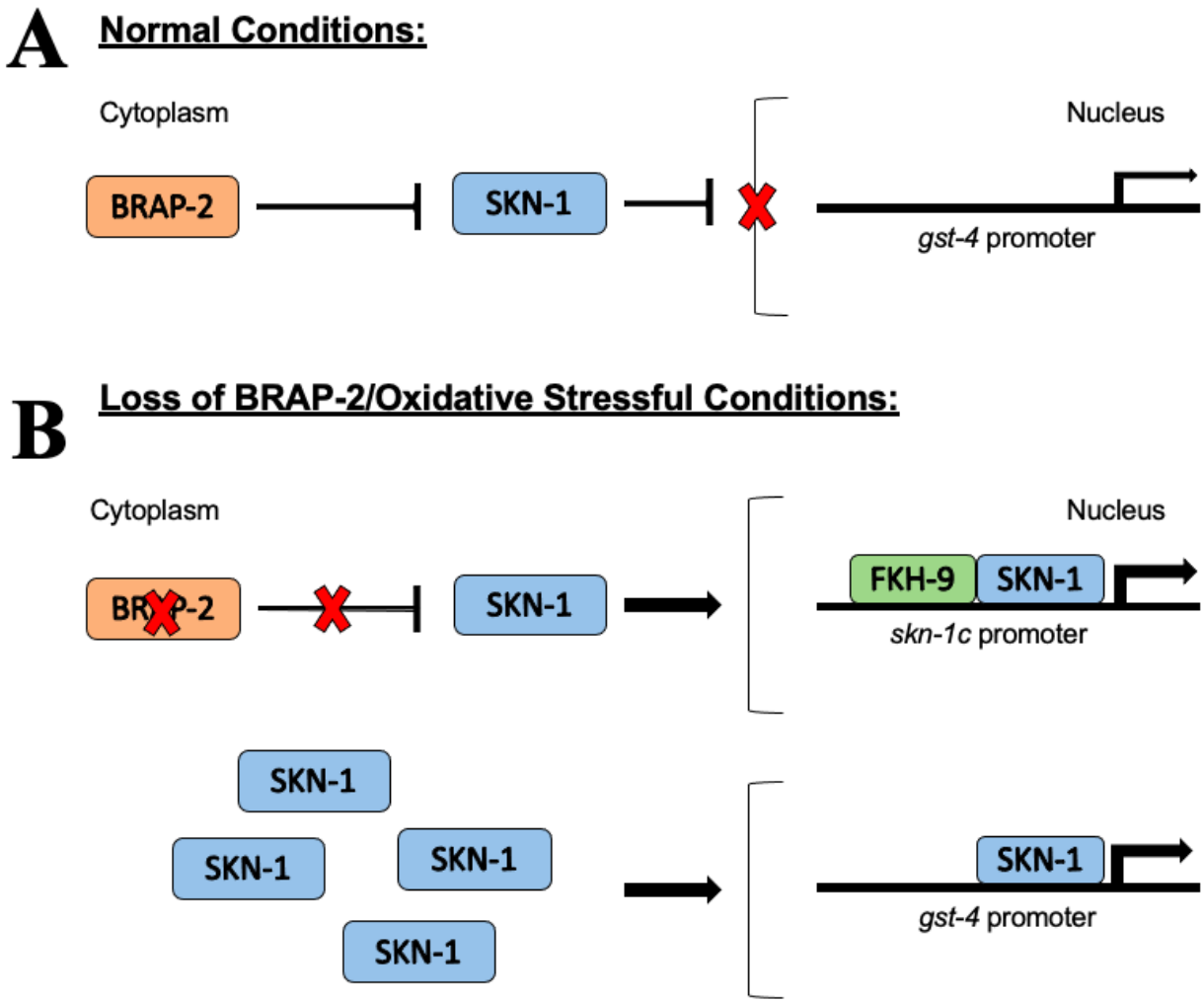

Figure 5.1: The Proposed Model for the Mechanism of FKH-9 Function in the Regulation of PII Detoxification Genes such as *gst-4*

(A) Under normal conditions, BRAP-2 can indirectly hold SKN-1 in the nucleus and prevent its translocation into the nucleus. This subsequently results in decreased transcriptional levels of *gst-4.* **(B)** Under conditions of the loss of BRAP-2 (mutation) or oxidative stressful conditions, SKN-1 is free to translocate into the nucleus where it potentially interacts with FKH-9 to increase SKN-1 transcriptional levels. SKN-1 is subsequently able to transcriptionally activate *gst-4*, which is needed to help combat elevated ROS levels. This proposed model helps explain high levels of *gst-4* observed in *brap-2(ok1492)* mutants, but significantly decreased levels in *brap-2(ok1492);fkh-9(ok1709)* double mutants, as we observe FKH-9 with activator-like functions. Thickness of arrows are indicator of robustness at the promoter.

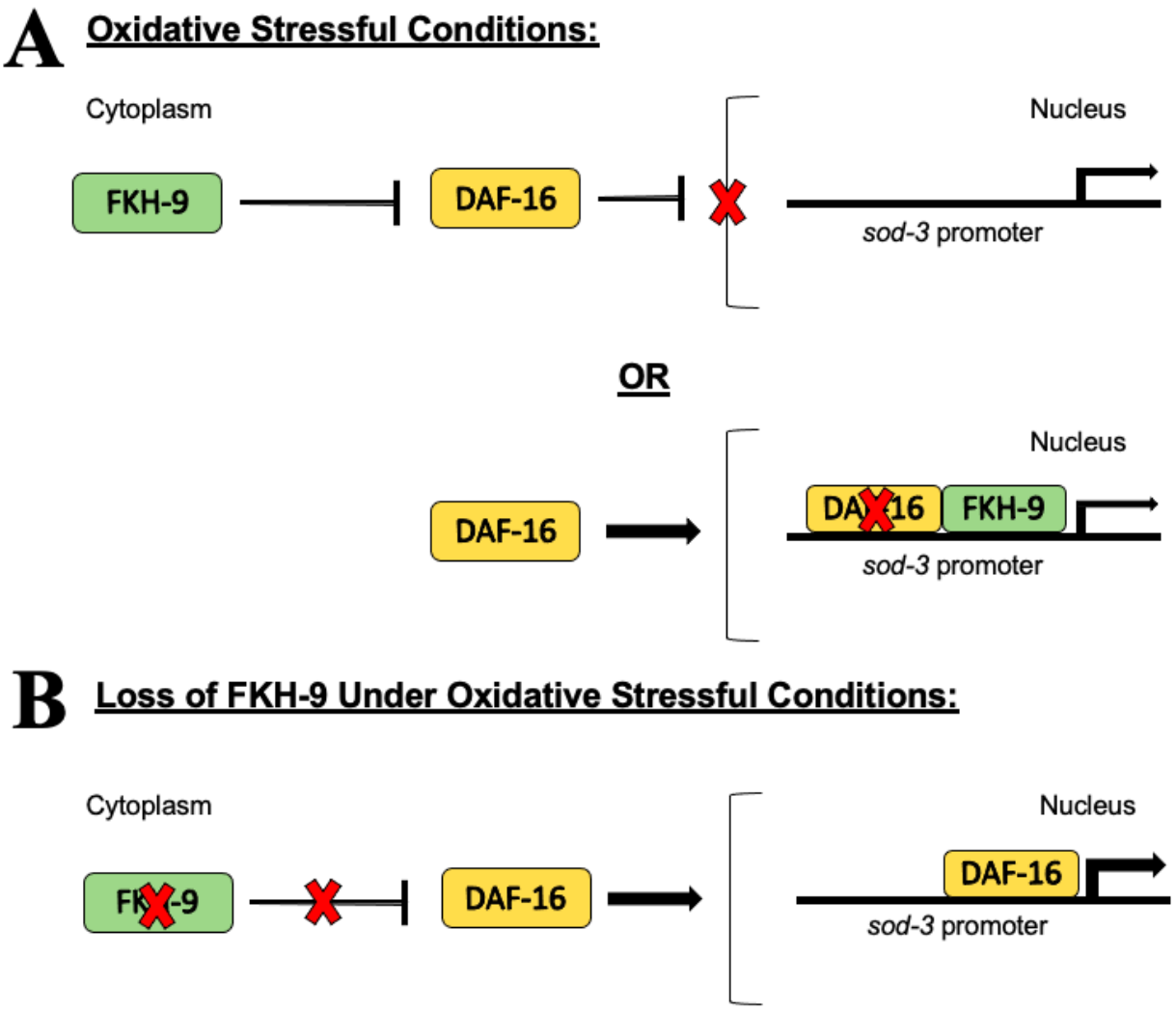

Figure 5.2: The Proposed Model for the Mechanism of FKH-9 Function in the Regulation of PI Detoxification Genes such as *sod-3*

(A) Under oxidative stressful conditions, FKH-9 potentially contributes to lowered expression of *sod-3*. FKH-9 may be able to directly or indirectly cause DAF-16's sequestration in the cytoplasm to prevent its nuclear translocation. Or FKH-9 may be able to suppress *sod-3* transcriptional activation directly at the promoter. **(B)** Under conditions of the loss of FKH-9 (mutation) during oxidative stressful conditions, DAF-16 is free to translocate into the nucleus to transcriptionally activate *sod-3*, which is needed to help combat elevated ROS levels. This proposed model helps explain high levels of *sod-3* observed in *fkh-9(ok1709)* mutants when treated with As, as we observe FKH-9 with repressor-like functions. Thickness of arrows are indicator of robustness at the promoter.

APPENDIX

Table 1: Statistics for the As Oxidative Stress Assay

	Strains	No. of Samples	Median Survival				Hours at % Mortality				
			Hours	Std. Error	95% C.I.	P-Value	25 %	50 %	75 %	90 %	100 %
Trial 1	Wildtype (N2)	36	6.69	0.55	5.63 ~ 7.76		4	6	9	12	13
	fkh-9 (ok1709)	36	4.69	0.38	3.96 ~ 5.43	0.0012	2	5	6	8	9
Trial 2	Wildtype (N2)	36	6.47	0.50	5.49 ~ 7.45		4	6	9	11	12
	fkh-9 (ok1709)	36	4.19	0.38	3.45 ~ 4.94	0.0006	2	4	5	8	9
Trial 3	Wildtype (N2)	36	6.28	0.42	5.46 ~ 7.10		4	6	8	9	12
	fkh-9 (ok1709)	36	4.53	0.36	3.82 ~ 5.24	0.0047	3	5	6	7	9

P-values are relative to wild type (N2).

Table 2: Statistics for the tBHP Oxidative Stress Assay

	Strains	No. of Samples	Median Survival				Hours at % Mortality				
			Hours	Std. Error	95% C.I.	P-Value	25 %	50 %	75 %	90 %	100 %
Trial 1	Wildtype (N2)	36	4.86	0.32	4.23 ~ 5.49		4	5	6	7	10
	fkh-9 (ok1709)	36	3.81	0.23	3.36 ~ 4.25	0.0084	3	4	5	6	7
Trial 2	Wildtype (N2)	36	5.06	0.32	4.43 ~ 5.69		4	5	6	7	8
	fkh-9 (ok1709)	36	3.28	0.23	2.83 ~ 3.72	<0.0001	2	3	4	5	6
Trial 3	Wildtype (N2)	36	5.11	0.39	4.35 ~ 5.88		3	5	7	8	9
	fkh-9 (ok1709)	36	3.53	0.27	3.00 ~ 4.06	0.0039	2	4	5	6	7

P-values are relative to wild type (N2).

Table 3: Statistics for the DTT ER Stress Assay

	Strains	No. of Samples	Median Survival				Hours at % Mortality				
			Hours	Std. Error	95% C.I.	P-Value	25 %	50 %	75 %	90 %	100 %
Trial 1	Wildtype (N2)	36	6.42	0.37	5.70 ~ 7.14		5	7	8	9	10
	fkh-9 (ok1709)	36	5.19	0.24	4.71 ~ 5.67	0.0006	4	5	6	7	8
Trial 2	Wildtype (N2)	36	4.25	0.37	3.53 ~ 4.97		2	4	6	7	9
	fkh-9 (ok1709)	36	3.92	0.33	3.27 ~ 4.56	0.3979	2	4	6	7	8
Trial 3	Wildtype (N2)	36	5.69	0.51	4.70 ~ 6.69		3	5	9	10	11
	fkh-9 (ok1709)	36	4.39	0.27	3.86 ~ 4.92	0.0078	3	4	6	7	8

P-values are relative to wild type (N2).

Table 4: Statistics for the Longevity Assay

	Strains	No. of Samples	Median Survival				Days at % Mortality				
			Days	Std. Error	95% C.I.	P-Value	25 %	50 %	75 %	90 %	100 %
Trial 1	Wildtype (N2)	25	19.72	1.41	16.95 ~ 22.49		15	18	22	32	36
	fkh-9 (ok1709)	25	15.04	1.30	12.49 ~ 17.59	0.0331	9	14	20	25	28
Trial 2	Wildtype (N2)	25	22.72	1.54	19.70 ~ 25.74		18	22	26	36	40
	fkh-9 (ok1709)	25	16.40	1.08	14.29 ~ 18.51	0.0016	12	16	20	25	27
Trial 3	Wildtype (N2)	25	23.56	1.51	20.61 ~ 26.51		18	23	29	34	37
	fkh-9 (ok1709)	25	19.04	1.42	16.26 ~ 21.82	0.0231	13	21	25	28	29

P-values are relative to wild type (N2).

Table 5: List of Mammalian Homologs of *C. elegans* Genes and their Functions

Information of the genes were obtained from WormBase and/or cited within this project.

***C. elegans* Gene**	**Mammalian Homolog**	**Description of Function in *C. elegans***
aak-2 (AMP-Activated Kinase)	Protein kinase AMP-activated catalytic subunit α 1 and 2 **(PRKAA1 and PRKAA2)**	- Enables AMP-activated protein kinase activity - Involved in determination of adult lifespan, positive regulation of dauer larval development and protein secretion
age-1 (AGEing Alteration)	Phosphatidylinositol-4,5-bisphosphate 3-kinase catalytic subunit α and δ **(PIK3CA and PIK3CD)**	- Enables 1-phosphatidylinositol-3-kinase and 1-phosphatidylinositol-4-phosphate 3-kinase activity - Involved in dauer entry, determination of adult lifespan and regulation of synaptic assembly at neuromuscular junction
akt-1/2 (AKT Kinase Family)	AKT serine/threonine kinase 1 and 2 **(AKT1 and AKT2)**	- Enables calmodulin and phosphatidylinositol-3,4,5-triphosphate binding activity and protein serine/threonine kinase activity - Involved in determination of adult lifespan, protein phosphorylation and signal transduction
brap-2 (BRCA1 Associated Protein)	BRCA1 associated protein 2 **(BRAP2)**	- Enables ubiquitin protein ligase activity - Involved in DNA damage induced germline apoptosis, and insulin signaling pathway
cdc-42 (Cell Division Cycle Related)	Cell Division Cycle 42 **(CDC42)**	- Enables GTP binding activity and GTPase activity - Involved in establishment of mitotic spindle orientation, regulation of nematode male tail tip morphogenesis and regulation of cellular component organization
daf-2 (Abnormal DAuer Formation)	Insulin like growth Factor 1 receptor **(IGF1R)**	- Enables PTB and SH2 domain binding activity and protein kinase binding activity

		- Involved in dauer exit, regulation of developmental and metabolic processes
daf-16 (Abnormal DAuer Formation)	Forkhead Box O **(FOXO1, FOXO3, and FOXO4)**	- Enables 14-3-3 protein, beta-catenin, and enzyme binding activity - Involved in defense responses, regulation of transcription and dauer larval development
dhs-8 (DeHydrogenases, Short Chain)	WW domain containing Oxidoreductase **(WWOX)**	- Enables oxidoreductase activity - Involved in protecting against oxidative stress
dod-3 (Downstream of DAF-16)	N/A	- Regulated by DAF-16, unknown function - Located/enriched at coelomocyte, head mesodermal cells, pharyngeal muscle cells and sensory neurons
fkh-9 (ForKHead Transcription Factor Family)	Forkhead Box	- Enables DNA-binding transcription factor activity, RNA polymerase II-specific and cis-regulatory region sequence-specific DNA binding activity - Involved in axon regeneration, determination of adult lifespan and learning/memory
fmo-1/2/3 (Flavin-Containing MonoOxygenase Family)	Flavin containing dimethylaniline monooxygenase **(FMO2/3/4)**	- Enables monooxygenase activity - Involved in lipid metabolic processes
gcs-1 (γ Glutamyl Cysteine Synthetase)	Glutamate-cysteine ligase catalytic subunit **(GCLC)**	- Enables glutamate-cysteine ligase activity - Involved in glutathione biosynthetic process, response to arsenic-containing substances and superoxide
gsk-3 (Glycogen Synthase Kinase Family)	Glycogen synthase kinase 3 α and δ **(GSK3A and GSK3B)**	- Enables protein serine/threonine kinase activity - Involved in engulfment of apoptotic cells, left/right axis specification and regulation of cellular component regulation
gst-4 (Glutathione S-Transferase)	Glutathione-S-Transferase **(GST)**	- Enables glutathione transferase activity - Involved in glutathione

		metabolic processes and ROS detoxification
gsto-2 (Glutathione S-Transferase, Omega Class)	Glutathione S-transferase Omega **(GSTO1/2)**	- Enables glutathione dehydrogenase and transferase activity - Involved in glutathione metabolic processes
him-5 (High Incidence of Males)	N/A	- Involved in meiotic DNA double-strand break formation involved in reciprocal meiotic recombination and chromosome segregation
hsp-4 (Heat Shock Protein)	Heat shock protein family A member 5 **(HSPA5)**	- Enables RNA polymerase II-specific DNA-binding transcription factor binding activity - Involved in ER unfolded protein response
jkk-1 (JNK Kinase)	Mitogen-activated protein kinase kinase 7 **MAP2K7**	- Enables JUN kinase kinase activity - Involved in hyperosmotic response and locomotion
jnk-1 (Jun N-terminal Kinase)	Mitogen-activated protein kinase 8/9/10 **(MAPK8/9/10)**	- Enables JUN kinase activity and RNA polymerase II-specific DNA-binding transcription factor binding activity - Involved in JUN phosphorylation, determination of adult lifespan and negative regulation of cellular response to manganese ions
mdt-15 (MeDiaTor)	Mediator complex subunit 15 **(MED15)**	- Enables nuclear receptor binding and transcription coactivator activity - Involved in determination of adult lifespan, nematode larval development and sequestering of triglyceride
mek-2 (MAP Kinase Kinase or Erk Kinase)	Mitogen-activated protein kinase kinase 1 and 2 **(MAP2K1/MAP2k2)**	- Enables protein serine/threonine/tyrosine kinase and scaffold protein activity - Involved in defense response to Gram-positive bacterium, intracellular signal transduction and vulval development

mpk-1 (MAP Kinase)	Mitogen activated protein kinase 1 **(MAPK1)**	- Enables MAP kinase activity - Involved in determination of adult lifespan, intracellular signal transduction and positive regulation of macromolecule metabolic processes
mtl-1/2 (MeTaLlothionein)	N/A	- Enables calcium and zinc ion binding activity - Involved in response to heat and metal ion
pdk-1 (PDK-Class Protein Kinase)	3-phosphoinositide dependant protein kinase 1 **(PDPK1)**	- Enables protein kinase activity - Involved in cellular response to oxygen species, dauer larval development and regulation of synaptic assembly at neuromuscular junction
pmk-1 (p38 MAPK Family)	Mitogen-activated protein kinase 11/14 **(MAPK11 and MAPK14)**	- Enables MAP kinase and transcription regulator activator activity - Involved in behavioural and defense responses
sdz-8 (SKN-1 Dependent Zygotic Transcript)	Carbonyl reductase 3 **(CBR3)**	- Encodes a protein with short chain dehydrogenase/reductase SDR and NAD(P)-binding domains - Affected by *daf-16*, *daf-2* and *skn-1* genes, enriched in body wall of muscle cells
skn-1 (SKiNhead)	Nuclear factor erythroid 2-related factor 2 **(Nrf2)**	- Enables Hsp70 protein binding activity and RNA polymerase II transcription regulatory region sequence-specific DNA binding activity - Involved in endoderm development, ER unfolded protein response and positive regulation of macromolecule metabolic processes
sod-1 (Superoxide Dismutase)	Superoxide dismutase 1 **(SOD1)**	- Enables copper ion binding, protein homodimerization and superoxide dismutase activity - Involved in regulation of brood size and vulva development and in removal of superoxide radicals
sod-2	Superoxide	- Enables protein

(Superoxide Dismutase)	dismutase 2 **(SOD2)**	homodimerization and superoxide dismutase activity - Involved in removal of superoxide radicals
sod-3 (Superoxide Dismutase)	Superoxide dismutase 3 **(SOD3)**	- Enables protein homodimerization and superoxide dismutase activity - Involved in removal of superoxide radicals
tba-1 (TuBulin, α)	Tubulin α 4a and 8 **(TUBA4A and TUBA8)**	- Enables GTP binding activity - Involved in embryonic development, mitotic spindle orientation and regulation of cytokines
ugt-13 (UDP-Glucuronosyl Transferase)	UDP Glucuronosyltransferase family 1 member A10 **(UGT1A10)**	- Enables glucuronosyltransferase activity - Involved in protection against oxygen species
vit-2 (VITellogenin Structural Genes)	N/A	- Enables lipid transporter activity - Involved in lipid transport
wdr-23 (WD Repeat Protein)	DDB1 and CUL4 associated factor 11 **(DCAF11)**	- Enables transcription factor binding activity - Involved in determination of adult lifespan, negative regulation of cellular response to manganese ions and positive regulation of neuron death
xbp-1 (X-box Binding Protein)	X-box binding protein 1 **(XBP1)**	- Enables RNA polymerase II transcription regulatory region sequence-specific DNA binding activity - Involved in defense response to Gram-negative bacterium, determination of adult lifespan and positive regulation of transcription from RNA polymerase II promoter involved in UPR

Table 6: List of Forward and Reverse Primers used for qRT-PCR

Genes	TM (°C)	Sequence
cdc-42	67.6 67.7	F: TCGACAATTACGCCGTCACA R: AGGCACCCATTTTTCTCGGA
daf-16	69.3 63.9	F: TGGAATTCAATCGTGTGGAA R: ATGAATATGCTGCCCTCCAG
dhs-8	64.2 65.4	F: AAAAGGATCGGGTGGGTACA R: AAACGACATGTGCTCCTGCT
fkh-9	57.7 57.3	F: GGCTCCAGAACCTTCTCACC R: AGAAAAGACTGGCTCTCGGC
fmo-1	57.3 56.8	F: GGAGCCGACTTGGACATGAA R: CACTTGTGCGTGATCGTTCG
fmo-2	64.0 63.5	F: GGAACAAGCGTGTTGCTGT R: GCCATAGAGAAGACCATGTCG
fmo-3	58.1 57.3	F: TTCTTGTTGTGGGTGCTGGG R: TGACCGTTGACAACTCGGTC
gcs-1	63.8 63.8	F: CCAATCGATTCCTTTGGAGA R: GCTACTTCCGGGAATGTGAA
gst-4	64.0 63.6	F: TGCTCAATGTGCCTTACGAG R: AGTTTTTCCAGCGAGTCCAA
gsto-2	66.6 65.5	F: TCCACCAGCTTCAGGAACCA R: TTCCCTCGTCGTGCTCTAGT
hsp-4	64.1 63.7	F: TGACTCGTGCCAAGTTTGAG R: GCTCCTTGCCGTTGAAGTAG
mdt-15	57.0 57.1	F: GCGAGGCAGGTCGAAGAATA R: CCAGCCGGAGTGTTTCCTAA
sdz-8	64.7 60.4	F: CTGCTGAGGTACGGAACGAA R: TCTGTAFFCGACAACTGGGA
skn-1c	66.8 66.6	F: TACTCACCGAGCATCCACCA R: TGATCAGCAGGAGCCACTTG
sod-1	65.7 68.1	F: ATTTCTGCCGGTCCACACTT R: CCATAGATCGGCCAACGACA
sod-2	67.5 65.9	F: GAGGCGGTCTCCAAAGGAAA R: GAACAGCCGACAGTTGATGCC
sod-3	63.9 64.0	F: GGATGGTGGAGAACCTTCAA R: AAGGATCCTGGTTTGCACAG
tba-1	66.4 67.4	F: AGACCAACAAGCCGATGGAG R: TCAGTTCCTTTCCGACGGTG
ugt-13	65.0 65.0	F: CCGGATTCCTGGATCGACTG R: TTGTCGCAGTAGTTGGGACC

Table 7: List of *C. elegans* strains used in this project

Strains	Description
N2	Bristol Wildtype
CF1553	*muls84(sod-3p::gfp)*
CL2166	*dvIs19(gst- 4p::gfp)III*
DR466	*him-5(e1490)V*
YF123	*fkh-9(ok1709)*
YF124	*brap-2(ok1492); fkh-9(ok1709)*
YF15	*brap-2(ok1492)*
YF221	*fkh-9(ok1709); dvIs19(gst-4p::gfp)III*
YF225	*fkh-9(ok1709); muls84(sod-3p::gfp)*
YF67	*brap-2(ok1492); dvIs19(gst-4p::gfp)III*

Table 8: List of Primers used for Genotyping *fkh-9* with SW-PCR

Name	TM (°C)	Sequence
TK133	66.1	GATTGCCAAAGGGCAAGTGT
TK135	64.4	GTGTGTCGCGTGTTTCTACG
TK139	64.3	GATGTTTCTCCGCTTCCAGA

References:

Alam, H., Williams, T. W., Dumas, K. J., Guo, C., Yoshina, S., Mitani, S., & Hu, P. J. (2010). EAK-7 Controls Development and Life Span by Regulating Nuclear DAF-16/FoxO Activity. *Cell Metabolism*, *12*(1), 30–41. https://doi.org/10.1016/j.cmet.2010.05.004

Albert, P. S., Brown, S. J., & Riddle, D. L. (1981). Sensory control of dauer larva formation inCaenorhabditis elegans. *The Journal of Comparative Neurology*, *198*(3), 435–451. https://doi.org/10.1002/cne.901980305

An, J. H., & Blackwell, T. K. (2003). SKN-1 links *C. elegans* mesendodermal specification to a conserved oxidative stress response. *Genes & Development*, *17*(15), 1882–1893. https://doi.org/10.1101/gad.1107803

An, J. H., Vranas, K., Lucke, M., Inoue, H., Hisamoto, N., Matsumoto, K., & Blackwell, T. K. (2005). Regulation of the *Caenorhabditis elegans* oxidative stress defense protein SKN-1 by glycogen synthase kinase-3. *Proceedings of the National Academy of Sciences*, *102*(45), 16275–16280. https://doi.org/10.1073/pnas.0508105102

Aronica, L., Ordovas, J. M., Volkov, A., Lamb, J. J., Stone, P. M., Minich, D., Leary, M., Class, M., Metti, D., Larson, I. A., Contractor, N., Eck, B., & Bland, J. S. (2022). Genetic Biomarkers of Metabolic Detoxification for Personalized Lifestyle Medicine. *Nutrients*, *14*(4), 768. https://doi.org/10.3390/nu14040768

Azadmanesh, J., & Borgstahl, G. (2018). A Review of the Catalytic Mechanism of Human Manganese Superoxide Dismutase. *Antioxidants*, *7*(2), 25. https://doi.org/10.3390/antiox7020025

Balaban, R. S., Nemoto, S., & Finkel, T. (2005). Mitochondria, Oxidants, and Aging. *Cell*, *120*(4), 483–495. https://doi.org/10.1016/j.cell.2005.02.001

Bergamini, C., Gambetti, S., Dondi, A., & Cervellati, C. (2004). Oxygen, Reactive Oxygen Species and Tissue Damage. *Current Pharmaceutical Design*, *10*(14), 1611–1626. https://doi.org/10.2174/1381612043384664

Blackwell, T. K., Bowerman, B., Priess, J. R., & Weintraub, H. (1994). Formation of a Monomeric DNA Binding Domain by Skn-1 bZIP and Homeodomain Elements. *Science*, *266*(5185), 621–628. https://doi.org/10.1126/science.7939715

Blackwell, T. K., Steinbaugh, M. J., Hourihan, J. M., Ewald, C. Y., & Isik, M. (2015). SKN-1/Nrf, stress responses, and aging in Caenorhabditis elegans. *Free Radical Biology and Medicine*, *88*, 290–301. https://doi.org/10.1016/j.freeradbiomed.2015.06.008

Braakman, I., Helenius, J., & Helenius, A. (1992). Manipulating disulfide bond formation and protein folding in the endoplasmic reticulum. *The EMBO Journal*, *11*(5), 1717–1722. https://doi.org/10.1002/j.1460-2075.1992.tb05223.x

Brenner, S. (1974). THE GENETICS OF *CAENORHABDITIS ELEGANS*. *Genetics*, *77*(1), 71–94. https://doi.org/10.1093/genetics/77.1.71

Calleman, C. J., Bergmark, E., & Costa, L. G. (1990). Acrylamide is metabolized to glycidamide in the rat: Evidence from hemoglobin adduct formation. *Chemical Research in Toxicology*, *3*(5), 406–412. https://doi.org/10.1021/tx00017a004

Choe, K. P., Przybysz, A. J., & Strange, K. (2009). The WD40 Repeat Protein WDR-23 Functions with the CUL4/DDB1 Ubiquitin Ligase to Regulate Nuclear Abundance and Activity of SKN-1 in *Caenorhabditis elegans*. *Molecular and Cellular Biology*, *29*(10), 2704–2715. https://doi.org/10.1128/MCB.01811-08

Clejan, L., & Cederbaum, A. I. (1989). Synergistic interactions between nadph-cytochrome P-450 reductase, paraquat, and iron in the generation of active oxygen radicals. *Biochemical Pharmacology*, *38*(11), 1779–1786. https://doi.org/10.1016/0006-2952(89)90412-7

Davis, R. J. (2000). Signal Transduction by the JNK Group of MAP Kinases. *Cell*, *103*(2), 239–252. https://doi.org/10.1016/S0092-8674(00)00116-1

Deng, J., Dai, Y., Tang, H., & Pang, S. (2020). SKN-1 Is a Negative Regulator of DAF-16 and Somatic Stress Resistance in *Caenorhabditis elegans*. *G3 Genes|Genomes|Genetics*, *10*(5), 1707–1712. https://doi.org/10.1534/g3.120.401203

Duchen, M. R. (2004). Mitochondria in health and disease: Perspectives on a new mitochondrial biology. *Molecular Aspects of Medicine*, *25*(4), 365–451. https://doi.org/10.1016/j.mam.2004.03.001

Gami, M. S., & Wolkow, C. A. (2006). Studies of Caenorhabditis elegans DAF-2/insulin signaling reveal targets for pharmacological manipulation of lifespan. *Aging Cell*, *5*(1), 31–37. https://doi.org/10.1111/j.1474-9726.2006.00188.x

Goh, G. Y. S., Martelli, K. L., Parhar, K. S., Kwong, A. W. L., Wong, M. A., Mah, A., Hou, N. S., & Taubert, S. (2014). The conserved Mediator subunit MDT-15 is required for oxidative stress responses in *Caenorhabditis elegans*. *Aging Cell*, *13*(1), 70–79. https://doi.org/10.1111/acel.12154

Goldstein, B. (2016). Sydney Brenner on the Genetics of *Caenorhabditis elegans*. *Genetics*, *204*(1), 1–2. https://doi.org/10.1534/genetics.116.194084

Golson, M. L., & Kaestner, K. H. (2016). Fox transcription factors: From development to disease. *Development*, *143*(24), 4558–4570. https://doi.org/10.1242/dev.112672

Goszczynski, B., Captan, V. V., Danielson, A. M., Lancaster, B. R., & McGhee, J. D. (2016). A 44 bp intestine-specific hermaphrodite-specific enhancer from the C. elegans vit-2 vitellogenin gene is directly regulated by ELT-2, MAB-3, FKH-9 and DAF-16 and indirectly regulated by the germline, by daf-2 /insulin signaling and by the TGF-β/Sma/Mab pathway. *Developmental Biology*, *413*(1), 112–127. https://doi.org/10.1016/j.ydbio.2016.02.031

Greer, E. L., Dowlatshahi, D., Banko, M. R., Villen, J., Hoang, K., Blanchard, D., Gygi, S. P., & Brunet, A. (2007). An AMPK-FOXO Pathway Mediates Longevity Induced by a Novel Method of Dietary Restriction in C. elegans. *Current Biology*, *17*(19), 1646–1656. https://doi.org/10.1016/j.cub.2007.08.047

Han, H. (2018). RNA Interference to Knock Down Gene Expression. In J. K. DiStefano (Ed.), *Disease Gene Identification* (Vol. 1706, pp. 293–302). Springer New York. https://doi.org/10.1007/978-1-4939-7471-9_16

Hannenhalli, S., & Kaestner, K. H. (2009). The evolution of Fox genes and their role in development and disease. *Nature Reviews Genetics*, *10*(4), 233–240. https://doi.org/10.1038/nrg2523

Hasegawa, K., & Miwa, J. (2010). Genetic and Cellular Characterization of Caenorhabditis elegans Mutants Abnormal in the Regulation of Many Phase II Enzymes. *PLoS ONE*, *5*(6), e11194. https://doi.org/10.1371/journal.pone.0011194

Hasegawa, K., Miwa, S., Tsutsumiuchi, K., & Miwa, J. (2010). Allyl Isothiocyanate that Induces GST and UGT Expression Confers Oxidative Stress Resistance on C. elegans, as Demonstrated by Nematode Biosensor. *PLoS ONE*, *5*(2), e9267. https://doi.org/10.1371/journal.pone.0009267

He, F., Ru, X., & Wen, T. (2020). NRF2, a Transcription Factor for Stress Response and Beyond. *International Journal of Molecular Sciences*, *21*(13), 4777. https://doi.org/10.3390/ijms21134777

Hourihan, J. M., Moronetti Mazzeo, L. E., Fernández-Cárdenas, L. P., & Blackwell, T. K. (2016). Cysteine Sulfenylation Directs IRE-1 to Activate the SKN-1/Nrf2 Antioxidant Response. *Molecular Cell*, *63*(4), 553–566. https://doi.org/10.1016/j.molcel.2016.07.019

Hu, Q., D'Amora, D. R., MacNeil, L. T., Walhout, A. J. M., & Kubiseski, T. J. (2017). The Oxidative Stress Response in *Caenorhabditis elegans* Requires the GATA Transcription Factor ELT-3 and SKN-1/Nrf2. *Genetics*, *206*(4), 1909–1922. https://doi.org/10.1534/genetics.116.198788

Huang, S., Howington, M. B., Dobry, C. J., Evans, C. R., & Leiser, S. F. (2021). Flavin-Containing Monooxygenases Are Conserved Regulators of Stress Resistance and Metabolism. *Frontiers in Cell and Developmental Biology*, *9*, 630188. https://doi.org/10.3389/fcell.2021.630188

Ient, B., Edwards, R., Mould, R., Hannah, M., Holden-Dye, L., & O'Connor, V. (2012). HSP-4 endoplasmic reticulum (ER) stress pathway is not activated in a C. elegans model of ethanol intoxication and withdrawal. *Invertebrate Neuroscience*, *12*(2), 93–102. https://doi.org/10.1007/s10158-012-0136-7

Inoue, H., Hisamoto, N., An, J. H., Oliveira, R. P., Nishida, E., Blackwell, T. K., & Matsumoto, K. (2005). The *C. elegans* p38 MAPK pathway regulates nuclear localization of the transcription factor SKN-1 in oxidative stress response. *Genes & Development*, *19*(19), 2278–2283. https://doi.org/10.1101/gad.1324805

Jaul, E., & Barron, J. (2017). Age-Related Diseases and Clinical and Public Health Implications for the 85 Years Old and Over Population. *Frontiers in Public Health*, *5*, 335. https://doi.org/10.3389/fpubh.2017.00335

Kaestner, K. H., Knochel, W., & Martinez, D. E. (2000). Unified nomenclature for the winged helix/forkhead transcription factors. *Genes & Development*, *14*(2), 142–146.

Kaletsky, R., Lakhina, V., Arey, R., Williams, A., Landis, J., Ashraf, J., & Murphy, C. T. (2016). The C. elegans adult neuronal IIS/FOXO transcriptome reveals adult phenotype regulators. *Nature*, *529*(7584), 92–96. https://doi.org/10.1038/nature16483

Karnoub, A. E., & Weinberg, R. A. (2008). Ras oncogenes: Split personalities. *Nature Reviews Molecular Cell Biology*, *9*(7), 517–531. https://doi.org/10.1038/nrm2438

Kenyon, C., Chang, J., Gensch, E., Rudner, A., & Tabtiang, R. (1993). A C. elegans mutant that lives twice as long as wild type. *Nature*, *366*(6454), 461–464. https://doi.org/10.1038/366461a0

Klass, M. R. (1983). A method for the isolation of longevity mutants in the nematode Caenorhabditis elegans and initial results. *Mechanisms of Ageing and Development*, *22*(3–4), 279–286. https://doi.org/10.1016/0047-6374(83)90082-9

Klotz, L.-O., & Steinbrenner, H. (2017). Cellular adaptation to xenobiotics: Interplay between xenosensors, reactive oxygen species and FOXO transcription factors. *Redox Biology*, *13*, 646–654. https://doi.org/10.1016/j.redox.2017.07.015

Kwon, E.-S., Narasimhan, S. D., Yen, K., & Tissenbaum, H. A. (2010). A new DAF-16 isoform regulates longevity. *Nature*, *466*(7305), 498–502. https://doi.org/10.1038/nature09184

Lee, T. I., & Young, R. A. (2013). Transcriptional Regulation and Its Misregulation in Disease. *Cell*, *152*(6), 1237–1251. https://doi.org/10.1016/j.cell.2013.02.014

Lemmon, M. A., & Schlessinger, J. (2010). Cell Signaling by Receptor Tyrosine Kinases. *Cell*, *141*(7), 1117–1134. https://doi.org/10.1016/j.cell.2010.06.011

Li, S., Ku, C.-Y., Farmer, A. A., Cong, Y.-S., Chen, C.-F., & Lee, W.-H. (1998). Identification of a Novel Cytoplasmic Protein That Specifically Binds to Nuclear Localization Signal

Motifs. *Journal of Biological Chemistry*, *273*(11), 6183–6189. https://doi.org/10.1074/jbc.273.11.6183

Lickwar, C. R., Mueller, F., Hanlon, S. E., McNally, J. G., & Lieb, J. D. (2012). Genome-wide protein–DNA binding dynamics suggest a molecular clutch for transcription factor function. *Nature*, *484*(7393), 251–255. https://doi.org/10.1038/nature10985

Longo, V. D., Antebi, A., Bartke, A., Barzilai, N., Brown-Borg, H. M., Caruso, C., Curiel, T. J., Cabo, R., Franceschi, C., Gems, D., Ingram, D. K., Johnson, T. E., Kennedy, B. K., Kenyon, C., Klein, S., Kopchick, J. J., Lepperdinger, G., Madeo, F., Mirisola, M. G., … Fontana, L. (2015). Interventions to Slow Aging in Humans: Are We Ready? *Aging Cell*, *14*(4), 497–510. https://doi.org/10.1111/acel.12338

López De Cerain, A., Marín, A., Idoate, M. A., Tuñón, M. T., & Bello, J. (1999). Carbonyl reductase and NADPH cytochrome P450 reductase activities in human tumoral versus normal tissues. *European Journal of Cancer*, *35*(2), 320–324. https://doi.org/10.1016/S0959-8049(98)00372-4

Matheny, S. A., Chen, C., Kortum, R. L., Razidlo, G. L., Lewis, R. E., & White, M. A. (2004). Ras regulates assembly of mitogenic signalling complexes through the effector protein IMP. *Nature*, *427*(6971), 256–260. https://doi.org/10.1038/nature02237

Mc Auley, M. T., Guimera, A. M., Hodgson, D., Mcdonald, N., Mooney, K. M., Morgan, A. E., & Proctor, C. J. (2017). Modelling the molecular mechanisms of aging. *Bioscience Reports*, *37*(1), BSR20160177. https://doi.org/10.1042/BSR20160177

Milkovic, L., Cipak Gasparovic, A., Cindric, M., Mouthuy, P.-A., & Zarkovic, N. (2019). Short Overview of ROS as Cell Function Regulators and Their Implications in Therapy Concepts. *Cells*, *8*(8), 793. https://doi.org/10.3390/cells8080793

Murphy, C. T., McCarroll, S. A., Bargmann, C. I., Fraser, A., Kamath, R. S., Ahringer, J., Li, H., & Kenyon, C. (2003). Genes that act downstream of DAF-16 to influence the lifespan of Caenorhabditis elegans. *Nature*, *424*(6946), 277–283. https://doi.org/10.1038/nature01789

Nita, M., & Grzybowski, A. (2016). The Role of the Reactive Oxygen Species and Oxidative Stress in the Pathomechanism of the Age-Related Ocular Diseases and Other Pathologies of the Anterior and Posterior Eye Segments in Adults. *Oxidative Medicine and Cellular Longevity*, *2016*, 1–23. https://doi.org/10.1155/2016/3164734

Oh, S. W., Mukhopadhyay, A., Svrzikapa, N., Jiang, F., Davis, R. J., & Tissenbaum, H. A. (2005). JNK regulates lifespan in *Caenorhabditis elegans* by modulating nuclear translocation of forkhead transcription factor/DAF-16. *Proceedings of the National Academy of Sciences*, *102*(12), 4494–4499. https://doi.org/10.1073/pnas.0500749102

O'Keefe, L. V., Colella, A., Dayan, S., Chen, Q., Choo, A., Jacob, R., Price, G., Venter, D., & Richards, R. I. (2011). Drosophila orthologue of WWOX, the chromosomal fragile site FRA16D tumour suppressor gene, functions in aerobic metabolism and regulates reactive oxygen species. *Human Molecular Genetics*, *20*(3), 497–509. https://doi.org/10.1093/hmg/ddq495

Okuyama, T., Inoue, H., Ookuma, S., Satoh, T., Kano, K., Honjoh, S., Hisamoto, N., Matsumoto, K., & Nishida, E. (2010). The ERK-MAPK Pathway Regulates Longevity through SKN-1 and Insulin-like Signaling in Caenorhabditis elegans. *Journal of Biological Chemistry*, *285*(39), 30274–30281. https://doi.org/10.1074/jbc.M110.146274

Oliveira, R. P., Abate, J. P., Dilks, K., Landis, J., Ashraf, J., Murphy, C. T., & Blackwell, T. K. (2009). Condition-adapted stress and longevity gene regulation by *Caenorhabditis elegans* SKN-1/Nrf. *Aging Cell*, *8*(5), 524–541. https://doi.org/10.1111/j.1474-9726.2009.00501.x

Paradis, S., & Ruvkun, G. (1998). *Caenorhabditis elegans* Akt/PKB transduces insulin receptor-like signals from AGE-1 PI3 kinase to the DAF-16 transcription factor. *Genes & Development*, *12*(16), 2488–2498. https://doi.org/10.1101/gad.12.16.2488

Park, S.-K., Tedesco, P. M., & Johnson, T. E. (2009). Oxidative stress and longevity in Caenorhabditis elegans as mediated by SKN-1: SKN-1 response to oxidative stress. *Aging Cell*, *8*(3), 258–269. https://doi.org/10.1111/j.1474-9726.2009.00473.x

Poetsch, A. R. (2020). The genomics of oxidative DNA damage, repair, and resulting mutagenesis. *Computational and Structural Biotechnology Journal*, *18*, 207–219. https://doi.org/10.1016/j.csbj.2019.12.013

Qin, Z., Johnsen, R., Yu, S., Chu, J. S.-C., Baillie, D. L., & Chen, N. (2018). Genomic Identification and Functional Characterization of Essential Genes in *Caenorhabditis elegans*. *G3 Genes|Genomes|Genetics*, *8*(3), 981–997. https://doi.org/10.1534/g3.117.300338

Riddle, D. L., Swanson, M. M., & Albert, P. S. (1981). Interacting genes in nematode dauer larva formation. *Nature*, *290*(5808), 668–671. https://doi.org/10.1038/290668a0

Robida-Stubbs, S., Glover-Cutter, K., Lamming, D. W., Mizunuma, M., Narasimhan, S. D., Neumann-Haefelin, E., Sabatini, D. M., & Blackwell, T. K. (2012). TOR Signaling and Rapamycin Influence Longevity by Regulating SKN-1/Nrf and DAF-16/FoxO. *Cell Metabolism*, *15*(5), 713–724. https://doi.org/10.1016/j.cmet.2012.04.007

Rodrigues, E. G., Kile, M., Hoffman, E., Quamruzzaman, Q., Rahman, M., Mahiuddin, G., Hsueh, Y., & Christiani, D. C. (2012). *GSTO* and *AS3MT* genetic polymorphisms and differences in urinary arsenic concentrations among residents in Bangladesh. *Biomarkers*, *17*(3), 240–247. https://doi.org/10.3109/1354750X.2012.658863

Senchuk, M. M., Dues, D. J., Schaar, C. E., Johnson, B. K., Madaj, Z. B., Bowman, M. J., Winn, M. E., & Van Raamsdonk, J. M. (2018). Activation of DAF-16/FOXO by reactive oxygen species contributes to longevity in long-lived mitochondrial mutants in Caenorhabditis elegans. *PLOS Genetics*, *14*(3), e1007268. https://doi.org/10.1371/journal.pgen.1007268

Singh, K. K. (2006). Mitochondria Damage Checkpoint, Aging, and Cancer. *Annals of the New York Academy of Sciences*, *1067*(1), 182–190. https://doi.org/10.1196/annals.1354.022

Solari, F., Bourbon-Piffaut, A., Masse, I., Payrastre, B., Chan, A. M.-L., & Billaud, M. (2005). The human tumour suppressor PTEN regulates longevity and dauer formation in Caenorhabditis elegans. *Oncogene*, *24*(1), 20–27. https://doi.org/10.1038/sj.onc.1207978

Somasundaram, K., Zhang, H., Zeng, Y.-X., Houvras, Y., Peng, Y., Zhang, H., Wu, G. S., Licht, J. D., Weber, B. L., & El-Deiry, W. S. (1997). Arrest of the cell cycle by the tumour-suppressor BRCA1 requires the CDK-inhibitor p21WAF1/CiPl. *Nature*, *389*(6647), 187–190. https://doi.org/10.1038/38291

Son, H. G., Altintas, O., Kim, E. J. E., Kwon, S., & Lee, S. V. (2019). Age-dependent changes and biomarkers of aging in *Caenorhabditis elegans*. *Aging Cell*, *18*(2). https://doi.org/10.1111/acel.12853

Sun, X., Chen, W.-D., & Wang, Y.-D. (2017). DAF-16/FOXO transcription factor in aging and longevity. *Frontiers in Pharmacology*, *8*. https://doi.org/10.3389/fphar.2017.00548

Tahara, E. B., Navarete, F. D. T., & Kowaltowski, A. J. (2009). Tissue-, substrate-, and site-specific characteristics of mitochondrial reactive oxygen species generation. *Free Radical Biology and Medicine*, *46*(9), 1283–1297. https://doi.org/10.1016/j.freeradbiomed.2009.02.008

Thompson, D., Szabo, C. I., Mangion, J., Oldenburg, R. A., Odefrey, F., Seal, S., Barfoot, R., Kroeze-Jansema, K., Teare, D., Rahman, N., Renard, H., KConFab Consortiumf, Mann, G., Hopper, J. L., Buys, S. S., Andrulis, I. L., Senie, R., Daly, M. B., West, D., … Stratton, M. R. (2002). Evaluation of linkage of breast cancer to the putative BRCA3 locus on chromosome 13q21 in 128 multiple case families from the Breast Cancer Linkage Consortium. *Proceedings of the National Academy of Sciences*, *99*(2), 827–831. https://doi.org/10.1073/pnas.012584499

Tillman, E. J., Richardson, C. E., Cattie, D. J., Reddy, K. C., Lehrbach, N. J., Droste, R., Ruvkun, G., & Kim, D. H. (2018). Endoplasmic Reticulum Homeostasis Is Modulated by the Forkhead Transcription Factor FKH-9 During Infection of *Caenorhabditis elegans*. *Genetics*, *210*(4), 1329–1337. https://doi.org/10.1534/genetics.118.301450

Tullet, J. M. A., Hertweck, M., An, J. H., Baker, J., Hwang, J. Y., Liu, S., Oliveira, R. P., Baumeister, R., & Blackwell, T. K. (2008). Direct Inhibition of the Longevity-Promoting

Factor SKN-1 by Insulin-like Signaling in C. elegans. *Cell*, *132*(6), 1025–1038. https://doi.org/10.1016/j.cell.2008.01.030

Udell, C. M., Rajakulendran, T., Sicheri, F., & Therrien, M. (2011). Mechanistic principles of RAF kinase signaling. *Cellular and Molecular Life Sciences*, *68*(4), 553–565. https://doi.org/10.1007/s00018-010-0520-6

Walker, A. K., See, R., Batchelder, C., Kophengnavong, T., Gronniger, J. T., Shi, Y., & Blackwell, T. K. (2000). A Conserved Transcription Motif Suggesting Functional Parallels between Caenorhabditis elegans SKN-1 and Cap'n'Collar-related Basic Leucine Zipper Proteins. *Journal of Biological Chemistry*, *275*(29), 22166–22171. https://doi.org/10.1074/jbc.M001746200

Wang, S., Zhao, Y., Wu, L., Tang, M., Su, C., Hei, T. K., & Yu, Z. (2007). Induction of Germline Cell Cycle Arrest and Apoptosis by Sodium Arsenite in *Caenorhabditis elegans*. *Chemical Research in Toxicology*, *20*(2), 181–186. https://doi.org/10.1021/tx0601962

Weigel, D., Jürgens, G., Küttner, F., Seifert, E., & Jäckle, H. (1989). The homeotic gene fork head encodes a nuclear protein and is expressed in the terminal regions of the Drosophila embryo. *Cell*, *57*(4), 645–658. https://doi.org/10.1016/0092-8674(89)90133-5

Weinkove, D., Halstead, J. R., Gems, D., & Divecha, N. (2006). Long-term starvation and ageing induce AGE-1/PI 3-kinase-dependent translocation of DAF-16/FOXO to the cytoplasm. *BMC Biology*, *4*(1), 1. https://doi.org/10.1186/1741-7007-4-1

Wickens, A. P. (2001). Ageing and the free radical theory. *Respiration Physiology*, *128*(3), 379–391. https://doi.org/10.1016/S0034-5687(01)00313-9

Xu, C., Li, C. Y.-T., & Kong, A.-N. T. (2005). Induction of phase I, II and III drug metabolism/transport by xenobiotics. *Archives of Pharmacal Research*, *28*(3), 249–268. https://doi.org/10.1007/BF02977789

Yadav, D. K., Kumar, S., Choi, E.-H., Chaudhary, S., & Kim, M.-H. (2019). Molecular dynamic simulations of oxidized skin lipid bilayer and permeability of reactive oxygen species. *Scientific Reports*, *9*(1), 4496. https://doi.org/10.1038/s41598-019-40913-y

Yang, W., Li, J., & Hekimi, S. (2007). A Measurable Increase in Oxidative Damage Due to Reduction in Superoxide Detoxification Fails to Shorten the Life Span of Long-Lived Mitochondrial Mutants of *Caenorhabditis elegans*. *Genetics*, *177*(4), 2063–2074. https://doi.org/10.1534/genetics.107.080788

Yoon, S., & Seger, R. (2006). The extracellular signal-regulated kinase: Multiple substrates regulate diverse cellular functions. *Growth Factors*, *24*(1), 21–44. https://doi.org/10.1080/02699050500284218

Yoshimura, J., Ichikawa, K., Shoura, M. J., Artiles, K. L., Gabdank, I., Wahba, L., Smith, C. L., Edgley, M. L., Rougvie, A. E., Fire, A. Z., Morishita, S., & Schwarz, E. M. (2019). Recompleting the *Caenorhabditis elegans* genome. *Genome Research*, *29*(6), 1009–1022. https://doi.org/10.1101/gr.244830.118

Yousef, M. I., & El-Demerdash, F. M. (2006). Acrylamide-induced oxidative stress and biochemical perturbations in rats. *Toxicology*, *219*(1–3), 133–141. https://doi.org/10.1016/j.tox.2005.11.008

Zečić, A., & Braeckman, B. P. (2020). DAF-16/FoxO in Caenorhabditis elegans and Its Role in Metabolic Remodeling. *Cells*, *9*(1), 109. https://doi.org/10.3390/cells9010109

Zha, J., Ying, M., Alexander-Floyd, J., & Gidalevitz, T. (2019). HSP-4/BiP expression in secretory cells is regulated by a developmental program and not by the unfolded protein response. *PLOS Biology*, *17*(3), e3000196. https://doi.org/10.1371/journal.pbio.3000196

Zhang, S., Li, F., Zhou, T., Wang, G., & Li, Z. (2020). Caenorhabditis elegans as a Useful Model for Studying Aging Mutations. *Frontiers in Endocrinology*, *11*, 554994. https://doi.org/10.3389/fendo.2020.554994

Zhang, W., & Liu, H. T. (2002). MAPK signal pathways in the regulation of cell proliferation in mammalian cells. *Cell Research*, *12*(1), 9–18. https://doi.org/10.1038/sj.cr.7290105

Zhao, Y., Yang, R., Rui, Q., & Wang, D. (2016). Intestinal Insulin Signaling Encodes Two Different Molecular Mechanisms for the Shortened Longevity Induced by Graphene Oxide in Caenorhabditis elegans. *Scientific Reports*, *6*(1), 24024. https://doi.org/10.1038/srep24024